

FINAL
IN-75-CR

Final Technical Report
NASA NAGW-838

Carbon Isotope Biogeochemistry of Methane from Anoxic Sediments

Submitted by: Neal E. Blair
Department of Marine, Earth and Atmospheric
Sciences
North Carolina State University
Raleigh, NC 27695-8208
(919) 515-7883

(NASA-CR-194620) CARBON ISOTOPE
BIOGEOCHEMISTRY OF METHANE FROM
ANOXIC SEDIMENTS Final Technical
Report (North Carolina State
Univ.) 166 p

N94-19231
--THRU--
N94-19235
Unclas

G3/45 0191315

Overview

The isotopic composition of naturally occurring methane has been used to constrain the tropospheric budget of that radiatively active gas. Numerous studies have shown that the isotopic composition is not constant, even for a specific source, and may vary temporally and spatially. This creates an uncertainty in the isotopic budgets but provides an opportunity to study methanogenic processes at a new mechanistic level.

The objective of this project was to develop a process-level model that reproduced the seasonal variations in the $^{13}\text{C}/^{12}\text{C}$ composition of methane observed at the coastal site, Cape Lookout Bight, North Carolina. The first step was to establish the seasonal isotopic systematics of the site. This was done by developing an isotope mass balance for Cape Lookout sediments on the year time scale. Details of the mass balance are provided in Part I of this report.

Carbon dioxide is one of the major precursors to methane. It is thus imperative that we understand the controls on the isotopic composition of CO_2 in sediments. Experiments and models designed to determine what factors influence the $^{13}\text{C}/^{12}\text{C}$ ratio of dissolved CO_2 (and bicarbonate, carbonate) are reported in Part II. Parts I and II are from the recently completed Ph.D. dissertation of Susan Boehme.

Acetate is the other important precursor to methane. Until recently, virtually nothing was known about the isotopic composition of that molecule in the natural environment. A systematic study of the isotopic composition of acetate from Cape

Lookout was undertaken and the results are reported in an article published in *Geochimica Cosmochimica Acta* in 1992. A reprint of that article is enclosed.

All of the factors thus described have been combined in a model that faithfully reproduces the seasonal $^{13}\text{C}/^{12}\text{C}$ variations observed at Cape Lookout. The model is described in Part III and has been published in the book *Biogeochemistry of Global Change: Radiative Trace Gases* (R.S. Oremland, ed.). Additional studies based on the model have been published in *Global Biogeochemical Cycles*. A reprint of that work is enclosed.

The factors that have been identified as most critical in controlling the $^{13}\text{C}/^{12}\text{C}$ ratio of methane in the marine environment are:

1. The isotopic compositions of acetate and CO_2 ,
2. The relative rates of CO_2 -reduction and acetate dissimilation,
3. The fractionation factors of the methane-producing processes,
4. The oxidation state of the fermentable organic carbon, and
5. The relative fluxes of fermentable carbon and oxidants (e.g. O_2 and SO_4^-).

Preliminary studies indicate that these same factors are important in freshwater environments. This level of mechanistic understanding is necessary for current efforts to predict the responses of methanogenic ecosystems to climatic changes.

Table of Contents

Part I:	A Carbon Isotope Mass Balance for an Anoxic Marine Sediment: Isotopic Signatures of Diagenesis	1
Part II:	The Carbon Isotope Biogeochemistry of ΣCO_2 Production in a Methanogenic Marine Sediment	51
Part III:	The Carbon Isotope Biogeochemistry of Methane Production in Anoxic Sediments 1. Field Observations..	97

Attachments:

"The Carbon Isotope Biogeochemistry of Acetate from a
Methanogenic Marine Sediment" *Geochim. Cosmochim. Acta*
56, 1247-1258 (1992), N.E. Blair and W.D. Carter, Jr.

"Factors that Control the Stable Carbon Isotopic Composition
of Methane Produced in an Anoxic Marine Sediment" *Global
Biogeochem. Cycles* 6, 271-291 (1992), M.J. Alperin, N.E.
Blair, D.B. Albert, T.M. Hoehler and C.S. Martens.

**A Carbon Isotope Mass Balance for an Anoxic Marine Sediment: Isotopic Signatures
of Diagenesis**

ABSTRACT

A carbon isotope mass balance was determined for the sediments of Cape Lookout Bight, NC to constrain the carbon budgets published previously (Martens and Klump, 1984; Martens et al., 1993). The diffusive, ebullitive and burial fluxes of ΣCO_2 and CH_4 , as well as the carbon isotope signatures of these fluxes, were measured. The flux-weighted isotopic signature of the remineralized carbon (-18.9 ± 2.7 per mil) agreed with the isotopic composition of the remineralized organic carbon determined from the particulate organic carbon (POC) $\delta^{13}\text{C}$ profiles (-19.2 ± 0.2), verifying the flux and isotopic signature estimates.

The measured $\delta^{13}\text{C}$ values of the ΣCO_2 and CH_4 diffusive fluxes were significantly different from those calculated from porewater gradients. The differences appear to be influenced by methane oxidation at the sediment-water interface, although other potential processes cannot be excluded.

The isotope mass balance provides important information concerning the locations of potential diagenetic isotope effects. Specifically, the absence of downcore change in the $\delta^{13}\text{C}$ value of the POC fraction and the identical isotopic composition of the POC and the products of remineralization indicate that no isotopic fractionation is expressed during the initial breakdown of the POC, despite its isotopically heterogeneous composition.

INTRODUCTION

Continental shelf and slope sediments are the dominant sites of carbon cycling in marine sediments, comprising only 10% of the seafloor but accounting for approximately 90% of the organic carbon remineralization (Henrichs and Reeburgh, 1987). These environments are thus critical to the global carbon cycle. Carbon remineralization rates in continental margin environments, however, are often difficult to quantify due to the temporal and spatial variability in processes.

Organic carbon reaching the sediments can be remineralized via a succession of oxidative processes requiring oxygen, nitrate, iron, manganese and sulfate as electron acceptors (Meharg, 1974). After these oxidants are depleted, if sufficient labile organic carbon remains, it may be fermented to CH_4 and CO_2 (Claypool and Kaplan, 1974). A common approach to estimating the rate of organic matter decomposition is the measurement of the sediment water fluxes of the remineralized products, ΣCO_2 and CH_4 and/or the oxidants (Henrichs and Farrington, 1984; Berelson et al., 1987; Mackin and Swider, 1989; McNichol et al., 1991; Reimers et al., 1992; and others).

Significant uncertainties in estimates of sediment-water carbon fluxes are caused by temporal variability in the input of organic matter and associated remineralization rates at individual sites (Martens and Klump, 1984; McNichol et al., 1991; Reimers et al., 1992). One approach to address these uncertainties is to determine a carbon mass balance of the various sources and sinks at individual field sites on time scales appropriate to the site (Martens and Klump, 1984; Berelson et al., 1987; Martens et al., 1993). In temporally variable systems, however, carbon budgets

may not be easily constrained without numerous measurements of fluxes.

An isotope mass balance, accomplished by measurement of the $\delta^{13}\text{C}$ of the individual carbon fluxes and determining the flux-weighted averages of each of the carbon pools, can serve to constrain further the fluxes and rates. Carbon isotope mass balances have been attempted in lake productivity studies (Quay et al., 1986; Herczeg, 1988) and in estuarine studies to quantify seasonal organic matter fluxes to the estuary floor (Lucotte et al., 1991). Alperin (1988) determined an isotope mass balance for the sediments of Skan Bay, Alaska in order to identify the relative rates of degradation of different organic sources. On a global scale, an isotope mass balance of atmospheric methane has been used to estimate source inputs (e.g. Craig et al., 1988; Quay et al., 1991). Most recently, Quay et al. (1992) and Tans et al. (1993) have attempted to use ΣCO_2 $\delta^{13}\text{C}$ measurements of surficial seawater to estimate increases in oceanic uptake. All of these isotope studies have attempted to use a mass balance to estimate a flux or rate that was not easily measured.

Our approach has been to use isotope measurements of all of the major carbon reservoirs and fluxes of the sediments of Cape Lookout Bight, NC, to verify the carbon budget proposed for this site (Martens and Klump, 1984; Martens et al., 1993). Measurement of the isotopic composition of the individual fluxes and reservoirs also allows us to address specific questions about processes at the sediment-water interface such as methane oxidation and to characterize diagenetic isotope effects caused by selective degradation. Cape Lookout was chosen because carbon mass balances for this site have been published previously (Martens and Klump, 1984;

Martens et al., 1993) and remineralization rates vary seasonally in a predictable fashion (Martens et al., 1986).

Remineralization processes (e.g. microbial methane production) can alter the isotopic composition of the individual carbon fluxes, causing a measurable isotope fractionation between the CH_4 and the CO_2 . Diagenetic isotope effects associated with selective remineralization of isotopically distinct organic fractions have also been hypothesized to alter the isotopic signature of the fluxes of the remineralized fraction, and by mass balance, the buried carbon fraction as well (Spiker and Hatcher, 1984; 1987; Alperin, 1988; Fischer, 1989; Benner et al., 1991). In principle, the ^{12}C and ^{13}C mass balance of all identified carbon fluxes (CH_4 , ΣCO_2 , corrected for carbonate dissolution and precipitation) should be the same as the isotopic composition of the remineralized carbon fraction determined from the particulate organic carbon isotope profiles.

FIELD SITE

Cape Lookout Bight (CLB) is a small (1 km^2) back barrier island lagoon with a water depth of 7 meters at the deepest location (Martens and Klump, 1980). All samples were collected at Station A-1, where previous carbon mass balance has been established (Martens and Klump, 1984; Martens et al., 1993). Circulation within the Bight is controlled predominantly by tidal flow (Martens and Klump, 1980; Wells, 1988). The water column above station A-1 remains oxygenated all year (Bartlett, 1981).

Cape Lookout Bight acts as a trap for fine-grained sediments and organic

debris transported seasonally from the Atlantic shelf during storms (Canuel et al., 1990) and from the shallow back barrier lagoons of coastal North Carolina by ebb tidal flows (Martens and Klump, 1980; Chanton et al., 1983). Sediment in Station A-1 accumulates at a rate of 8.4 to 11.8 cm/yr averaged over the upper meter of sediment (Chanton et al., 1983; Canuel et al., 1990). Organic carbon content in the upper meter ranges from approximately 3 to 4 wt. % (Martens and Klump, 1984; Haddad and Martens, 1987; this study) and appears to be derived primarily from phytoplankton and seagrass debris (Haddad and Martens, 1987). Bioirrigation and sediment mixing by animals are not important processes for most of the year at Station A-1 (Bartlett, 1982).

Sulfate reduction is the dominant remineralization process within the upper 10 to 15 cm of the sediment (Martens and Klump, 1984; Crill and Martens, 1987). Methane production occurs below this zone. During summer months (May through October) methane ebullition occurs during low tide conditions when hydrostatic pressure is decreased (Martens and Klump, 1980). Sediment temperatures can vary by more than 20°C through the year and are the driving force behind seasonal changes in rates of microbial processes such as sulfate reduction and methanogenesis (Martens and Klump, 1984).

Based on grain size distributions and annually reproducible pore water nutrient profiles (Klump and Martens, 1981), Martens and Klump, (1984) suggested that "quasi steady state" conditions have existed at Station A-1 at least since the early 1970's. Haddad and Martens (1987) used lignin oxidation product analysis and

isotopic measurements of sediment organic matter as well as degradation rates of metabolizable materials to document yearly steady state input of organic matter on an annual time scale at Station A-1. The agreement in the sedimentation rate determined using ^{210}Pb and ^7Be radiotracers in studies conducted almost 10 years apart (Chanton et al., 1983; Canuel et al., 1990) is further evidence of annual steady state sediment accumulation at Cape Lookout Bight. Laminations seen in sediment cores in the upper 5 cm of winter sediment cores and ^7Be profiles (Canuel et al., 1990) indicate, however, that sedimentation is not uniform on time scales of less than one year. Pore water depth-concentration profiles, fluxes across the sediment-water interface and isotope profiles change rapidly in response to increasing temperature, suggesting that steady state conditions may not be attained on time scales of weeks. Nevertheless, pore water depth integrated and measured rates suggests that the system is near steady state on time scales less than a year.

METHODS

Cores were collected by divers from Station A-1 at 4-8 week intervals from February 1986 through February 1987. Samples also were obtained with a Soutar box core in March, 1986 and 1988. Porewater samples were isolated with a sediment membrane filtration squeezer (Reeburgh, 1967).

ΣCO_2 analyses were performed by injecting one to two ml of porewater into 120 ml evacuated serum bottles capped with crimped, lightly greased rubber stoppers (Alltech #6633). Duplicate or triplicate cores were analyzed. In May, 1986, duplicate samples from the same core as well as samples from a second core were

analyzed. Pore water samples were frozen immediately after collection and maintained frozen until analysis (-18 to -56°C). One ml of 1M phosphoric acid saturated with copper sulfate was added to each porewater sample immediately before analysis. The copper sulfate was added to the sample to precipitate sulfides in order to avoid interference from H₂S. The CO₂ was removed from the bottle by vacuum distillation, purified, and collected cryogenically for isotopic analysis. Sample size was determined manometrically. Bicarbonate and tank CO₂ standards were processed to verify that the procedure was not causing isotopic fractionation and to insure complete gas collection. The precision and accuracy of concentration measurements were 0.4mM and 0.1mM, respectively, based on bicarbonate standards. Reproducibility of the triplicate samples from May, 1986 was 0.5mM.

After purification the CO₂ was collected and sealed in borosilicate tubing and its carbon isotopic composition was measured in one of three laboratories: the Stable Isotope Laboratory, North Carolina State University; NASA-Ames, California; and the Center for Applied Isotope Studies, Athens, Georgia. Interlab comparison among these three labs gave comparable results (± 0.2 per mil, Blair and Carter, 1992). The accuracy and precision of the ΣCO_2 measurements were 0.4 and 0.2 per mil, respectively. Reproducibility from triplicate standard analyses was 0.95 per mil.

Porewater samples were collected on four field dates for analysis of calcium. Following acidification and filtration (0.45 μm), samples for calcium were diluted to 1:20. Samples were analyzed on a Perkin-Elmer 560 Atomic Absorption spectrometer (NCSU - Forestry Department Analytical Laboratory) using a 0.5% Lanthanum

solution. Duplicate analyses had a precision of 0.2mM. A comparison of samples analyzed for Ca^{++} at SUNY-Stony Brook (P. Rude, Marine Sciences) and NCSU agreed to within 0.2mM.

Sediment cores were collected for CH_4 isotopic analysis. Cores were sectioned in 2-3 cm depth intervals and placed in Mason jars containing 10 to 20 ml of 1-3M NaOH. Headspace gas was removed from the Mason jars by syringe through a rubber stopper (Bellco Biotechnology) that had been fitted into the lid. After removing water and CO_2 cryogenically, the methane was converted to CO_2 by passing it through an 790°C furnace packed with CuO using helium as a carrier gas (Matthews and Hayes, 1978). The resultant CO_2 was purified and collected cryogenically. The precision and accuracy of the analyses, based on a methane standard (Scott Specialty Gas), were both 0.3 per mil. Duplicate core samples expressed a maximum difference of 1.6 per mil.

Bubble samples were collected as described in Martens et al. (1986). One ml samples of the bubble gas were removed via syringe from a serum bottle and processed in the same way as the sedimentary methane samples. Tank CH_4 standards, duplicate samples from individual bottles and duplicate and triplicate bottles were analyzed. Precision and accuracy of this procedure are the same as the values given for the sedimentary methane procedure. Reproducibility of samples taken from the same bottle were 0.02 per mil and reproducibility of analyses from individual bottles collected on the same date were 0.2 per mil.

Concentration and isotopic composition measurements of the particulate organic

carbon (POC) were made downcore on sediments collected in August, 1986. Bomb combustion techniques are described in Blair et al. (1987). Precision and accuracy of this procedure, based on NBS-20 standards, are 0.3 and 0.5 per mil, respectively.

Particulate inorganic carbon (PIC) was analyzed on a sediment core collected in May, 1987. The sediment was rinsed with deionized water three times and freeze dried. Ten to 60 mg of sediment was placed in a 120ml serum bottle and sealed with a rubber stopper. The bottle was evacuated and one ml of 0.5M phosphoric acid was injected and allowed to react overnight. Vacuum line collection procedures were the same as for ΣCO_2 porewater samples. Duplicate analyses of the 0-1 cm depth interval gave PIC concentrations within 0.1% and $\delta^{13}\text{C}$ values within 0.01 per mil.

An in situ flux experiment was undertaken in April, 1986. Lucite chambers were placed on the sediment surface and then pushed downward a few cm into the sediment. A battery operated stirring system was used to keep chamber waters mixed. Overlying water samples within the chamber were collected for ΣCO_2 concentration and isotope analyses shortly after emplacement and again at the end of the experiment prior to the next low tide ebullitive event. Cores were taken adjacent to the chambers and analyzed for ΣCO_2 concentration and isotope profiles.

Flux experiments were performed in the laboratory in February 1987 and March 1988. Lucite box core chambers were used to collect an undisturbed section of sediment and overlying water. The chambers were sealed from below and transported in seawater back to the laboratory and placed in a seawater circulation tank to maintain near ambient temperatures. Overlying water samples were taken immediately

after the chambers were stabilized and sampled again twice during the following day. Chambers were circulated at a rate of approximately 15 ml/minute by circulating the overlying water with a peristaltic pump. At the end of the experiment the chambers were subcored and the porewater was extracted for ΣCO_2 concentration and isotopic analyses. During the March, 1988 experiment, overlying water and sediment samples were also collected for CH_4 concentrations and isotopic analyses.

RESULTS

Particulate Organic Carbon

POC content decreases exponentially with values ranging from 4% at the surface to less than 3% at depth (Fig. 2.1a). The $\delta^{13}\text{C}$ values of the POC from this study as well as profiles from Blair et al. (1987) and Blair and Carter (1992) (Fig 2.1b) behave conservatively as a function of depth, indicating that the fraction remineralized must have a $\delta^{13}\text{C}$ value similar to the site average of -19.08 ± 0.26 (Blair and Carter, 1992). More formally, a mass balance calculation can be used to estimate the $\delta^{13}\text{C}$ signal of the remineralized organic carbon:

$$\delta G_0 = \frac{(\%G_{\text{remin}})(\delta G_{\text{remin}}) + (100 - \%G_{\text{remin}})(\delta G_{\text{buried}})}{100} \quad (2)$$

where $\%G_{\text{remin}}$ is the percent of the POC remineralized. Martens and Klump (1984) determined the percent of organic matter remineralized to be $28 \pm 7\%$, based on five POC profiles. The isotopic composition of the POC at the surface (δG_0) is -19.1 ± 0.2 and at depth (δG_{buried}) is -19.2 ± 0.1 (Fig 2.1b). Solving Eqn. (2) for δG_{remin} gives an isotopic signature of the remineralized fraction of the organic matter

of -19.2 ± 0.2 per mil.

ΣCO_2 Diffusive Flux

The results of the ΣCO_2 flux chamber experiments (Table 2.1) were integrated with previous flux measurements (Martens and Klump, 1984) to yield an estimated annual flux of 30.3 ± 4.8 moles- m^{-2} - yr^{-1} . The error estimate of $\pm 16\%$ is based on the interannual variability of March flux measurements in 1977, 1978 (Martens and Klump, 1984), and 1988 (this study). The ΣCO_2 diffusive flux across the sediment-water interface represents 80% of the remineralized organic carbon that is recycled to the overlying water. This value is consistent with the $84 \pm 18\%$ measured by Martens and Klump (1984). The isotopic signal of the annual diffusive ΣCO_2 flux is estimated to be -15.5 ± 1.2 per mil based on the results of directly measured fluxes (Table 2.1).

Fluxes and isotopic signatures were calculated from pore water gradients for the three flux experiments to compare to the measured flux values (Table 2.1). Calculated fluxes were determined using Fick's 1st Law of diffusion modified for chemical transport in sediments,

$$J_{\text{diffusive}} = -\phi_0 \left(\frac{\partial C}{\partial z} \right)_0 D_s \quad (3)$$

where:

- ϕ_0 = sediment porosity at sediment surface ($0.926 \text{ cm}^3_{\text{pw}}/\text{cm}^3_{\text{wet sed.}}$)
Martens and Klump, 1980)
- D_s = sediment diffusion coefficient (cm^2/sec) (D_0 taken from Li and Gregory (1974) and corrected for sediment tortuosity (Berner 1980))
- $(\partial C/\partial z)_0$ = linear gradient of ΣCO_2 , $\Sigma^{12}\text{CO}_2$ or $\Sigma^{13}\text{CO}_2$ profiles at the sediment water interface (mM/cm)

Calculated and measured fluxes and their isotopic signatures are compared in Table 2.1. The calculated isotopic signal of the March ΣCO_2 flux was also determined by solving for the individual $\Sigma^{12}\text{CO}_2$ and $\Sigma^{13}\text{CO}_2$ concentrations and then calculating the distribution and isotopic signature of each of the following species based on sediment temperature, salinity, pressure and pH: $^{12}\text{CO}_2$, $^{13}\text{CO}_2$, $\text{H}^{12}\text{CO}_3^-$, $\text{H}^{13}\text{CO}_3^-$, $^{12}\text{CO}_3^{=}$, $^{13}\text{CO}_3^{=}$; Deines et al., 1974; Stumm and Morgan, 1981) (Table 2.2; See appendix for description). pH data were taken from Chanton (1985). Individual gradients for each of these species were calculated and the corresponding diffusion coefficients were used in Eqn. 3 (Unver and Himmelblau, 1964; Li and Gregory, 1974; Friedman and O'Neil, 1977; O'Leary, 1984). The resulting isotopic signal of ΣCO_2 flux was compared to a flux based only on the gradients of $\Sigma^{12}\text{CO}_2$ and $\Sigma^{13}\text{CO}_2$ (Table 2.2). The individual species were calculated because previous studies had found significant diffusion of $\text{CO}_3^{=}$ into the sediment despite the net flux of ΣCO_2 out of the sediment (Sayles and Curry, 1988; McNichol et al., 1991). There was no difference in the calculated isotope signal of the ΣCO_2 flux using either approach and so individual species gradient calculations were not applied to the February and April fluxes. Application of a range of pH values (6-8) for the 0-1 cm interval shifted the resulting isotopic signal by less than 1 per mil.

The isotope signature of the calculated ΣCO_2 flux was consistently 6 to 7 per mil enriched in ^{13}C compared to the measured values (Table 2.1). The measured fluxes were slightly larger than the calculated fluxes except in the April *in situ* experiment in which the flux was calculated using porewater gradients from a core

near the chamber.

Burial of ΣCO_2

Burial of ΣCO_2 accounts for a flux of 6.6 ± 0.5 moles- m^{-2} - yr^{-1} with an isotopic signature of $+8.3 \pm 1.5$ per mil. The burial flux was determined using an average of ΣCO_2 concentrations measured at depths between 35 and 40 cm depth (Fig. 2.2) and applying the following equation:

$$J_{\text{burial}} = C_{\infty} \omega_{\infty} \phi_{\infty} \quad (4)$$

where

ϕ_{∞} = sediment porosity at depth ($0.85 \text{ cm}^3_{\text{pw}}/\text{cm}^3_{\text{wet sed.}}$; Chanton, 1985)
 ω_{∞} = sediment accumulation rate at depth (10 cm/yr: Chanton et al., 1983),
 C_{∞} = average concentration of ΣCO_2 at 35 to 40cm (mM/cm).

The burial depth of 40 cm was chosen because the ΣCO_2 concentration profiles are nearly asymptotic and greater than 95% of the remineralization occurs above this horizon (Martens and Klump, 1984). The isotopic signal of the buried ΣCO_2 of $+8.3 \pm 1.5$ per mil was determined by averaging the isotopic values measured at depths of 35 to 40 cm.

CH_4 Bubble Flux

Methane ebullitive fluxes were measured previously (Martens and Chanton, 1989; Martens et al., 1986). The annual ebullitive flux is calculated to be 6.4 ± 0.8 moles- m^{-2} - yr^{-1} based on fluxes measured from 1976 to 1986 (Table 2.3). The isotopic signature of the ebullitive flux of -60.0 ± 1.2 is based on flux-weighted average monthly methane measurements (Martens et al., 1986; Fig. 2.3). The isotope

measurements (Fig. 2.3) show strong seasonality, with relatively ^{13}C -enriched methane consistently released during the period of peak production (July-August).

CO₂ Bubble Flux

Ebullition strips a portion of the dissolved CO₂ from the porewater. The CO₂ ebullitive flux, 0.13 ± 0.05 moles-m⁻²-yr⁻¹ has an annual $\delta^{13}\text{C}$ value of -8.5 ± 1.4 per mil (Martens et al., 1986). The more negative CO₂ $\delta^{13}\text{C}$ values were measured in the summer months corresponding to the period of highest remineralization rates and the most depleted ΣCO_2 values measured in the sediment (Fig. 2.2; Martens et al., 1986).

CH₄ Diffusive Flux

The annual methane diffusive flux of 0.85 ± 0.8 moles-m⁻²-yr⁻¹ was taken from Martens and Klump (1980) and is based on pore water methane profiles and saturation calculations. The measured isotope signature of the methane flux is estimated to be -50.5 ± 0.3 per mil, based on the two flux chamber measurements from this study. The diffusive signal is 9.5 per mil enriched in ^{13}C relative to the annual methane ebullient isotope signal (Martens et al., 1986; this study) and is 4 per mil enriched compared to the diffusive flux calculated from pore water gradients of methane for March (-54.0 ± 0.3 per mil; Table 2.1).

No attempt to determine the seasonality of this signature was made, however, a sensitivity of this flux to the overall isotopic signature of the remineralized fraction was performed. Assuming that either all or none of the diffusive flux was oxidized (the probable cause for the isotopic signature that is different from the methane

produced in the sediment) resulted in less than a 0.5 per mil shift in the isotopic signature of the remineralized carbon.

CH₄ Burial Flux

The burial rate of methane has been calculated to be 0.14 ± 0.02 moles-m⁻²-yr⁻¹ (Martens et al., 1993). The $\delta^{13}\text{C}$ value of the buried CH₄ (-59.9 ± 1.9) was determined by averaging the isotopic signal of the sedimentary methane at 40 cm (Fig. 2.4). This signal is not significantly different than the methane bubble flux value of -60.0 ± 1.2 per mil, indicating that the ebullitive and burial processes are not influenced by oxidation or transport isotope effects (Martens et al., 1986; Chanton and Dacey, 1991).

Solid Phase Inorganic Carbon

Ca⁺⁺ concentration profiles increase from overlying water values in the upper few centimeters and then decrease with depth (Fig. 2.5a). The rates of dissolution and precipitation of particulate inorganic carbon (PIC) were estimated from these porewater Ca⁺⁺ profiles by assuming that an increase in the Ca⁺⁺ concentration profile was caused by dissolution and a decrease in concentration was caused by precipitation of PIC. The Ca⁺⁺ porewater linear concentration gradients were used in the 0-5 and 5-25 cm intervals to estimate the dissolution and precipitation rate of CaCO₃ respectively. The bulk sediment diffusivity for Ca⁺⁺ (D_g) was determined by correcting the diffusion coefficients for Ca⁺⁺ measured in seawater (Li and Gregory, 1974) for the given temperature and sediment tortuosity (Bernier, 1980).

The isotopic composition of the PIC that was assumed to have dissolved in the

0-5cm depth interval was determined by averaging the measured isotopic composition of the PIC within the dissolution zone (Fig. 2.5b). The isotopic composition of the assumed precipitated carbonate of -3.8 ± 3.8 per mil is based on the average isotopic value of the DIC pool in the 5-25 cm depth interval from the same months as the measured Ca^{++} profiles (see Fig. 2.2). The use of the Ca^{++} profiles to determine the PIC flux implies that CaCO_3 is the dominant species involved in the dissolution and precipitation processes. To a first approximation, this appears to be true since Mg^{++} concentration profiles showed no significant trends and Sr^{++} concentrations, which mimicked the Ca^{++} profiles, were an order of magnitude lower in concentration than the Ca^{++} values (see Appendices for Mg^{++} and Sr^{++} results). The decrease in Ca^{++} concentration at depth may be a result of precipitation after core recovery because of the oversaturated nature of the porewaters, thus the calculated precipitation rate should be regarded as an upper limit.

The Carbon Isotope Mass Balance

The carbon isotope mass balance determined as described above is summarized in Table 2.4 and shown schematically in Fig. 2.6. The total flux (J_{total}) is defined as the sum of the buried, bubble and diffusive fluxes of ΣCO_2 and CH_4 . To determine the isotopic composition of the portion of J_{total} that results directly from remineralization of the POC (J_{remin}), the contributions of carbonate dissolution and precipitation need to be accounted for:

$$J_{\text{total}} = J_{\text{remin}} + J_{\text{diss}} + J_{\text{precip}} \quad (5)$$

$$(J_{total}) (\delta_{total}) = (J_{remin}) (\delta_{remin}) + (J_{diss}) (\delta_{diss}) + (J_{precip}) (\delta_{precip}) \quad (6)$$

Using eqns. 5 and 6, the isotopic composition of the remineralized carbon is estimated to be -18.9 ± 2.7 per mil, which is in excellent agreement with the remineralized organic matter signal determined from the POC profiles (-19.2 ± 0.2 per mil).

The error associated with the estimated signature of the remineralized carbon pool of 2.7 per mil is primarily due to interannual variability in fluxes and the errors associated with the isotopic composition of the diffusive ΣCO_2 flux. The annual ΣCO_2 flux makes up approximately 70% of the remineralized carbon fraction, and therefore, the budget is very sensitive to the isotopic value assigned to this flux. The internal consistency of the mass balance suggests that despite the small data sets used to determine the methane and ΣCO_2 diffusive fluxes and the interannual variability, the values are realistic estimates of the isotopic signature of these fluxes.

The isotopic composition of the diffusive CH_4 flux was calculated from a single experiment conducted in March. There is undoubtedly some seasonality to this signal that is not included in the estimate used here, but as noted, the small size of this flux precludes it from strongly affecting the overall isotopic signature of the remineralized carbon.

The isotopic composition of the dissolved organic carbon (DOC) flux has not been measured and consequently is not included in this budget. The diffusive and burial DOC fluxes should not significantly influence the overall isotope mass balance

because they represent only 5% of the remineralized carbon flux (Martens et al., 1993), and the isotopic composition of DOC fractions in similar environments are typically within 2-3 per mil of the particulate organic carbon pool (Williams and Gordon, 1970; Nissenbaum et al., 1972; Brown et al., 1972; Orem et al., 1986; Alperin, 1988).

DISCUSSION

The successful isotopic mass balance of the isotopic signature of the sources and sinks of carbon verifies the carbon budget determined for Cape Lookout as well as the isotopic signatures of the different carbon fluxes at a site that experiences significant seasonal variations. More importantly, the isotope mass balance allows us to constrain further our interpretations of certain processes occurring in this system to a degree previously not possible. These processes are discussed below in the context of the balanced carbon isotope budget.

Surficial processes influencing ΣCO_2 and CH_4 fluxes

The diffusive fluxes of both ΣCO_2 and CH_4 and their associated isotopic signatures were directly measured in chamber experiments. Pore water analyses of the flux chamber sediments were made so that the fluxes and their isotopic signature could be estimated from the concentration gradients at the sediment-water interface using Fick's 1st Law (Eqn. 3). Our original intent was to use the monthly ΣCO_2 profiles (Fig. 2.2) to determine the annual $\delta^{13}\text{C}$ value of the diffusive flux. The comparison of measured and calculated ΣCO_2 fluxes and their associated isotopic signatures revealed that the calculated isotopic compositions of the fluxes were consistently 6-7

per mil enriched in ^{13}C relative to the measured values (Table 2.1). The calculated diffusive flux of CH_4 was greater and depleted in ^{13}C relative to the measured CH_4 flux (Table 2.1). Several possible mechanisms that could account for the discrepancies between the calculated and measured isotopic signatures of these fluxes are discussed below.

In theory, differential diffusion of the inorganic carbon species, CO_2 , HCO_3^- , and $\text{CO}_3^{=}$, because of pH gradients across the sediment-water interface, could influence the isotopic composition of the flux of ΣCO_2 and the sedimentary ΣCO_2 pool. The apparent production of ΣCO_2 that is significantly enriched in ^{13}C relative to the organic carbon has been noted in coastal and deep-sea sediments and has been interpreted to result from the diffusion of ^{13}C -depleted CO_2 out of and relatively ^{13}C -enriched $\text{CO}_3^{=}$ into the sediment (McNichol, 1986; Sayles and Curry, 1988; McNichol et al., 1991). Calculations of the individual fluxes and isotopic signals of CO_2 , HCO_3^- and $\text{CO}_3^{=}$ from the March flux experiment demonstrate that the magnitude of the $\text{CO}_3^{=}$ flux is insufficient to alter significantly the overall isotopic ΣCO_2 signal and thus this mechanism can be ruled out for Cape Lookout sediments (Table 2.2).

Differences in the diffusion coefficient of isotopically substituted species would, if they exist, contribute to apparent diffusion isotope effects. For example, the ratio of the diffusion coefficient for $^{12}\text{CO}_2$ and $^{13}\text{CO}_2$ in water ($^{12}\text{D}/^{13}\text{D}$) is 1.0007 ± 0.0002 at 25°C (O'Leary, 1984). This fractionation has been included in the calculations of the ΣCO_2 isotopic signal (Table 2.1). To our knowledge, the potential

isotope effects associated with the diffusion of HCO_3^- , $\text{CO}_3^{=}$ or CH_4 have not been measured.

We consider methane oxidation in surficial sediments to be a source of ^{13}C -depleted material to the diffusive ΣCO_2 flux. Methane oxidation could also explain the discrepancies in the measured and calculated CH_4 fluxes. Evidence for CH_4 oxidation includes $^{14}\text{CH}_4$ -tracer studies (M. Alperin, pers. comm.), and the ^{12}C -depleted CH_4 in the winter surface sediments at Station A-1 (Fig. 2.4). Methane oxidizing bacteria preferentially utilize $^{12}\text{CH}_4$ (Silverman and Oyama, 1968; Barker and Fritz, 1981; Coleman et al., 1981; Whiticar and Faber, 1986; King et al., 1989). The fractionation factor ($^{12}\text{k}/^{13}\text{k}$) for aerobic oxidation of CH_4 ranges from 1.005 to 1.031 in culture (See Table 1 in Whiticar and Faber, 1986). An estimate of the fractionation factor for methane oxidation in the surficial sediments of CLB can be determined if it is assumed that the difference between the measured and calculated methane isotope signal of the March flux experiment is entirely the result of methane oxidation:

$$\delta_{\text{calc}} = (\delta_{\text{meas}} (1 - F_{\text{ox}})) + (\delta_{\text{ox}} F_{\text{ox}}) \quad (7)$$

where F_{ox} is the fraction of the potential diffusive flux of methane that has been oxidized, and δ_{calc} and δ_{meas} are the isotopic compositions of the calculated and measured fluxes (-54.0 ± 0.3 and -50.5 ± 0.3 , respectively) (Table 2.1). F_{ox} was estimated to be 0.32 using the equation:

Accordingly, δ_{ox} is -61.5 per mil and the fractionation factor (α) can be estimated using the following relationship:

$$F_{ox} = 1 - \left(\frac{J_{meas}}{J_{calc}} \right) \quad (8)$$

$$\alpha = \frac{(\delta_{meas} + 10^3)}{(\delta_{ox} + 10^3)} \quad (9)$$

The calculated α is 1.012 ± 0.005 , which falls within the range of both the culture studies mentioned above, and the range determined by Whiticar and Faber (1986) for methane oxidation in natural systems ($\alpha = 1.002$ to 1.014).

If it is assumed that the difference between measured and calculated CH_4 fluxes is due to CH_4 oxidation alone, then only $14 \mu\text{moles}\cdot\text{m}^{-2}\cdot\text{yr}^{-1}$ of CO_2 are added to the ΣCO_2 flux with an isotopic signal of -61.5 per mil (Table 2.1). This small addition of ^{13}C -depleted CO_2 shifts the calculated ΣCO_2 flux by less than one per mil, and thus does not fully explain the discrepancy between the measured and calculated isotopic values of the ΣCO_2 flux.

Diagenetic Isotope Effects

The carbon isotope mass balance allows us to address the effects of early diagenesis on the isotopic composition of the organic matter that is deposited at Cape Lookout Bight. For the purposes of this discussion, a diagenetic isotope effect is defined as any process that alters the isotopic composition of the organic carbon or creates isotopically distinct pools of carbon after the original organic matter is deposited in a sediment. Selective degradation of isotopically heterogeneous fractions, or kinetic isotope effects associated with various diagenetic processes could result in a

diagenetic isotope effect. The well known isotopic discrimination associated with biogenic methane formation is included in this definition.

In principle, Cape Lookout Bight is an ideal location to investigate potential isotopic effects because of its nearly steady state annual input of organic matter. In addition, Cape Lookout Bight receives organic matter from a variety of isotopically distinct sources such as phytoplankton and seagrasses, as indicated by isotopic measurements, lignin and lipid analyses (Haddad, 1989; Blair and Carter, 1992). Isotopic differences apparently exist between compound classes at this site as well, as indicated by the average $\delta^{13}\text{C}$ values of fatty acids (-22.1 ± 0.5), neutral lipids (-22.9 ± 0.3) and POC (-19.08 ± 0.26) fractions (Blair and Carter, 1992). Thus, given that nearly 30% of the organic matter delivered to site A-1 is remineralized, a diagenetic isotope effect might be expected, if any of these organic fractions were selectively degraded. Surprisingly, the downcore profiles of the POC $\delta^{13}\text{C}$ values and the isotope mass balance of the ΣCO_2 and CH_4 fluxes provide no evidence for selective degradation or preservation of isotopically distinct organic pools. McArthur (1989), Cronin and Morris (1982), Reimers and Suess (1983) and others, also found no indication of an isotopic diagenetic effect in the organic carbon record from a variety of sediment types and ages. This is in contrast to observations made in marine sediments of Skan Bay (Alperin, 1988) where changes in the isotopic composition of the organic matter downcore could be attributed to different rates of remineralization of the dominant organic matter sources, and Mangrove Lake, Bermuda where a ^{12}C enrichment downcore in the sediments was attributed to selective preservation (Spiker

and Hatcher, 1984).

The absence of any expressed isotope effect associated with the input and early diagenesis of organic matter at CLB is surprising since the inputs are isotopically distinct. The analyses of both the deposited and buried fractions of the organic matter of Haddad (1989) and Martens et al. (1993) indicated that the organic matter that was remineralized was most similar to an algal/bacterial source based on the C/N ratios and the loss of biochemical components downcore. The carbon isotope mass balance can be explained most simply by a remineralized fraction that is a mixture of two sources, predominantly algal/bacterial and a vascular plant component.

The large isotopic difference observed between the POC and CH₄ indicates that isotope fractionation occurs during some step or steps in the production of methane from the breakdown of organic matter. Large isotope effects are associated with the reduction of CO₂ and the dissimilation of acetate to form CH₄ at this site (Blair and Carter, 1992; Blair et al., 1993). The carbon isotope budget should allow us to determine if CO₂ reduction and acetate dissimilation are masking other diagenetic isotope effects occurring during the initial breakdown of organic matter at Cape Lookout.

The carbon isotope mass balance, when considered in light of the downcore $\delta^{13}\text{C}$ acetate measurements of Blair and Carter (1992) indicate that there is little or no fractionation in the breakdown of high molecular weight compounds (biopolymers) to form the low molecular weight biomonomers. If there was isotopic fractionation in the initial breakdown of the organic matter, one would expect to see $\delta^{13}\text{C}$ acetate

measurements in the sulfate zone that were very different from the $\delta^{13}\text{C}$ POC measurements downcore, and the isotopic composition of the flux weighted sum of organic carbon remineralization (δ_{total}) would be isotopically different than the organic matter. Isotope discrimination might occur during the fermentation of lower weight organic matter to form acetate and other intermediates, however its signal may not be expressed if most of the organic matter flows through the acetate pathway (Blair and Carter, 1992). An acetate $\delta^{13}\text{C}$ measurement from the sulfate reduction zone of Cape Lookout Bight sediments of -17.6 per mil indicates that the expressed isotope effect is probably less than 2 per mil during the oxidation of acetate (Blair and Carter, 1992). These observations suggest that the isotopic fractionation of the carbon during the formation of methane via CO_2 reduction and acetate dissimilation occurs in the final steps of CH_4 production and little or no fractionation is expressed in the breakdown of higher molecular weight compounds to form low molecular weight compounds such as acetate. This conclusion is in contrast to the less well-constrained speculations about sedimentary processes that would cause intramolecular isotope effects such as bond rupture (Macko, 1992), polymerization, and decarboxylation (Galimov, 1980) and thus alter the isotopic composition of the residual organic matter.

SUMMARY AND CONCLUSIONS

The carbon isotopic signal of the remineralized organic matter in Cape Lookout Bight sediments is -18.9 ± 2.7 per mil based on a mass balance of the remineralized carbon fractions. This estimate is indistinguishable from the calculated $\delta^{13}\text{C}$ signal of the remineralized organic matter determined from vertically uniform POC profiles of -19.2 ± 0.2 per mil. The agreement confirms that the major sources and sinks of carbon and their isotopic signals have been quantified. The comparison of directly measured and calculated CH_4 and ΣCO_2 isotope fluxes suggest that a surficial process is altering the isotopic composition of these species diffusing out of the sediment. Methane oxidation has altered the isotopic compositions of both the ΣCO_2 and CH_4 leaving the sediment, but can account for little of the discrepancy in calculated versus measured $\delta^{13}\text{C}$ values of the ΣCO_2 fluxes.

The isotope mass balance revealed little variation in the isotopic composition of the organic matter being deposited, remineralized, or buried. This is in contrast to numerous recent studies that have focused on organic matter source variations, individual biochemical components and their selective loss or preservation, and also intramolecular isotope effects to explain downcore changes in $\delta^{13}\text{C}$ values of POC (Galimov, 1980; Spiker and Hatcher, 1984; 1987; Benner et al., 1987; Alberts et al., 1988; Hayes et al., 1990; McArthur et al., 1992). The absence of an expressed diagenetic isotope effect in a system with a mixture of organic matter sources suggests that the processes that have been speculated to cause the isotopic variations in sedimentary organic matter profiles may not typically be expressed in the sedimentary

record, and the variations seen may more often be source related (Dean et al., 1986).

A carbon isotope mass balance was achieved by seasonal measurements of the dominant components of the carbon cycle in this system, highlighting the importance of considering seasonality when determining an isotopic signal for a specific environment. This is particularly important in coastal systems where the rates of remineralization processes and the isotopic signals of the various fluxes should vary seasonally.

Fig. 2.1 Cape Lookout Bight particulate organic carbon concentration (A) and $\delta^{13}\text{C}$ values as a function of depth in the seabed. (B) POC profiles are from Chanton et al. (1983); Blair et al. (1987), Blair and Carter (1992) and this study.

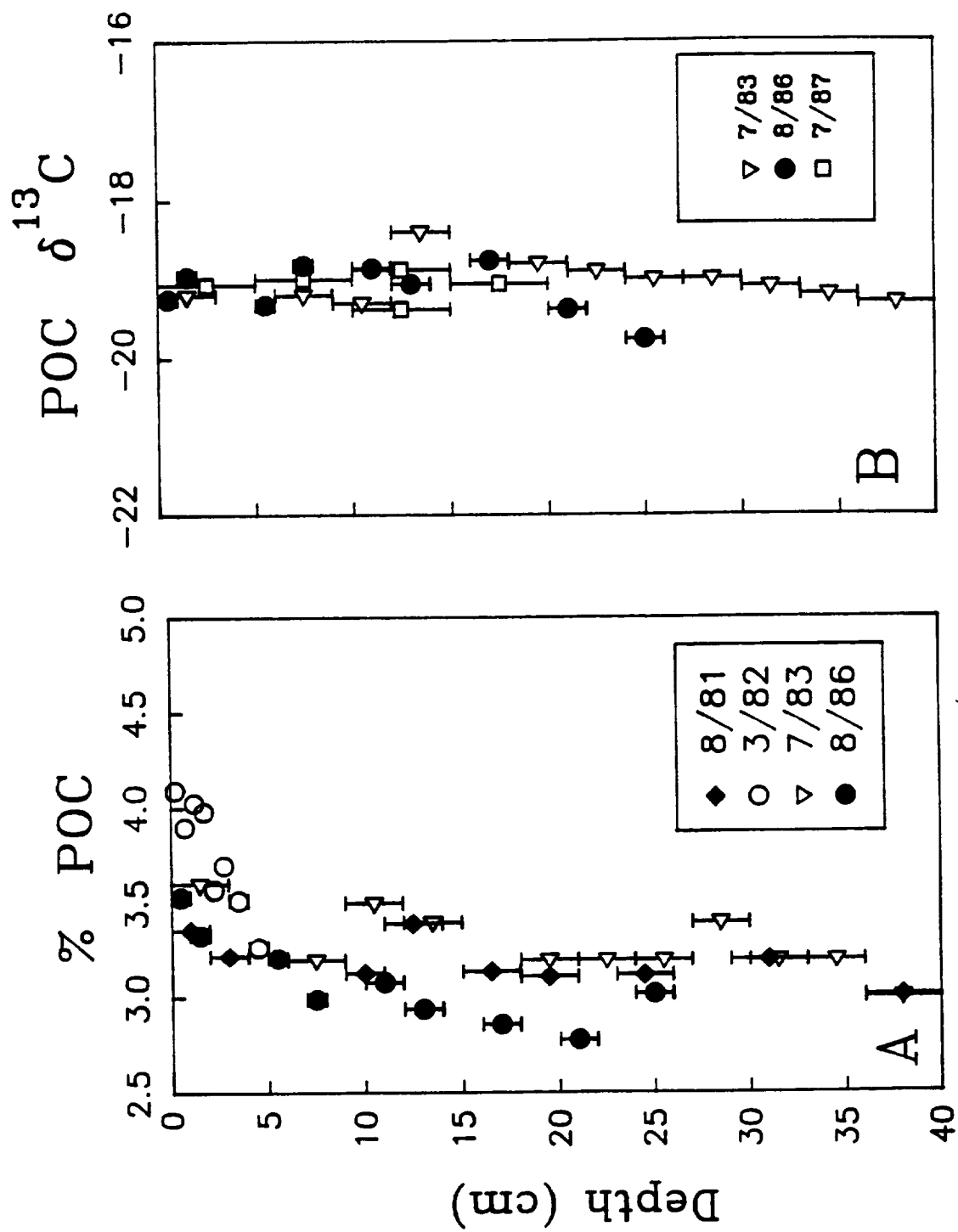
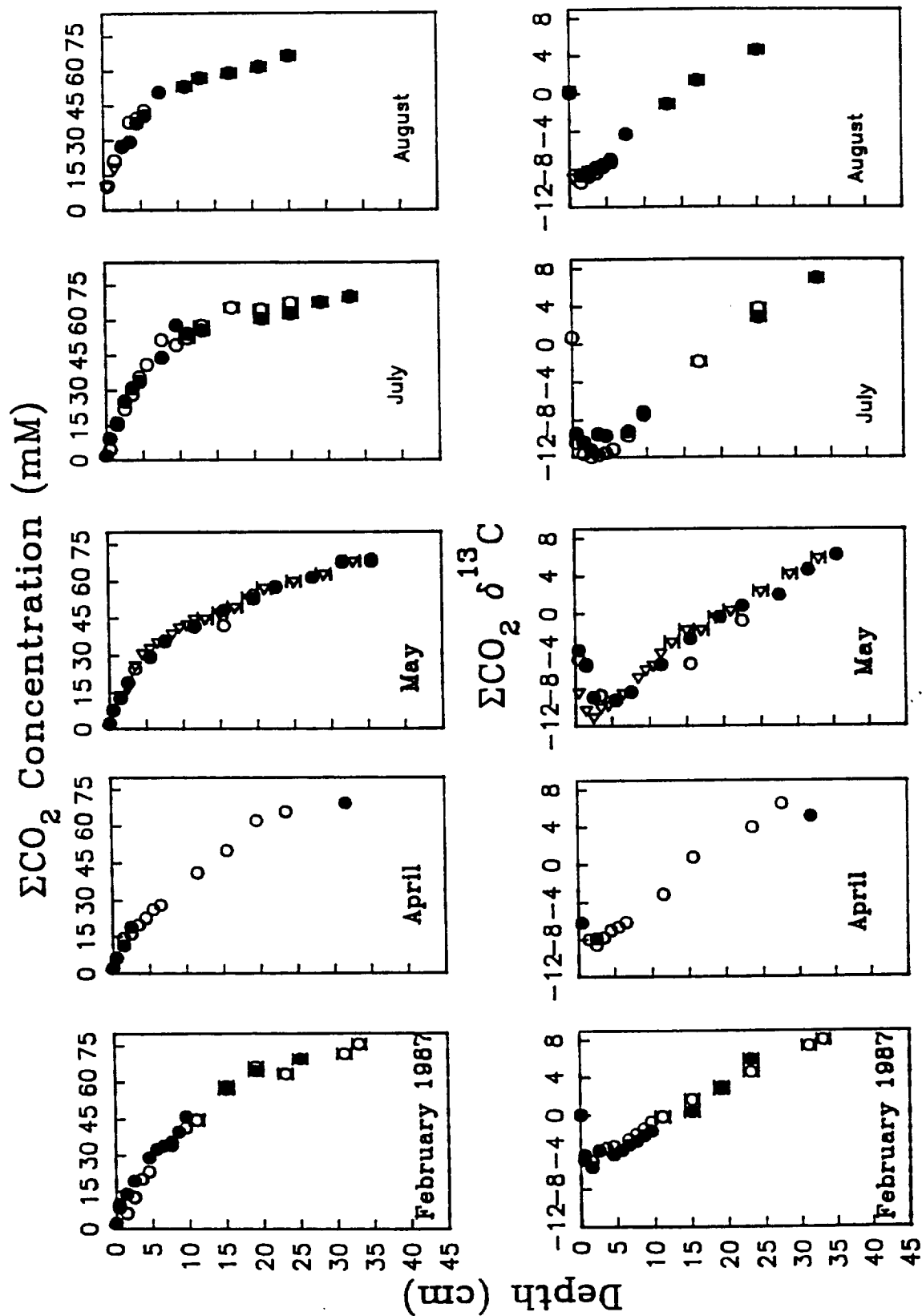


Fig. 2.2 ΣCO_2 concentration and $\delta^{13}\text{C}$ profiles from Cape Lookout Bight. Samples were collected in 1986 except where noted. Individual symbols represent separate cores collected on the same sampling date. The open and filled circles for the May 1986 profiles represent duplicate samples from the same core. Note differences in concentration, depth, and $\delta^{13}\text{C}$ scales for March profiles.



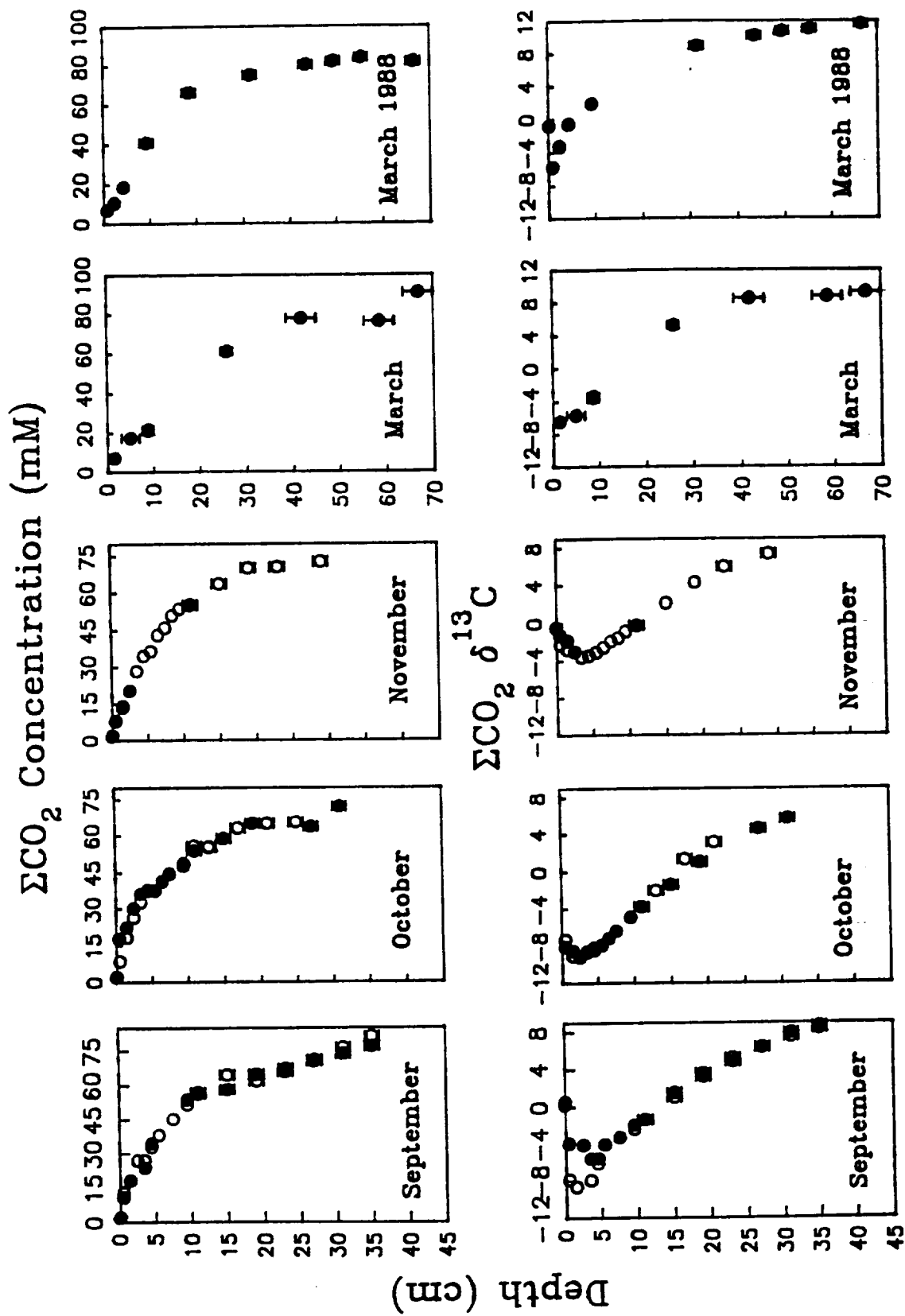
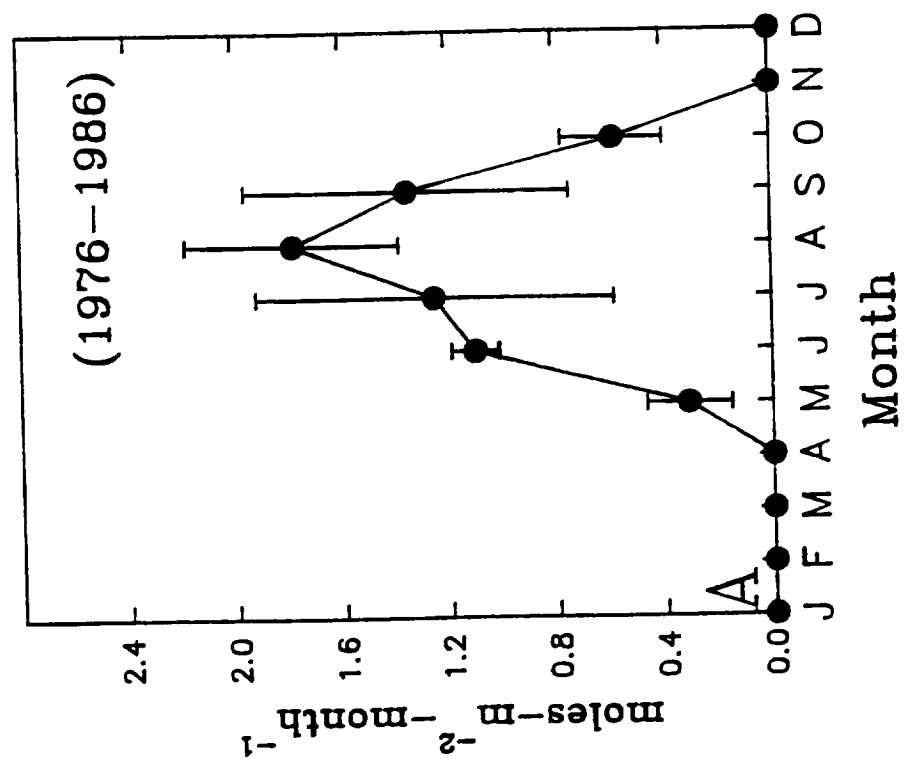


Fig. 2.3 Methane flux and $\delta^{13}\text{C}$ bubble data from Cape Lookout. The ebullitive fluxes from mid October to May are essentially zero. Flux and 1983-1984 $\delta^{13}\text{C}$ bubble data are from Martens et al. (1986). $\delta^{13}\text{C}$ bubble data for 1986 are from this study.

Methane Flux



Methane Bubbles

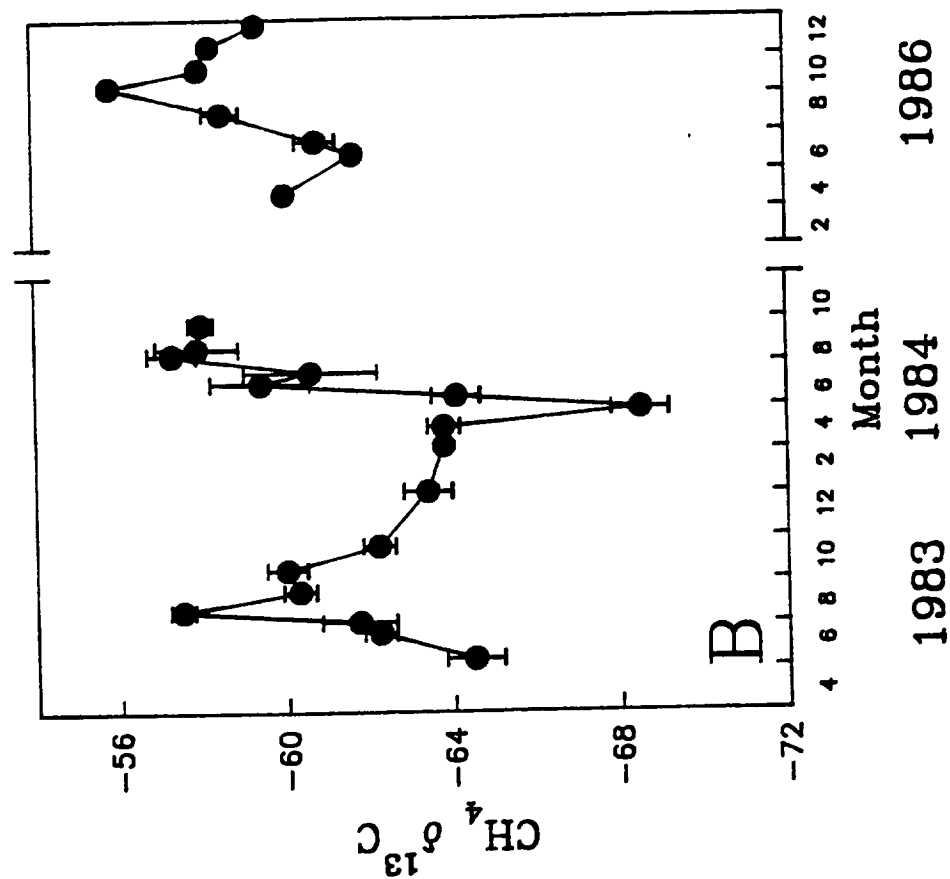


Fig. 2.4 Sedimentary CH₄ $\delta^{13}\text{C}$ profiles from Cape Lookout Bight.

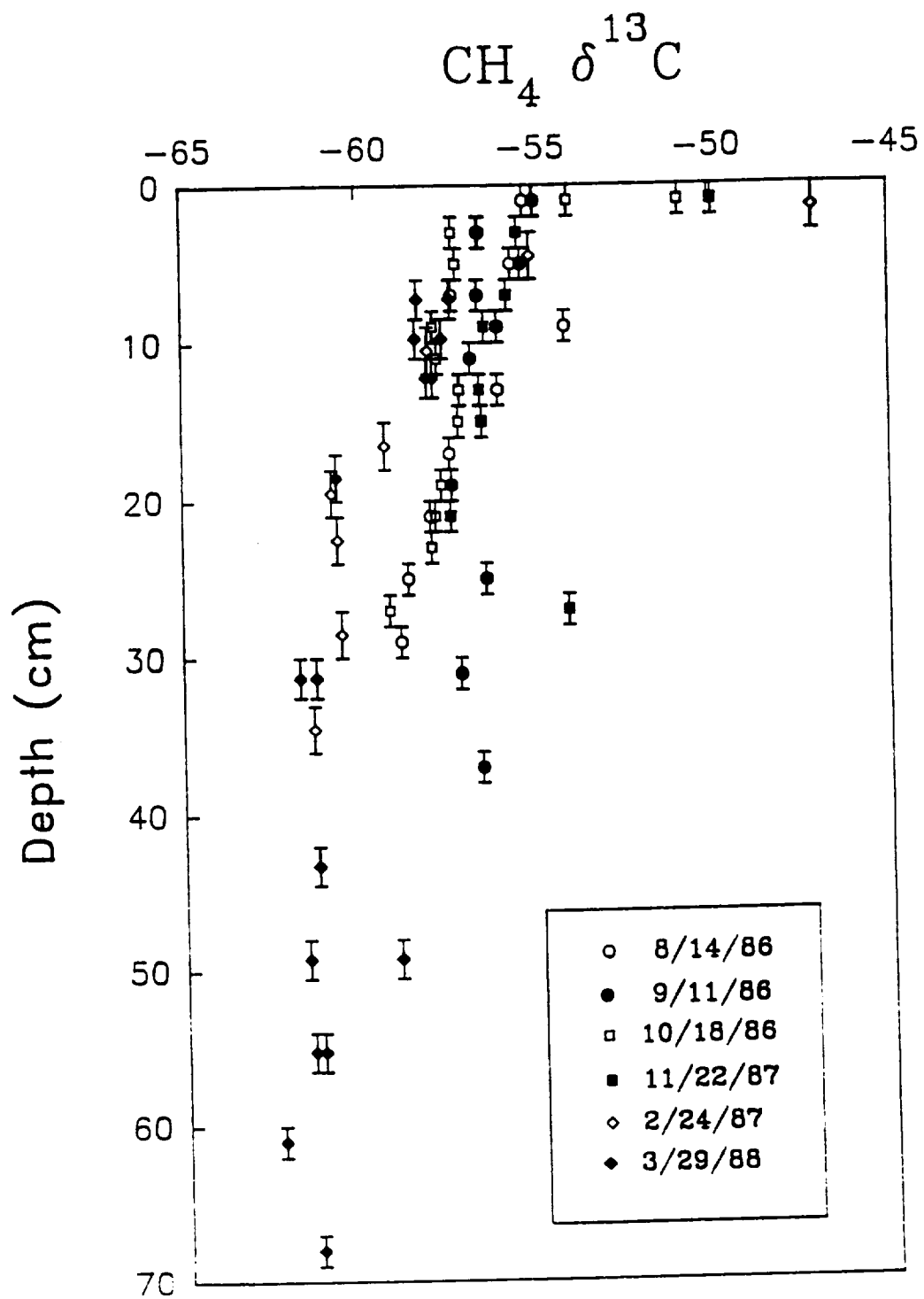


Fig. 2.5 Cape Lookout Bight porewater calcium profiles from 1990-91 (A) and particulate inorganic carbon concentration (PIC) and $\delta^{13}\text{C}$ profiles (B). The dotted line at 5 cm indicates the maximum depth assumed for net dissolution and 5 to 25 cm is considered the zone of precipitation.

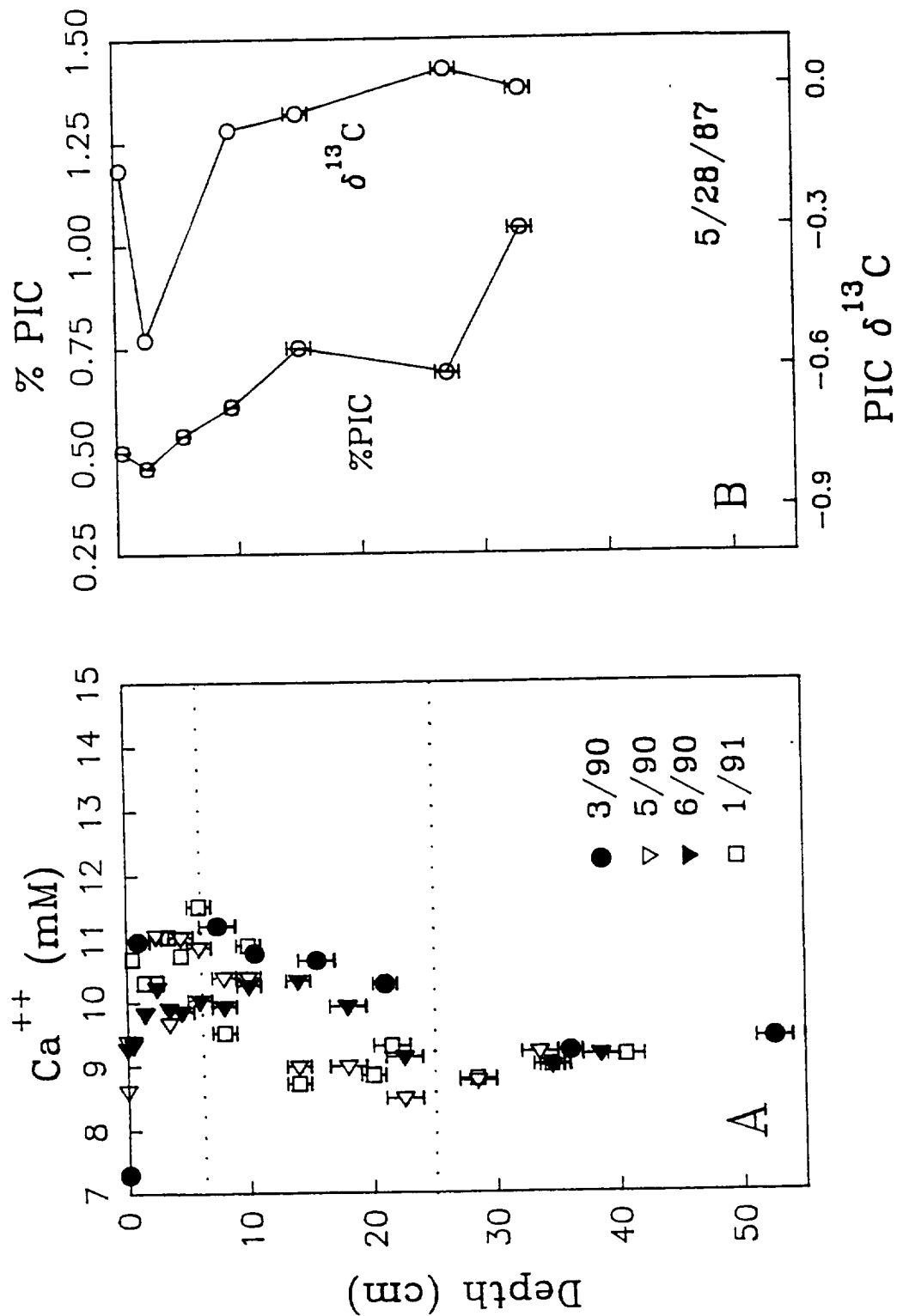


Fig. 2.6 The carbon flow and isotopic composition of the major fluxes at CLB.
The double arrows for methane and CO₂ represent diffusion and bubble ebullition. Carbon fluxes are given in parentheses.

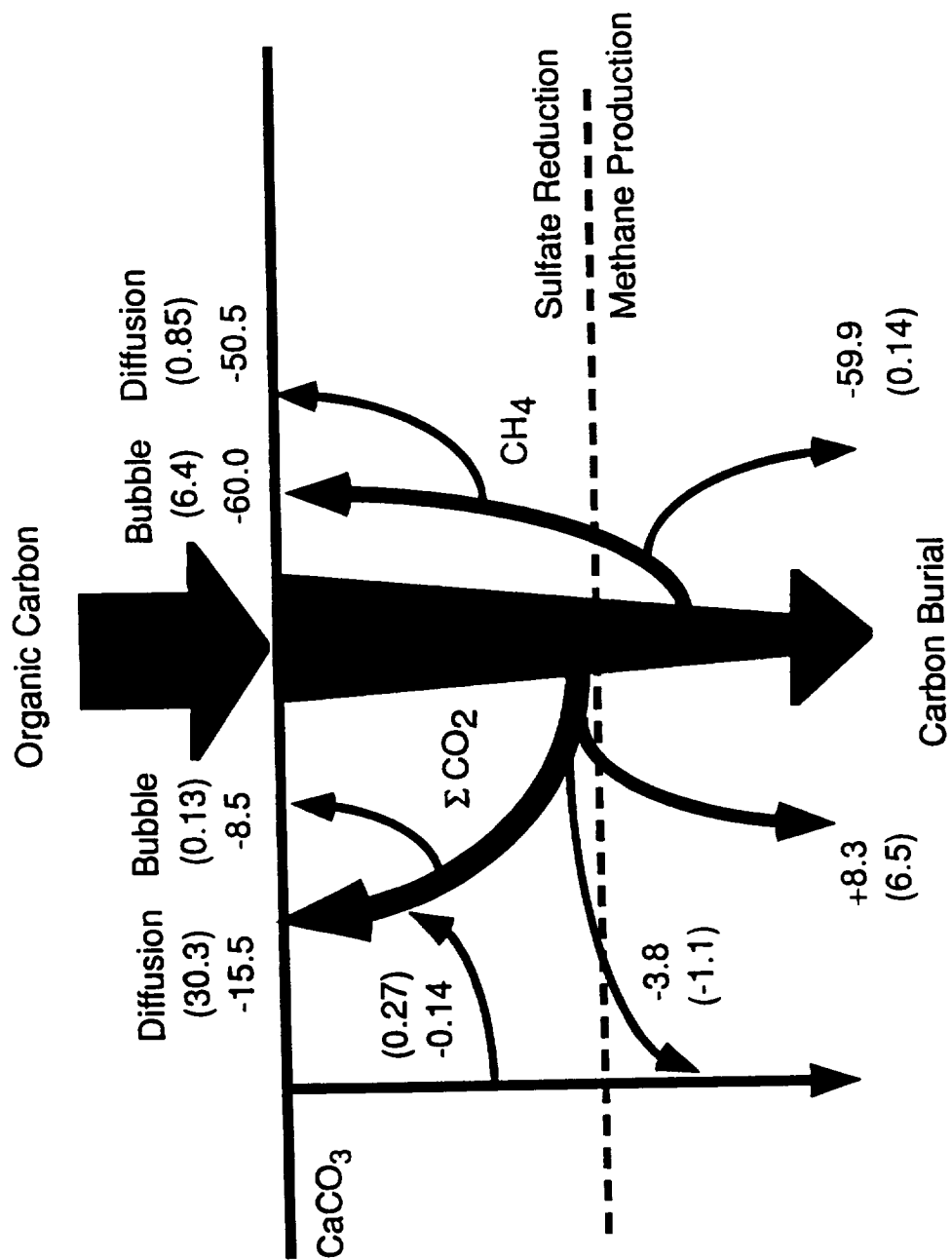


Table 2.1 Fluxes and $\delta^{13}\text{C}$ values of diffusive ΣCO_2 and CH_4

ΣCO_2		Measured		Calculated ¹	
Date	°C	$\text{mmol}\cdot\text{m}^{-2}\cdot\text{hr}^{-1}$	$\delta^{13}\text{C}$	$\text{mmol}\cdot\text{m}^{-2}\cdot\text{hr}^{-1}$	$\delta^{13}\text{C}$
4/28/86	17.0	2.20(0.8)	-16.8(2.7)	2.31 ²	-9.7 ²
2/24/87	9.0	1.57	-15.4	1.36	-8.4
3/28/88	15.5	2.54(0.02)	-14.6(2.7)	2.21(0.2)	-8.2(1.4)

CH_4		Measured		Calculated ¹	
Date	°C	$\text{umol}\cdot\text{m}^{-2}\cdot\text{hr}^{-1}$	$\delta^{13}\text{C}$	$\text{umol}\cdot\text{m}^{-2}\cdot\text{hr}^{-1}$	$\delta^{13}\text{C}$
3/28/88	15.5	29.2(9.1)	-50.5(0.3)	42.8(7.3) ³	-54.0(0.3)

¹Fluxes were calculated using Eqn. 3. Numbers in parentheses are the range of the average of two chambers. Calculated isotopic signatures are determined from isotopic gradients.

²The April 1986 flux experiment was conducted in-situ. The cores were collected beside rather than directly beneath the chamber for the determination of a calculated flux.

³Methane diffusion coefficient taken from Alperin (1988) and corrected for temperature and porosity.

Table 2.2 Concentration and $\delta^{13}\text{C}$ of ΣCO_2 and individual dissolved inorganic species in flux experiments for March 1988.

ΣCO_2			[mM]			$\delta^{13}\text{C}$			Flux*		
Chamber	Depth	pH	[mM]	$\delta^{13}\text{C}$ ΣCO_2	CO_2	HCO_3^-	$\text{CO}_3^{=}$	CO_2	HCO_3^-	$\text{CO}_3^{=}$	$\delta^{13}\text{C}$ BW to 1cm
P	BW	7.76	2.77	-3.10	0.05	2.63	0.09	-11.8	-2.9	-4.8	-6.8
	0-1cm	7.18	7.28	-5.41	0.48	6.73	0.07	-13.7	-4.8	-6.7	(-6.8)**
Q	BW	7.76	2.87	-3.60	0.05	2.73	0.09	-12.3	-3.4	-5.3	-9.6
	0-1cm	7.18	6.64	-7.03	0.44	6.14	0.06	-15.3	-6.4	-8.4	(-9.7)**

*Flux and isotopic signal of each species determined individually then the following equation was used to solve for $\delta^{13}\text{C}$ ΣCO_2 total flux:

$$\delta^{13}\text{C}_{\text{flux}} = \frac{(J_{[\text{CO}_2]} \delta_{[\text{CO}_2]} + J_{[\text{HCO}_3^-]} \delta_{[\text{HCO}_3^-]} + J_{[\text{CO}_3^{=}]})}{J_{[\Sigma\text{CO}_2]}}$$

**Values in parentheses are calculated fluxes based on ΣCO_2 treated as whole species where $(\partial\text{C}/\partial z)$ (Eqn. 3) is based on the ΣCO_2 gradient from bottom water (T_{final}) to 0-1 cm.

Table 2.3 CH₄ Bubble Flux from Martens et al. (1986) and Martens and Chanton (1989).

(moles-m ⁻² -month ⁻¹)							
Month	1976	1977	1978	1985	1986	Average	s.d.
May				0.08	0.54	0.31	0.32
June		0.98		1.23		1.10	0.18
July		0.31		2.21		1.26	1.35
Aug	0.70	1.71	1.57	2.94	2.02	1.79	0.81
Sept	0.46		0.86	2.75		1.36	1.22
Oct	0.71		0.16	0.89		0.59	0.38
Sum (mol-m ⁻² -yr ⁻¹):						6.4	2.1*

*Error was determined as:

$$\sigma = \sqrt{\sum (s.d.)^2}$$

Table 2.4 Carbon isotope mass balance for Cape Lookout, Station A-1.

	moles-m ⁻² -yr ⁻¹	δ ¹³ C
CH₄		
Buried	0.14(0.02)	-59.9(1.9)
Bubble	6.4(2.1)	-60.0(1.2)
Diffusive	0.85(0.8)	-50.5(0.3)
ΣCO₂		
Buried	6.5(0.5)	+8.3(1.5)
Bubble	0.13(0.05)	-8.5(1.4)
Diffusive	30.3(4.8)	-15.5(1.2)
J_{total}	44.3(12.6)	-19.2(2.7)¹
PIC		
Dissolved	0.27(0.4)	-0.14(0.2)
Precipitated	-1.1(0.3)	-3.8(3.8)
J_{remin}²	45.13(12.6)	-18.9(2.7)

¹The estimated δ¹³C of the flux (J_{total}) was determined using the following equation:

$$\delta^{13}C(J_{total}) = \frac{\sum [(\delta J_i) (J_i)]}{\sum (J_i)}$$

where i = the diffusive, ebullitive and burial fluxes of CH₄ and ΣCO₂.

²Calculated using Eqn. 5.

REFERENCES

- ALBERTS J.J., FILIP Z., PRICE M.T., WILLIAMS D.J. and WILLIAMS M.C. (1988) Elemental composition, stable carbon isotope ratios and spectrophotometric properties of humic substances occurring in a salt marsh estuary. *Org. Geochem.* 12, 455-467.
- ALPERIN M.J. (1988) The carbon cycle in an anoxic marine sediment: concentrations, rates, isotope ratios, and diagenetic models. Ph.D dissertation, University of Alaska, Fairbanks.
- BARKER J.F. and FRITZ P. (1981) Carbon isotope fractionation during microbial methane oxidation. *Appl. Environ. Microbiol.* 293, 289-291.
- BARTLETT K.A. (1981) Macroinfauna distribution and seasonal influences on interstitial water chemistry of Cape Lookout Bight, N.C. M.S. Thesis, University of North Carolina at Chapel Hill.
- BENNER R., FOGEL M.L., SPRAGUE E.K. and HODSON R.E. (1987) Depletion of ^{13}C in lignin and its implications for stable isotope studies. *Nature* 329, 708-710.
- BENNER R., FOGEL M.L. and SPRAGUE E.K. (1991) Diagenesis of belowground biomass of *Spartina alterniflora* in salt-marsh sediments. *Limnol. Oceanogr.* 36, 1358-1374.
- BERELSON W.M., HAMMOND D.E. and JOHNSON K.S. (1987) Benthic fluxes and the cycling of biogenic silica and carbon in two southern California borderland basins. *Geochim. Cosmochim. Acta* 51, 1345-1363.
- BERNER R.A. (1980) Early diagenesis. Princeton University Press.
- BLAIR N.E., MARTENS C.S., and DES MARAIS D.J. (1987) Natural abundances of carbon isotopes in acetate from a coastal marine sediment. *Science* 236, 66-68.
- BLAIR N.E. and CARTER W.D. (1992) The carbon isotope biogeochemistry of acetate from a methanogenic marine sediment. *Geochim. Cosmochim. Acta.* 56, 1247-1258.
- BLAIR N.E., BOEHME S.E., and CARTER W.D. (1993) The carbon isotope biogeochemistry of methane production in anoxic sediments 1. field observations. In *The Biogeochemistry of Global Change: Radiative Trace Gases* (ed. R.S. Oremland) Chapman and Hall.

- BROWN F.S., BAEDECKER M.J., NISSENBAUM, A., and KAPLAN, I.R. (1972) Early diagenesis in Saanich Inlet, a reducing fjord, British Columbia. Part III: Changes in organic constituents of sediment. *Geochim. Cosmochim. Acta* 36, 1185-1203.
- CANUEL E.A., MARTENS C.S. and BENNINGER L.K. (1990) Seasonal variations in ^7Be activity in the sediments of Cape Lookout Bight, North Carolina. *Geochim. Cosmochim. Acta* 54, 237-245.
- CHANTON J.P., MARTENS C.S. and GOLDBERGER M.B. (1987) Biogeochemical cycling in an organic-rich coastal marine basin. 7. Sulfur mass balance, oxygen uptake and sulfide retention. *Geochim. Cosmochim. Acta* 51, 1187-1199.
- CHANTON J.P. (1985) Sulfur mass balance and isotopic fractionation in an anoxic marine sediment. Ph.D. Dissertation, University of North Carolina, Chapel Hill.
- CHANTON J.P., MARTENS C.S., and KIPPHUT G.W. (1983) Lead-210 sediment geochronology in an organic-rich coastal marine basin. *Geochim. Cosmochim. Acta* 49, 1791-1804.
- CLAYPOOL G.E. and KAPLAN I.R. (1974) The origin and distribution of methane in marine sediments. In *Natural Gases in Marine Sediments* (ed. I.R. Kaplan) pp. 99-139. Plenum Press.
- COLEMAN D.D., RISATTI J.B. and SCHOELL M. (1981) Fractionation of carbon and hydrogen isotopes by methane oxidizing bacteria. *Geochim. Cosmochim. Acta* 45, 1033-1037.
- CRAIG H., CHOU C.C., WELHAN J.A., STEVENS C.M. and ENGELKEMEIR A. (1988) The isotopic composition of methane in polar ice cores. *Science* 242, 1535-1538.
- CRILL P.M. and MARTENS C.S. (1987) Biogeochemical cycling in an organic-rich coastal marine basin. 6. Temporal and spatial variations in sulfate reduction rates. *Geochim. Cosmochim. Acta* 51, 1175-1186.
- CRONIN J.R. and MORRIS R.J. (1982) The occurrence of high molecular weight humic material in recent organic-rich sediment from the Namibian Shelf. *Est. Coast. Shelf Sci.* 15, 17-27.
- DEAN W.E., ARTHUR M.A. and CLAYPOOL G.E. (1986) Depletion of ^{13}C in cretaceous marine organic matter: source, diagenetic, or environmental signal? *Mar. Geol.* 70, 119-157.

- DEINES P., LANGMUIR D., HARMON R.S. (1974) Stable carbon isotope ratios and the existence of a gas phase in the evolution of carbonate groundwaters. *Geochim. Cosmochim. Acta* 38, 1147-1164.
- FISCHER G. (1989) Stabile kohlenstoff-isotope in partikulärer organischer substanz aus dem südpolarmeer (Atlantischer Sektor) Ph.D. dissertation, Universität Bremen.
- FRIEDMAN I. and O'NEIL J.R. (1977) Compilation of stable isotope fractionation factors of geochemical interest. *U.S. Geological Survey Professional Paper* 440-KK.
- GALIMOV E.M., (1985) *The Biological Fractionation of Isotopes*. Academic Press. 261pp.
- HADDAD R.I. (1989) Sources and reactivity of organic matter accumulating in a rapidly depositing, coastal environment. Ph.D. Dissertation, University of North Carolina, Chapel Hill.
- HADDAD R.I. and MARTENS C. S. (1987) Biogeochemical cycling in an organic-rich coastal marine basin: 9. Sources and accumulation rates of vascular plant-derived organic material. *Geochim. Cosmochim. Acta* 51, 2991-3001.
- HAYES J.M., FREEMAN K.H., POPP B.N., and HOHAM C.H. (1990) Compound-specific isotopic analyses: A novel tool for reconstruction of ancient biogeochemical processes. *Org. Geochem.* 16, 1115-1128.
- HENRICHS S.M. and REEBURGH W.S. (1987) Anaerobic mineralization of marine sediment organic matter: Rates of anaerobic processes in the oceanic carbon economy. *Geomicrob. J.* 5, 191-237.
- HENRICHS S.M. and FARRINGTON J.W. (1984) Peru upwelling region sediments near 15°S. 1. Remineralization and accumulation of organic matter. *Limnol. Oceanogr.* 29, 1-19.
- HERCZEG A.L. (1988) Early diagenesis of organic matter in lake sediments: A stable carbon isotope study of pore waters. *Chem. Geol.* 72, 199-209.
- KING S.L., QUAY P.D. and LANSDOWN J.M. (1989) The $^{13}\text{C}/^{12}\text{C}$ kinetic isotopic effect for soil oxidation of methane at ambient atmospheric concentrations. *J. Geophys. Res.* 94, 18273-18277.

- KLUMP J.V. and MARTENS C.S. (1981) Biogeochemical cycling in an organic-rich coastal marine basin. 2. Nutrient sediment-water exchange processes. *Geochim. Cosmochim. Acta* 45, 101-121.
- LI Y.H. and GREGORY S. (1974) Diffusion of ions in sea water and in deep-sea sediments. *Geochim Cosmochim. Acta*, 38, 703-714.
- LUCOTTE M., HILLAIRES-MARCEL C. and LOUCHOUARN P. (1991) First-order organic carbon budget in the St. Lawrence lower estuary from ^{13}C data. *Est. Coast. Shelf Sci.* 32, 297-312.
- MACKIN J.E. and SWIDER K.T. (1989) Organic matter decomposition pathways and oxygen consumption in coastal marine sediments. *J. Mar. Res.* 47, 681-716.
- MACKO S.A. (1992) The characterization of organic matter in abyssal sediments, pore waters and sediment traps. In *Deep-Sea Food Chains and the Global Carbon Cycle* (eds. T. Rowe and V. Pariente) pp. 325-338. Kluwer Academic Publishers.
- MARTENS C.S. and KLUMP J.V. (1980) Biogeochemical cycling in an organic-rich coastal marine basin - 1. Methane sediment-water exchange processes. *Geochim. Cosmochim. Acta* 44, 471-490.
- MARTENS C.S. and KLUMP J.V. (1984) Biogeochemical cycling in an organic-rich coastal marine basin. 4. An organic carbon budget for sediments dominated by sulfate reduction and methanogenesis. *Geochim. Cosmochim. Acta* 48, 1987-2004.
- MARTENS C.S., BLAIR N.E., GREEN C.D. and DES MARAIS D.J. (1986) Seasonal variations in the stable carbon isotopic signature of biogenic methane in a coastal sediment. *Science* 233, 1300-1303.
- MARTENS C.S. and CHANTON J.P. (1989) Radon as a tracer of biogenic equilibration and transport from methane-saturated sediments *J. Geophys. Res.* 94, 3451-3459.
- MARTENS C.S., HADDAD R.I., and CHANTON, J.P. (1993) Organic matter accumulation, remineralization and burial in an anoxic coastal sediment. In: *Organic Matter: Productivity, Accumulation and Preservation in Recent and Ancient Sediment* (eds. J.K. Whelan and J.W. Farrington) Columbia University Press, NY.
- MATTHEWS D.E. and HAYES J.M. (1978) Isotope-ratio-monitoring gas chromatography-mass spectrometry. *Anal. Chem.* 50, 1465-1473.

- MCARTHUR J.M. (1989) Carbon isotopes in pore water, calcite, and organic carbon from distal turbidites of the Madeira Abyssal Plain. *Geochim. Cosmochim. Acta* 53, 2997-3004.
- MCARTHUR J.M., TYSON R.V., THOMSON J. and MATTEY D. (1992) Early diagenesis of marine organic matter: Alteration of the carbon isotopic composition. *Mar. Geol.* 105, 51-61.
- MCNICHOL A.P. (1986) A study of the remineralization of organic carbon in nearshore sediments using carbon isotopes. Ph.D. Dissertation, WHOI/MIT, WHOI-86-27.
- MCNICHOL A.P., DRUFFEL E.R.M. and LEE C. (1991) Carbon cycling in coastal sediments: 2. An investigation of the sources of ΣCO_2 to pore water using carbon isotopes. In: *Organic Substances and Sediments in Water* (ed. R.A. Baker) Lewis Publishers, Chelsea, MI.
- MECHALAS B.J. (1974) Pathways and environmental requirements for biogenic gas production in the ocean. In *Natural Gases in Marine Sediments* (ed. I.R. Kaplan) pp. 151-177, Plenum Press.
- NISSENBAUM A., BAEDECKER M.J. and KAPLAN I.R. (1972) Studies on dissolved organic matter from interstitial water of a reducing marine fjord. *Adv. in Org. Geochem.* (ed. Braunschweig) Pergammon Press, Oxford, 427-440.
- O'LEARY (1984) Measurement of the isotope fractionation associated with diffusion of carbon dioxide in aqueous solution. *J. Phys. Chem.* 88, 823-825.
- OREM W.H., HATCHER P.G., SPIKER E., SZEVERENYI N.M. and MACIEL G.E. (1986) Dissolved organic matter in anoxic pore waters from Mangrove Lake, Bermuda *Geochim. Cosmochim. Acta* 50, 609-618.
- QUAY P.D., EMERSON S.R., QUAY B.M. and DEVOL A.H. (1986) The carbon cycle for Lake Washington - A stable isotope study. *Limnol. Oceanogr.* 31, 596-611.
- QUAY P.D., TILBROOK B. and WONG C.S. (1992) Oceanic uptake of fossil fuel CO_2 : Carbon-13 evidence. *Science* 256, 74-79.

- QUAY P.D., KING S.L., STUTSMAN J., WILBUR D.O., STEELE L.P., FUNG I., GAMMON R.H., BROWN T.A., FARWELL G.W., GROOTES P.M. and SCHMIDT F.H. (1991) Carbon isotopic composition of atmospheric CH₄: Fossil and biomass burning source strengths. *Global Biogeochem. Cycles* 5, 25-47.
- REEBURGH W. S., (1967) An improved interstitial water sampler. *Limnol. Oceanogr.* 12, 163-165.
- REIMERS C.E. and SUESS E. (1983) Late Quaternary fluctuations in the cycling of organic matter off central Peru: a proto-kerogen record. In *Coastal Upwelling: Its Sedimentary Record* Part A (NATO Conf. Ser.) (eds. E. Suess and J. Thiede) pp. 497-526. Plenum Press.
- REIMERS C.E., JAHNKE R.A. and MCCORKLE D.C. (1992) Carbon fluxes and burial rates over the continental slope and rise off central California with implications for the global carbon cycle. *Global Biogeochem. Cycles* 6, 199-224.
- SAYLES F.L. and CURRY W.B. (1988) $\delta^{13}\text{C}$, TCO₂, and the metabolism of organic carbon in deep sea sediments. *Geochim. Cosmochim. Acta* 52, 2963-2978.
- SILVERMAN M.P. and OYAMA V.I. (1968) Automatic apparatus for sampling and preparing gases for mass spectral analysis in studies of carbon isotope fractionation during methane metabolism. *Anal. Chem.* 40, 1833-1837.
- SPIKER E.C. and HATCHER P.G. (1984) Carbon isotope fractionation of sapropelic organic matter during early diagenesis. *Org. Geochem.* 4, 283-290.
- SPIKER E.C. and HATCHER P.G. (1987) The effects of early diagenesis on the chemical and stable carbon isotopic composition of wood. *Geochim. Cosmochim. Acta* 51, 1385-1391.
- STUMM W. and MORGAN J.J. (1981) *Aquatic Chemistry*. John Wiley and Sons, New York.
- TANS P.P., BERRY J.A. and KEELING R.F. (1993) Oceanic $^{13}\text{C}/^{12}\text{C}$ observations: A new window on ocean CO₂ uptake. *Global Biogeochem. Cycles* 7, 353-368.
- UNVER A.A. and HIMMELBLAU D.M. (1964) Diffusion Coefficients of CO₂, C₂H₄, C₃H₆, and C₄H₈ in Water from 6° to 65°C. *J. Chem. Engineer. Data* 9, 428-431.

- WELLS J.T. (1988) Accumulation of fine-grained sediments in a periodically energetic clastic environment, Cape Lookout Bight, North Carolina. *J. Sed. Pet.* 58, 596-606.
- WHITICAR M.J. and FABER E. (1986) Methane oxidation in sediment and water column environments--Isotope evidence. *Org Geochem.* 10, 759-768.
- WILLIAMS P.M. and GORDON L.I. (1970) Carbon-13:carbon-12 ratios in dissolved and particulate organic matter in the sea. *Deep-Sea Research* 17, 19-27.

The Carbon Isotope Biogeochemistry of ΣCO_2 Production in a
Methanogenic Marine Sediment

ABSTRACT

To investigate the relationship between ΣCO_2 $\delta^{13}\text{C}$ values and rates of the dominant remineralization processes at the organic-rich field site of Cape Lookout Bight, NC, the isotopic composition of porewater ΣCO_2 was measured on a seasonal basis. The ΣCO_2 $\delta^{13}\text{C}$ values varied seasonally in response to changes in rates of sulfate reduction and methanogenesis, the dominant remineralization processes at this site.

A tube incubation experiment was also performed to determine the isotopic signature of the ΣCO_2 produced by sulfate reduction and methanogenesis. The $\delta^{13}\text{C}$ of the ΣCO_2 produced in the sulfate reduction zone determined from the tube incubation was -14.3 ± 1.9 , a value enriched in ^{13}C relative to the labile organic fraction. The ^{13}C -enrichment may be caused by low rates of methanogenesis occurring in the sulfate reduction zone. The $\delta^{13}\text{C}$ of the ΣCO_2 produced in the methanogenic zone was estimated to be +44 per mil, whereas the co-produced methane was -65 per mil. The fractionation factor for CO_2 reduction was calculated to be 1.055, a value in agreement with previous estimates at this site. The measured concentration and $\delta^{13}\text{C}$ of the ΣCO_2 at Cape Lookout was closely reproduced by a diagenetic model using the measured rates of sulfate reduction and ΣCO_2 production, and the isotopic signature of the ΣCO_2 production in the two biogeochemical zones.

INTRODUCTION

The isotopic composition of total dissolved inorganic carbon (ΣCO_2) in sediments is a unique record of diagenetic processes. Presley and Kaplan (1968) used the isotopic signatures of ΣCO_2 to confirm that the downcore increases in ΣCO_2 from nearshore sediments were a result of metabolic activity of organisms in the sediment. Nissenbaum et al. (1972) identified the effects of methane production on the isotopic composition of ΣCO_2 . These studies were followed by numerous applications of isotopic measurements of ΣCO_2 to identify the processes that produce and utilize ΣCO_2 in sediments (e.g. LaZerte, 1981; Reeburgh, 1982; McCorkle et al., 1985; Herczeg, 1988; McCorkle and Emerson, 1988).

Closed system box models were first used to try to reproduce the isotopic signatures that were measured in the field (Nissenbaum et al., 1972; Claypool and Kaplan, 1974; Reeburgh, 1982). Applying open system models to stable isotope studies of both freshwater and marine studies allowed for the inclusion of diffusion, bioturbation and sedimentation effects and yielded more information about the processes affecting these profiles such as carbonate dissolution (McCorkle et al., 1985; Alperin, 1988; McNichol et al., 1991), carbon input rates (McCorkle et al., 1985), and methane oxidation (Whelen et al., 1976; Reeburgh, 1982; Herczeg, 1988; Alperin, 1988). To date, diagenetic models of isotopic profiles have required assumptions about the isotopic composition of the ΣCO_2 produced during sulfate reduction and methanogenesis, as well as the isotopic composition of the remineralized organic carbon.

Typical ΣCO_2 $\delta^{13}\text{C}$ depth profiles from organic-rich marine sediments exhibit two major trends. The ΣCO_2 initially becomes depleted in ^{13}C relative to overlying seawater ΣCO_2 values (typically near zero per mil) and then, at depth, reverses this trend and becomes ^{13}C -enriched. The initial $^{13}\text{C}/^{12}\text{C}$ gradient has been attributed to sulfate reduction which produces ΣCO_2 with an isotopic composition similar to the organic matter that has been remineralized (typically -19 to -24 per mil in marine sediments (Fry and Sherr, 1984). Methanogenesis is thought to cause the gradient reversal by utilizing ^{13}C -depleted ΣCO_2 and leaving behind ^{13}C -enriched ΣCO_2 (Nissenbaum et al., 1972). To observe such profiles in typical coastal or deep sea sediments may require analysis of several to 100's of meters of sediment because of the slow rates of remineralization. The sediments of Cape Lookout Bight, North Carolina (Station A-1; Martens, 1976) were chosen for this study because these trends are fully established in the upper 40 cm of sediment due to the extremely high remineralization rates (Chapter 2; Boehme et al., in revision).

The present study attempts to address some of the assumptions applied to isotopic studies of ΣCO_2 and to identify and quantify the controls on the isotopic composition of ΣCO_2 in a methanogenic sediment. Specifically, this study was undertaken to determine quantitatively the processes controlling the isotopic composition of ΣCO_2 in a methane producing marine sediment overlain by a typical sulfate reduction zone. By coupling field and laboratory studies, the parameters that had to be assumed in earlier models could be directly measured in order to estimate the relative importance of the dominant processes controlling the $\delta^{13}\text{C}$ composition of

the ΣCO_2 . Field measurements of ΣCO_2 $\delta^{13}\text{C}$ sedimentary profiles indicated a relationship between rates of the dominant processes and the resultant ΣCO_2 $\delta^{13}\text{C}$ profiles. Sediment incubations were used to determine rates of ΣCO_2 production and sulfate reduction as well as the $\delta^{13}\text{C}$ of ΣCO_2 produced. From these measurements it was possible to test the hypothesis that the ΣCO_2 $\delta^{13}\text{C}$ porewater profiles from anoxic sediments resulted from a balance of ΣCO_2 produced by sulfate reduction and that produced by methanogenesis.

Field Site

Cape Lookout Bight, North Carolina is a partially enclosed marine basin located 110 km southwest of Cape Hatteras. Samples were collected at Station A-1, which has been actively studied for almost 20 years (Martens, 1976; Chanton et al., 1983; Martens and Klump, 1984; and references therein). The dominant remineralization processes within the sediment are sulfate reduction and methanogenesis (Crill and Martens, 1983; 1986; Martens and Klump, 1984). Accumulation rates of 8-12 cm per year for the upper 40 cm of the sediment have been measured at Station A-1 (Chanton et al, 1983; Canuel et al., 1990). Seasonal temperature variations of 20°C drive changes in remineralization rates and fluxes of the diagenetic products. Despite this seasonality, near-steady state conditions occur on yearly time scales. Good agreement between measured and modelled nutrient profiles suggest near steady state conditions may occur on shorter time scales as well (Klump and Martens, 1981; Martens and Klump, 1984; Haddad and Martens, 1990; Chapter 2, Boehme et al., in revision; this study).

METHODS

The collection and analysis of field samples for monthly profiles of ΣCO_2 from Station A-1 have been described previously (Chapter 2; Boehme et al., in revision). A 9.5 cm diameter sediment core was collected at A-1 in June 1991 and sectioned in the lab at 2 cm intervals down to 20 cm to conduct an incubation experiment. Sediment temperature was 25°C, in the field at the time of core collection. Sediments from each depth interval were homogenized and transferred into five 15 ml centrifuge tubes via syringes. The centrifuge tubes from each of the 10 depth intervals were capped and stored in a glove bag and kept under nitrogen at 25°C for the duration of the incubation experiment.

One sample from each of the ten depth intervals was processed immediately ($T=0$) and then every 40 to 75 hours by centrifugation (3500 rpm for 30 minutes). The extracted porewater was taken up in a syringe, and filtered through a 0.45 μm nylon filter (Micron Separations Inc.). One ml of porewater was injected into a 2.5 ml serum bottle, capped and crimped for analysis of the concentration and $\delta^{13}\text{C}$ of the ΣCO_2 . The ΣCO_2 samples were maintained frozen until the end of the experiment so that the five samples from each depth could be analyzed on the same day. One to 3 ml of porewater was acidified and stored for Ca^{++} analyses. The remaining porewater was treated with a drop of concentrated ZnCl_2 to precipitate sulfide, filtered, and stored refrigerated for sulfate analysis.

Porewater ΣCO_2 samples were analyzed on a GC-TCD adapted with a vacuum line to collect the CO_2 gas for isotopic analysis (Blair and Carter, 1992; Schaff et al.,

1993). The ΣCO_2 serum bottles were injected with 0.2 ml of 1M H_3PO_4 and the resulting CO_2 was swept into the GC column containing Unibeads-1s or 2s silica gel (Alltech) with He as the carrier gas. Water was removed using a Nafion drying tube (Permapure Products). Sample concentrations were determined with a thermal conductivity detector. The CO_2 was trapped in an 1/8 inch o.d. stainless steel trap under liquid nitrogen, and transferred to 6 mm borosilicate glass tubing for storage. Isotopic analyses were done on a modified Finnigan Mat Delta E isotope ratio mass spectrometer (Hayes, 1983). All isotope values are given in the $\delta^{13}\text{C}$ notation (See Eqn. 1). The precision and accuracy of the ΣCO_2 concentration measurements determined from standards is 0.5 mM and 1.0 mM respectively, and for ΣCO_2 $\delta^{13}\text{C}$ measurements, 0.3 per mil and 0.6 per mil respectively.

Porewater $\text{SO}_4^{=}$ samples were processed by gravimetric analysis of the precipitated barium salt (Chanton, 1985; Chanton et al, 1987). The precision and accuracy of this technique was 0.6 mM and 1.0 mM, respectively.

Porewater Ca^{++} samples were treated as described in Chapter 2. The Ca^{++} measurements were analyzed on a Perkin-Elmer Atomic Absorption spectrometer in the Soil Science Laboratory (NCSU).

RESULTS

The concentration of ΣCO_2 increased and that of sulfate decreased as a function of time in the upper 10 cm during the incubation experiment, with the most rapid changes occurring in the upper 0-2 cm interval (Fig. 3.1). ΣCO_2 $\delta^{13}\text{C}$ became progressively depleted in ^{13}C with time for the 0-8 cm intervals, whereas the 8-10 cm

interval became enriched in ^{13}C with time (Fig. 3.1). The rates of ΣCO_2 production and sulfate reduction were determined by linear fits to the concentration data for each of the upper 0-10 cm intervals (r^2 values are given in Table 3.1). The $\text{SO}_4^{=}$ and ΣCO_2 concentrations, and the ΣCO_2 $\delta^{13}\text{C}$ values showed little change with time in the samples below 10 cm due to slow rates of remineralization and the relatively short 10-day incubation and therefore are not shown. The Ca^{++} concentrations show little change below the 0-2 cm interval (Fig. 3.5) for the upper 10 cm. The Ca^{++} T=0 profile did not agree well with the porewater collected by squeezer on the same day (Chapter 2; Fig. 2.5). The poor agreement between the squeezer and centrifuged profiles may indicate that one of these techniques causes changes in the porewater concentrations, and therefore this data set was only used to show that there were not large changes in porewater Ca^{++} over the 10 day experiment.

Using the ΣCO_2 concentration and $\delta^{13}\text{C}$ values, ^{12}C and ^{13}C production rates were determined. Rate measurements of ΣCO_2 production, and $\text{SO}_4^{=}$ reduction for the upper 10 cm (Fig. 3.2a) as well as $\Sigma^{13}\text{CO}_2$ and $\Sigma^{12}\text{CO}_2$ production rates calculated using the isotopic signatures of the ΣCO_2 produced (Fig. 3.2b) were fit to an exponential curve of the form:

$$R_z = R_0 \exp(-az) \quad (10)$$

where

R_z = rate of production or reduction of process (mM/hr),
 R_0 = rate at the sediment-water interface (mM/hr),
 a = attenuation coefficient (cm^{-1}), and
 z = depth into sediment (cm).

Values of R_0 and a were solved iteratively from measured values of R_z with the Sigmaplot curve fitting routine (Jandel Scientific). Curve fitting parameters are given in Table 3.2. The ΣCO_2 concentration and $\delta^{13}\text{C}$ values were used to estimate the $\delta^{13}\text{C}$ signal of the ΣCO_2 produced for each depth interval using the following equation:

$$\delta_{\text{add}} = \frac{C_t \delta_t - C_o \delta_o}{C_{\text{add}}} \quad (11)$$

where

$$\begin{aligned} C_t &= \Sigma\text{CO}_2 \text{ concentration at given time} \\ \delta_t &= \delta^{13}\text{C of } \Sigma\text{CO}_2 \text{ at given time} \\ C_o &= \Sigma\text{CO}_2 \text{ concentration at initial time zero for given depth} \\ \delta_o &= \delta^{13}\text{C of } \Sigma\text{CO}_2 \text{ at initial time zero for given depth} \\ C_{\text{add}} &= \Sigma\text{CO}_2 \text{ concentration added between } C_o \text{ and } C_t \\ \delta_{\text{add}} &= \delta^{13}\text{C of } \Sigma\text{CO}_2 \text{ added between } C_o \text{ and } C_t. \end{aligned}$$

The δ_{add} was solved for by curvefitting the ΣCO_2 concentration and ΣCO_2 $\delta^{13}\text{C}$ for each depth interval and the horizontal error bars represent the standard error for each of the values (Fig. 3.2).

The advection-diffusion model (Berner, 1980) was used to convert the measured rates of sulfate reduction, ΣCO_2 production, $\Sigma^{12}\text{CO}_2$ production and $\Sigma^{13}\text{CO}_2$ production to test whether these rates are representative of in situ conditions. An analytical solution of the advection-diffusion equation

$$\frac{\partial C}{\partial t} = D_s \frac{\partial^2 C}{\partial z^2} - \omega \frac{\partial C}{\partial z} - R \quad (12)$$

was found assuming $\partial C / \partial t = 0$ and the following boundary conditions: as $C_z \rightarrow \infty$, $\partial C / \partial z = 0$; for ΣCO_2 , $C_0 = 2.11 \text{ mM}$, $\delta^{13}\text{C} = 0.0 \text{ per mil}$; for sulfate, $C_0 = 29.6$.

Eqn. 12 becomes

$$C_z = C_0 + \frac{R_0}{a^2 D_s + a \omega} (1 - \exp^{-az}), \quad (13)$$

where

D_s	=	Diffusion coefficient ($D_s = \phi^2 D_0$; $\phi = 0.9$ for upper 20 cm; Chanton et al., 1983; $D_s(\text{HCO}_3^-) = 0.0344$ cm/hr; $D_s(\text{SO}_4^{=}) = 0.0312$ cm/hr),
C_z	=	Concentration of species at given depth z
a	=	attenuation coefficient (cm^{-1})
ω	=	sedimentation rate (10.6 cm/yr; Chanton et al., 1983).

Diffusion coefficients for HCO_3^- and $\text{SO}_4^{=}$ were taken from Li and Gregory (1974) and corrected for sediment tortuosity as noted above (Ullman and Aller, 1982). The effects of changing porosity with depth have been shown to alter the results by less than 4% for Cape Lookout sediments and so porosity was assumed to be constant with depth (Klump and Martens, 1989). The comparison of measured and calculated concentrations and the ΣCO_2 $\delta^{13}\text{C}$ profiles are shown in Fig. 3.3. The steady state assumption appears to be justified given the agreement between measured and estimated ΣCO_2 profiles determined from the rate measurements (Klump and Martens, 1981; 1989; this study). The estimated ΣCO_2 $\delta^{13}\text{C}$ profile shown in Fig. 3.3b, agrees with the measured values for the upper 0-12 cm. The two profiles diverge below this depth, because the lower boundary condition forces $\partial C / \partial z$ to 0 at depth. The modelled and measured $\text{SO}_4^{=}$ concentration also agree well, verifying the sulfate reduction rate measurements.

The depth-integrated rates of ΣCO_2 production and sulfate reduction as well as $\Sigma^{12}\text{CO}_2$ and $\Sigma^{13}\text{CO}_2$ were determined by integrating Eqn. 11 and multiplying by a

porosity term ($\phi = 0.9 \text{ cm}^3_{\text{pw}}/\text{cm}^3_{\text{sed}}$) (Eqn. 12), to compare to previous depth integrated rate measurements:

$$\Sigma R_z = \int_0^{10\text{cm}} R_0 \exp^{-az}. \quad (14)$$

The calculated depth integrated rate of sulfate reduction of $21.3 \text{ moles-m}^{-2}\text{-yr}^{-1}$ is in excellent agreement with a previously measured incubation experiment sulfate reduction rate of $21.0 \text{ moles-m}^{-2}\text{-yr}^{-1}$ (Klump and Martens 1989) and comparable to previously measured rates of sulfate reduction for June 1978 of $19.3 \pm 3.4 \text{ moles-m}^{-2}\text{-yr}^{-1}$ and June 1979 of $24.3 \pm 3.0 \text{ moles-m}^{-2}\text{-yr}^{-1}$ (Martens and Klump, 1984). The depth integrated ΣCO_2 production of $34.6 \text{ moles-m}^{-2}\text{-yr}^{-1}$ also agrees well with a previous incubation experiment rate of $34.0 \text{ moles-m}^{-2}\text{-yr}^{-1}$ (Klump and Martens 1989) and is comparable to ΣCO_2 fluxes of $38.9 \pm 0.8 \text{ moles-m}^{-2}\text{-yr}^{-1}$ measured in June 1978 (Martens and Klump, 1984).

DISCUSSION

The ΣCO_2 $\delta^{13}\text{C}$ profiles measured at Cape Lookout are typical of anoxic marine sediments, with a zone of ^{13}C -depletion overlying a zone of ^{13}C enriched ΣCO_2 . These profiles are thought to result from sulfate reduction producing ΣCO_2 that is isotopically similar to the organic matter being oxidized in the upper zone and methanogenesis generating ^{13}C -enriched ΣCO_2 at depth. Additionally, ^{13}C -depletions have been attributed to methane oxidation adding ^{13}C -depleted ΣCO_2 in the sulfate reduction zone, particularly near the transition between the sulfate reduction and methane production zones (Reeburgh, 1982; Whiticar and Faber, 1986). In studies

where methane oxidation has been shown to be important, the resultant ΣCO_2 may be distinguishable by the ^{13}C -depleted nature and the concave-up sedimentary methane concentration profiles. At Cape Lookout, methane oxidation is not an obvious control on the ΣCO_2 $\delta^{13}\text{C}$ values, and appears to affect only the surficial sediments based on flux experiments and sedimentary CH_4 $\delta^{13}\text{C}$ profiles (See Chapter 2, Fig. 2.4; Boehme et al., in revision). The agreement between methane production rates and observed fluxes (Crill and Martens, 1986) is further evidence against significant methane oxidation at this site.

The ΣCO_2 $\delta^{13}\text{C}$ profiles from Cape Lookout also exhibit seasonal changes (Chapter 2; Boehme et al., in revision). If sulfate reduction and methanogenesis are controlling the isotopic signature of the ΣCO_2 , then the seasonal trends seen in the isotope profiles should correlate to the changing rates of these processes. This can be tested directly using the measured monthly profiles of ΣCO_2 $\delta^{13}\text{C}$.

Further, if these processes are occurring in distinct zones, namely sulfate reducing bacteria out-competing the methanogenic consortia down to the depth at which sulfate is depleted, then the isotopic signal of ΣCO_2 being produced should reflect this zonation and should be expressed in the incubation experimental results. The measured isotopic signature for the ΣCO_2 produced in the sediment generally reflects this zonation (Fig. 3.2b).

The use of exponential fits to the $\Sigma^{12}\text{CO}_2$ and the $\Sigma^{13}\text{CO}_2$ rate measurements results in an estimated $\delta^{13}\text{C}$ produced that does not reflect the observed zonation in $\Sigma^{12}\text{CO}_2$ and $\Sigma^{13}\text{CO}_2$ production (Fig 3.2b). This is not surprising considering that the

$\Sigma^{12}\text{CO}_2$ and $\Sigma^{13}\text{CO}_2$ rate data may not be described by a simple exponential function because these rates result from the addition of two separate processes, sulfate reduction and methanogenesis, with different rates. The exponential fits, despite these problems reproduced the concentration and estimated isotope signatures of the ΣCO_2 measured in the sediment (Fig. 3.3; see discussion below). A comparison of exponential fits to cubic spline fits resulted in little differences in the estimated ΣCO_2 $\delta^{13}\text{C}$ profiles. The curve fits were used to determine depth integrated rates for modelling of individual processes. The depth integrated rates determined are consistent with previously measured rates for this site.

Field Studies

Seasonal changes in the ΣCO_2 $\delta^{13}\text{C}$ profiles from Cape Lookout (Chapter 2, Fig. 2.2; Boehme et al., in revision) appear to result from the changing rates of sulfate reduction and methanogenesis, the changing depths of sulfate depletion and possibly by changes in methanogenic pathways. This relationship can be seen qualitatively in the steepening concentration gradients and changing porewater ΣCO_2 isotope profiles in Fig. 2.2. In an attempt to quantify this relationship, sulfate concentration gradients and the isotopic gradient for the upper 3 cm of the sediment are compared in Fig. 3.4. Increasing rates generally correlate with increasingly ^{13}C -depleted gradients, however, this comparison does not include the effects of methanogenesis on the isotope profiles. Methane production is altering the isotopic signature of the ΣCO_2 flux. Further, for most of the year methane is produced predominantly via CO_2 reduction, however in July and August, some fraction of the

methane appears to be produced by acetate dissimilation (Crill and Martens, 1986; Blair et al., 1993). The smaller fractionation factor associated with acetate dissimilation may further alter the relationship between the sulfate concentration gradient and isotopic gradient for the months when acetate dissimilation is important.

The comparison shown in Fig. 3.4 suggests a simple correlation, that ΣCO_2 $\delta^{13}\text{C}$ values at the sediment surface are dependent on the concentration gradients of sulfate reduction. This may be a useful observation for understanding the range of isotopic signatures that are measured in other field sites, especially environments where methane production is not important. The data imply that if the isotopic signature of the two dominant processes controlling ΣCO_2 concentration in Cape Lookout sediments can be determined, then the overall ΣCO_2 isotopic signature should be predictable based on the changing rates of these two processes.

Incubation Experiment

The incubation experiment was performed to measure directly the isotopic signature of the ΣCO_2 being produced as a function of depth. Variation with depth in the isotopic composition of the ΣCO_2 produced for the upper 10 cm are shown in Fig. 3.2b. For the upper 8 cm, the isotopic signature is relatively constant. The 8-10 cm interval is markedly ^{13}C -enriched with an isotopic signature of $+2 \pm 1.9$ per mil. The two distinct zones are consistent with biogeochemical arguments that have theorized little overlap between the sulfate reduction and methanogenic zones. The isotopic signature of the ΣCO_2 in the upper 8 cm is enriched in ^{13}C relative to the metabolizable organic carbon being at Cape Lookout (-19 per mil; Chapter 2; Boehme

et al., in revision). This may indicate some methane production in the sulfate reduction zone. This hypothesis is consistent with previous measurements of methane production in the sulfate reduction zone (Crill and Martens, 1986). There are other possible causes for this enrichment of the ΣCO_2 that can be considered.

One source of ^{13}C enriched ΣCO_2 to porewaters is the dissolution of calcium carbonate. Porewater concentrations of Ca^{++} were measured during the incubation experiment and suggest some dissolution in the upper 0-4 cm (Fig. 3.5). The previous Ca^{++} measurements for this site also show an increase in the upper two cm indicating dissolution (Chapter 2, Fig. 2.5; Boehme et al., in revision). The increases, however, are not large enough to account for an offset of -5 per mil (-19 per mil organic carbon to the -14 per mil average isotope value for the upper 8 cm) assuming an isotopic composition of the CaCO_3 of -0.1 per mil (the average isotopic composition of the particulate inorganic carbon at Cape Lookout). Further, the Ca^{++} profiles measured during the incubation experiment do not indicate dissolution below the 0-2 cm interval over the 10 day incubation experiment (Fig. 3.5). Thus, the isotopic composition of the ΣCO_2 produced should therefore not be significantly affected by calcium carbonate dissolution. This conclusion could be erroneous if dissolution was coupled with precipitation in an exchange reaction. Exchange reactions have been hypothesized to account for differences in modelled and measured ΣCO_2 $\delta^{13}\text{C}$ profiles from turbidites (McArthur, 1989) but have typically been ignored because they are considered to be too slow to significantly alter the isotopic composition of rapidly depositing sediments (Nissenbaum et al., 1972). The isotopic

composition of the particulate inorganic carbon is relatively constant with depth (Boehme et al., in revision; Boehme, 1989), however, the possibility of isotopic exchange reactions during dissolution and precipitation of CaCO_3 has not been adequately addressed.

Another possible cause of the relatively ^{13}C -enriched ΣCO_2 in the sulfate reduction zone is the preferential remineralization of a ^{13}C -enriched organic carbon fraction during sulfate reduction. A long-term incubation study using sediments from Cape Lookout estimated the $\delta^{13}\text{C}$ of the organic matter remineralized during sulfate reduction to be -15.6 per mil (Alperin et al., 1992). If the sulfate reducing bacteria do not significantly fractionate the organic matter during remineralization, then the ΣCO_2 should be similar to the remineralized organic carbon. Preferential remineralization is not consistent with the particulate organic carbon (POC) $\delta^{13}\text{C}$ profiles for this site that indicate that the δ value of the organic carbon does not change with depth (Haddad, 1989; Blair and Carter, 1992; Chapter 2; Boehme et al., in revision). If sulfate reduction, the dominant remineralization process in these sediments, is preferentially removing organic carbon with a different isotopic signature than the bulk organic carbon, then this should cause be evident in the POC $\delta^{13}\text{C}$ profiles.

If methane production is occurring within the sulfate reduction zone, ^{13}C -enriched ΣCO_2 would be added to the pool of ΣCO_2 produced by sulfate reduction. This is consistent with incubation measurements of methanogenic rates measured by Crill and Martens (1983; 1986) in which low rates of methanogenesis via CO_2

reduction were measured within the sulfate reduction zone using incubation experiments and ^{14}C tracers, especially in the summer months when sulfate is rapidly depleted by 8 to 10 cm. As will be shown later, these rates of sulfate reduction and methanogenesis can be used in conjunction with an estimate of the isotopic signature of the ΣCO_2 produced from these processes to estimate a ΣCO_2 $\delta^{13}\text{C}$ value produced in the sulfate reduction zone. Studies have shown that methane production via non-competitive substrates such as methanol and methylamines can also result in methane production (and presumably ΣCO_2 production as well) in salt marsh sediments (King, 1984; King et al., 1985; Oremland et al., 1982; 1993).

The successful use of the rate measurements to estimate ΣCO_2 concentration and $\delta^{13}\text{C}$ profiles indicates that a simple two component mixing model can be used to estimate the isotopic signature of the ΣCO_2 produced from an anoxic sediment like Cape Lookout. The mixing model assumes that the isotopic signature of the ΣCO_2 results from the mixing of two sources--oxidative source (sulfate reduction) and methanogenic. This hypothesis can be described mathematically as a mass balance of the processes producing ΣCO_2 in the sediment,

$$R_{\text{tot}}\delta_{\text{tot}} = R(\Sigma\text{CO}_2)_{\text{SR}}\delta_{\text{SR}} + R(\Sigma\text{CO}_2)_{\text{M}}\delta_{\text{M}} \quad (15)$$

where:

R_{tot}	= ΣCO_2 total production rate (mM/hr),
δ_{tot}	= isotopic signature of ΣCO_2 produced,
$R(\Sigma\text{CO}_2)_{\text{SR}}$	= ΣCO_2 production from sulfate reduction rate (mM/hr),
δ_{SR}	= isotopic signature of ΣCO_2 from SR
$R(\Sigma\text{CO}_2)_{\text{M}}$	= ΣCO_2 production from methanogenesis rate (mM/hr),
δ_{M}	= isotopic signature of ΣCO_2 from methanogenesis.

The sources of the ^{13}C -enriched ΣCO_2 produced in the sulfate reduction zone cannot be resolved by this study, but the measurement of this isotope signature allows us to model the processes producing these signals in an effort to test some of the hypotheses given here.

The ΣCO_2 produced and its isotopic signature were used to determine the ^{12}C and ^{13}C production rate profiles individually. These profiles were curve fit and extrapolated to estimate the isotopic signature of the ΣCO_2 added to the surface sediments due to sulfate reduction, -19.2 per mil. This value is assumed to be the best guess value for the isotopic composition of the ΣCO_2 produced from sulfate reduction alone (δ_{SR}) because the surface sediments should be the least affected by methanogenesis.

The sulfate reduction rate, R_{SR} , can be used to determine the depth integrated rate of ΣCO_2 produced from sulfate reduction,

$$R(\Sigma\text{CO}_2)_{\text{SR}} = R_{\text{SR}}\tau, \quad (16)$$

where $\tau = 1.78$, the ratio of ΣCO_2 produced to sulfate reduced at the sediment-water interface. The stoichiometric coefficient, τ , is assumed to be constant downcore. This assumption is supported by degradation studies of algae where the calculated composition of the refractory material (calculated as percent proteins, lipids and carbohydrates) was similar to the original composition of the algae (Foree and McCarty 1970) suggesting that no one algal component was preferentially utilized producing a different ratio of ΣCO_2 produced to algae degraded. Previous estimates

of τ for Cape Lookout surface sediments, of 1.7 ± 0.1 (Alperin et al, 1992) and 1.9 (average of upper 6 cm; Klump and Martens, 1989) supports the τ value used in this study. Factors controlling τ are discussed in further detail in a later section.

The net production of ΣCO_2 during methanogenesis, R_M is calculated by subtracting $R(\Sigma\text{CO}_2)_{\text{SR}}$ from R_{tot} . The depth integrated δ value of ΣCO_2 produced, δ_{tot} was estimated from the isotopic signature of the depth integrated $\Sigma^{12}\text{CO}_2$ and $\Sigma^{13}\text{CO}_2$ production rates, -13.1 per mil. Solving Eqn. 15 for δ_M gives +44.2 per mil for the isotopic composition of the ΣCO_2 produced during methanogenesis. Using the values for ΣCO_2 production from sulfate reduction (-19.2 per mil) and methanogenesis (+44.2 per mil) and the estimated production rates, a ΣCO_2 $\delta^{13}\text{C}$ mixing curve was calculated and compared to the measured isotopic signature of the ΣCO_2 produced (Fig. 3.2b). The mixing curve misses the zonation of sedimentary processes, similar to the exponential curve fit results, but the mixing curve is derived from the exponential fits and so the similarity is not unexpected. As noted previously, the estimated concentration from the rate curve fits agrees well with the data. The differences in the curve fits and the measured data are probably not strongly reflected in the estimated isotope profiles because the production rates are low at depth.

Based on mass balance arguments, it should be possible to estimate the isotopic composition of the CH_4 produced in the incubation experiment using the following equation,

$$[R_{\text{tot}} + R_{\text{CH}_4}] \delta_{\text{remin}} = R_{\text{tot}} \delta_{\text{tot}} + R_{\text{CH}_4} \delta_{\text{CH}_4} \quad (17)$$

where

$$\begin{aligned} R_{CH_4} &= \text{rate of methanogenesis (mM/hr),} \\ \delta_{CH_4} &= \text{isotopic signature of methane produced,} \\ \delta_{remin} &= (-18.9 \text{ per mil; Boehme et al., in revision).} \end{aligned}$$

To estimate the rate of methane production, the rate of ΣCO_2 produced during methanogenesis can be used in the following stoichiometric relationship:

$$(R_{CH_4}) = \frac{R(\Sigma CO_2)_M}{(\tau - 1)}. \quad (18)$$

The $\tau - 1$ parameter was determined based on oxidation state arguments and will be discussed later. Solving Eqn. 17, the isotopic composition of the methane produced in the sediments is -65.9 per mil. This value is very similar to the measured isotopic signature of methane bubbles collected at the same site in June 1983 and 1984 (-64.3 \pm 0.7; Martens et al., 1986). The mass balance equations accurately estimate the isotopic composition of the methane being produced in this sediment. This is further verification that the mass balance achieved using measured rates of ΣCO_2 production and sulfate reduction adequately represents controlling diagenetic processes.

As noted earlier, the calculated $\delta^{13}C$ for ΣCO_2 produced via sulfate reduction (-19 per mil) and methanogenesis (+44 per mil) can be used to estimate the isotopic signature of the ΣCO_2 produced in the sulfate reduction zone using previously measured rates from Crill and Martens (1983). The rates of sulfate reduction and methane production from the summer months were averaged for the upper 1- 4 cm and 6-11cm (the depths above where sulfate was depleted) and converted to ΣCO_2 production rates using τ and $\tau - 1$. The resultant rates were used with the calculated

$\delta^{13}\text{C}$ for ΣCO_2 produced via sulfate reduction (-19 per mil) and methanogenesis (+44 per mil) to estimate a $\delta^{13}\text{C}$ for ΣCO_2 produced of -18 per mil for the upper 4 cm and -13 per mil for the 6-11cm interval. These calculations suggest that methane production in the sulfate reduction zone can significantly affect the $\delta^{13}\text{C}$ of the ΣCO_2 produced and may be responsible for the ^{13}C -enriched ΣCO_2 seen in the sulfate reduction zone.

The determination of the isotopic composition of the methane produced in the sediment allows us to calculate the fractionation factor for the production of methane,

$$\alpha = \frac{\delta^{13}\text{C}_{(\text{CO}_2)} + 10^3}{\delta^{13}\text{C}_{(\text{CH}_4)} + 10^3}, \quad (19)$$

where $\delta^{13}\text{C}_{(\text{CH}_4)}$ is -65.9 per mil as calculated above and δCO_2 is the isotopic composition of the CO_2 measured in the methanogenic zone. Using a pH of 6.95 for A-1 sediments (Chanton, 1985; N.E. Blair et al., 1993), the relative contributions of HCO_3^- , CO_2 , and $\text{CO}_3^{=}$ can be determined (Stumm and Morgan, 1981). At 8-10 cm, the measured ΣCO_2 $\delta^{13}\text{C}$ is -7.0 per mil (Fig. 3.3). To determine the isotopic composition of the CO_2 species, the following equations (Deines et al., 1974; Friedman and O'Neil, 1977; Blair et al., 1993) were solved simultaneously:

$$\delta^{13}\text{C}(\Sigma\text{CO}_2) = d\delta^{13}\text{C}(\text{CO}_2) + e\delta^{13}\text{C}(\text{HCO}_3^-) + f\delta^{13}\text{C}(\text{CO}_3^{=}) \quad (20)$$

$$\alpha\left(\frac{\text{HCO}_3^-}{\text{CO}_2}\right) = \frac{10^3 + \delta^{13}\text{C}(\text{HCO}_3^-)}{10^3 + \delta^{13}\text{C}(\text{CO}_2)} \quad (21)$$

$$\delta^{13}\text{C}(\text{HCO}_3^-) = \delta^{13}\text{C}(\text{CO}_3^{2-}) \quad (22)$$

The variables d, e, and f represent the fractions of the dissolved ΣCO_2 components. The $\delta^{13}\text{C}$ of HCO_3^- and CO_3^{2-} are assumed to be the same (Eqn. 22). The equilibrium fractionation factor for the HCO_3^- and CO_2 equilibrium is given by:

$$\ln \alpha \left(\frac{\text{HCO}_3^-}{\text{CO}_2} \right) = \left(\frac{9.552}{T} \right) - 0.0241 \quad (23)$$

Temperature is in Kelvin (Deines et al., 1974) Solving Eqns. 20, 21, 22 and 23 gives a $\delta^{13}\text{C}$ value for CO_2 of -14.0 per mil. Substituting this value into Eqn. 19 gives an α for methane production of 1.055. This fractionation factor is remarkably similar to an independent estimate for this site, based on a mechanistic model (1.056 at 25°C; Blair et al., 1993) and is within the range determined in culture studies (1.03 to 1.06; Games et al., 1976; Fuchs et al., 1979; Balabane et al., 1987; Belyaev et al., 1983) and estimated from measured profiles of ΣCO_2 and CH_4 (1.05 to 1.09; Whiticar et al., 1986). The agreement is further evidence to support the model results. This is the first in situ fractionation factor for methane production from CO_2 reduction determined using directly measured rates and the associated isotopic signatures.

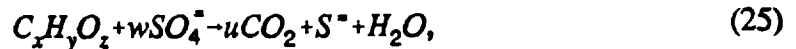
Model Sensitivity to Reaction Stoichiometry

The isotopic composition of the ΣCO_2 produced during sulfate reduction and methanogenesis, and the isotopic composition of the methane that were estimated using the mass balance approach are sensitive to the stoichiometries of the sulfate reduction and methane production reactions. The δ_{CH_4} is especially sensitive to the

stoichiometry as is seen in Fig. 3.6. These stoichiometries are dependent on the apparent oxidation state of the organic carbon that is remineralized. For the generalized formula $C_xH_yO_z$, the apparent oxidation state of the carbon is defined as

$$OS = \frac{2z-y}{x} \text{ for } -4 \leq OS \leq 4. \quad (24)$$

for the reaction



where

$$\tau = \frac{u}{w} = \frac{8}{4-OS}. \quad (26)$$

Similarly for the methanogenic reaction,



the ratio of CO_2 produced to CH_4 produced (u/v) is given by

$$\frac{u}{v} = \frac{4+OS}{4-OS} = \tau - 1. \quad (28)$$

The relationship between $\tau-1$, the ratio of CH_4 to ΣCO_2 produced, and oxidation state has been demonstrated in culture experiments (Tarvin and Buswell, 1934; Fig. 3.7).

Solving Eqn. 28 for oxidation state using $\tau = 1.78$ from the model, gives an apparent oxidation state of the organic matter of -0.49. Using the τ determined by

Alperin et al. (1992) of 1.7 ± 0.1 gives an OS values of -0.72 ± 0.28 and using the τ determined by Klump and Martens (1989) of 1.9 gives an OS value of -0.21.

An independent estimate of oxidation state of the remineralized organic matter can be determined from the composition of the remineralized organic matter. At Cape Lookout, $64 \pm 17\%$ of the metabolized organic carbon has been identified as carbohydrates, lipids and amino acids, in a ratio of 1.0:1.0:1.9. Using the equation,

$$OS = \frac{(3a+2b+2z-y)}{x} \quad (29)$$

to describe the oxidation state of amino acids with the formula $C_xH_yN_aO_zS_b$ and the amino acid distributions identified at Cape Lookout sediments (Burdige and Martens, 1988), the average oxidation state of the amino acid carbon is estimated to be 0.07. The carbohydrate carbon is assumed to have an average oxidation state of zero. The C_{16} fatty acid was used as a representative lipid for this system (Haddad, 1989) with an oxidation state of -1.75. Given the relative contribution of these fractions to the identified pool, the apparent oxidation state of the identified metabolizable pool is -0.41, in good agreement with the modeled value of -0.49. The OS determined from the organic matter can be applied to Eqns. 26 and 28 to estimate a τ of 1.81, in excellent agreement with the 1.78 determined from this study. McCorkle and Emerson (1988) calculated CO_2/O_2 ratios for a variety of oxic and suboxic sediments. Assuming that oxidation state is the only factor controlling this ratio, their value of -0.54 is consistent with the τ determined for Cape Lookout. Gujer and Zehnder (1983) also noted a relationship between oxidation state, substrate, and CO_2 to CH_4

ratios for anaerobic digesters. Based on their correlations, the substrates that correlate to the oxidation state estimated for Cape Lookout are algae, bacteria, carbohydrates and proteins. The agreement of these various approaches to determining the OS and stoichiometries of sulfate reduction and methanogenesis is further evidence that despite the sensitivity of the model to these parameters (Fig. 3.6), our model is accurately describing the processes and their isotopic signatures in this system.

Implications for Control of Marine CH_4 $\delta^{13}\text{C}$

Marine CH_4 $\delta^{13}\text{C}$ values exhibit a wide range of values (-110 to -60 per mil; Whiticar et al., 1986). Possible sources of this variation must be due to differences in the relative rates of methanogenic pathways (predominantly CO_2 -reduction and acetate dissimilation), differences in fractionation factors, and the isotopic composition of the precursors. The mass balance model presented here indicates that the δCH_4 is also dependent on the relative rates of non-methanogenic oxidative processes (sulfate reduction in this study) and methanogenesis. Further, the model's sensitivity to oxidation state suggests that oxidation state may be important as well.

CONCLUSIONS

The ΣCO_2 $\delta^{13}\text{C}$ profiles from Cape Lookout have been shown to be dependent on the rates of the remineralization processes, similar to the results of McCorkle and Emerson (1988). In the methanogenic sediments of Cape Lookout, the ΣCO_2 $\delta^{13}\text{C}$ primarily reflects changes in sulfate reduction rate and methanogenesis. The sedimentary profiles are best described by the mixing of ΣCO_2 from two processes: sulfate reduction, producing ΣCO_2 with an isotopic signature of -19.2 per mil, and

methanogenesis, resulting in ΣCO_2 with an isotopic signature of +44.2 per mil. The mass balance calculations generated a reasonable isotope value for methane and a reasonable fractionation factor for methane production. However the calculation is very sensitive to the reaction stoichiometry.

The mass balance approach used suggests that the isotopic signature of both the ΣCO_2 and methane are sensitive to the ratios of $\Sigma\text{CO}_2/\text{SR}$ and $\Sigma\text{CO}_2/\text{CH}_4$ that are ultimately dependent on the oxidation state of the organic matter being remineralized. The oxidation state determined from the incubation experiment agreed with a calculated OS based on the identified fraction of the organic carbon remineralized. We hypothesize that the ratio of sulfate reduction to methanogenesis may be an important contribution to the range of CH_4 isotope values observed in the marine environment. This may ultimately be useful in interpreting ΣCO_2 $\delta^{13}\text{C}$ profiles in other environments as well as the isotopic signature of diagenetic carbonates.

Fig. 3.1 ΣCO_2 , sulfate and ΣCO_2 $\delta^{13}\text{C}$ data for the five depth intervals. The ΣCO_2 , $\Sigma^{12}\text{CO}_2$, $\Sigma^{13}\text{CO}_2$ and sulfate concentrations were fit to a line to determine rates for each depth interval.

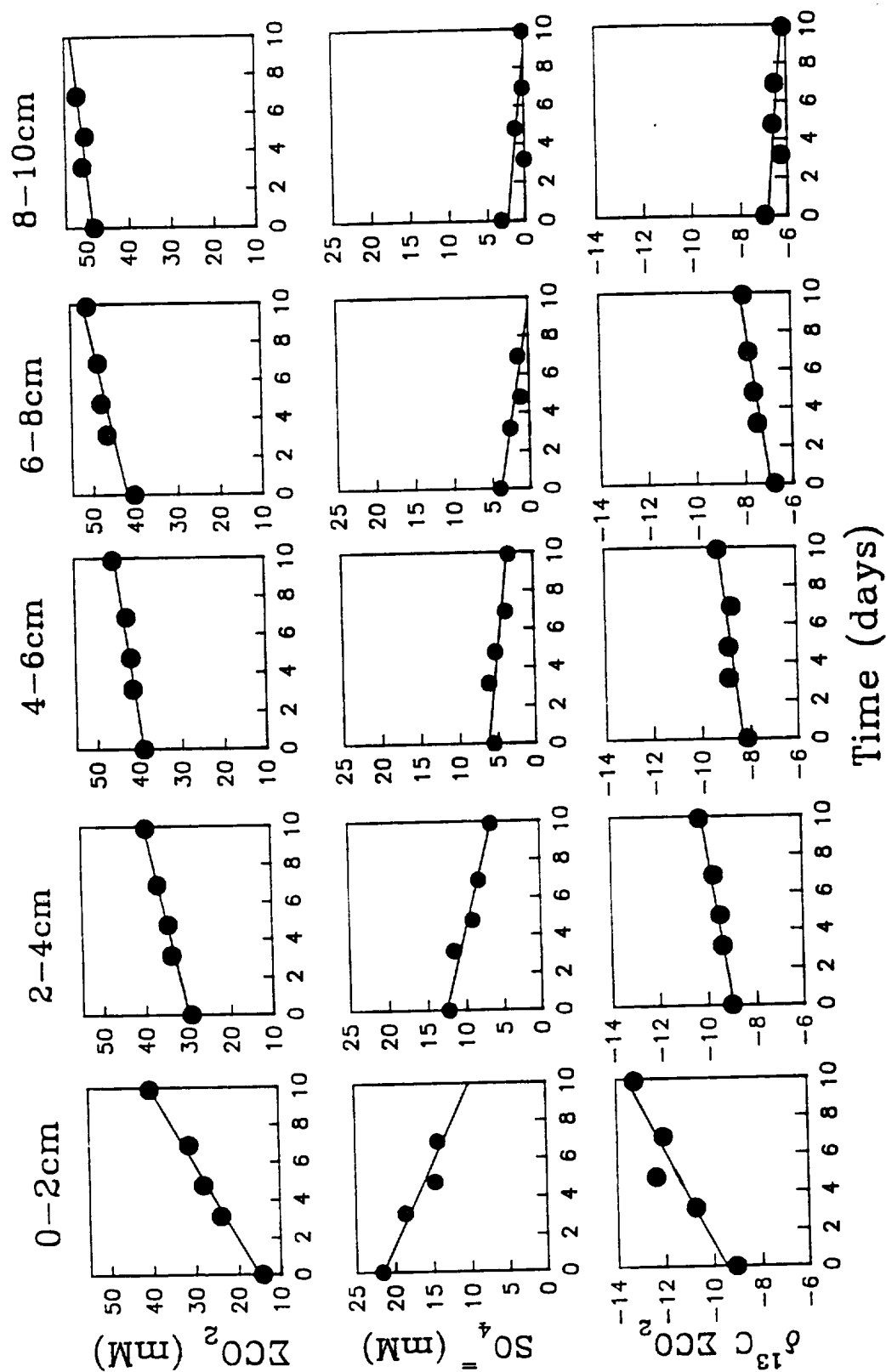


Fig. 3.2 (A) Measured rates (symbols) and curvefits to rates (lines) of ΣCO_2 production and sulfate reduction. (B) Isotopic signature of the ΣCO_2 produced in the upper 10 cm (symbols) determined using Eqn. 11. The solid line is the $\delta^{13}\text{C}$ of the ratio of the curvefits of the individual $\Sigma^{12}\text{CO}_2$ and $\Sigma^{13}\text{CO}_2$ production profiles. The dotted line (.....) is a mixing curve based on the calculated rates of sulfate reduction and methanogenesis and the associated end member isotopic signatures. The dashed line (- - -) is the ratio of depth-dependent production rates of $\Sigma^{12}\text{CO}_2$ and $\Sigma^{13}\text{CO}_2$ solved for using the measured ΣCO_2 concentration and $\delta^{13}\text{C}$ profile and the diagenetic equation (Eqn. 12).

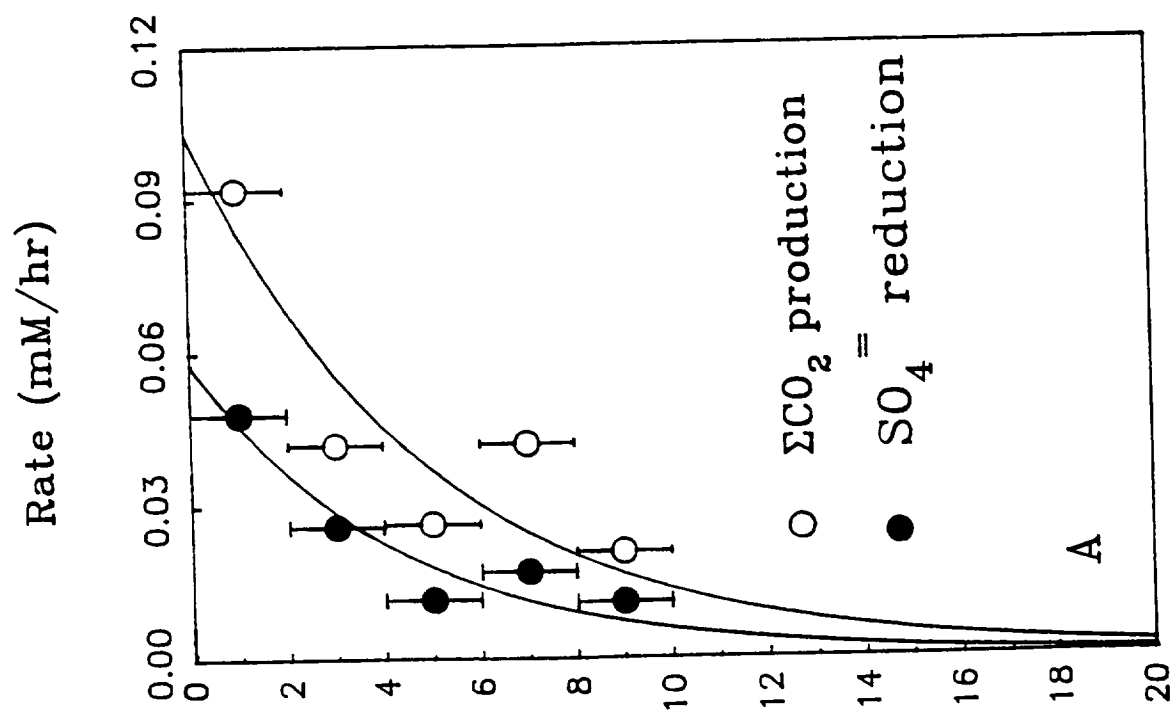
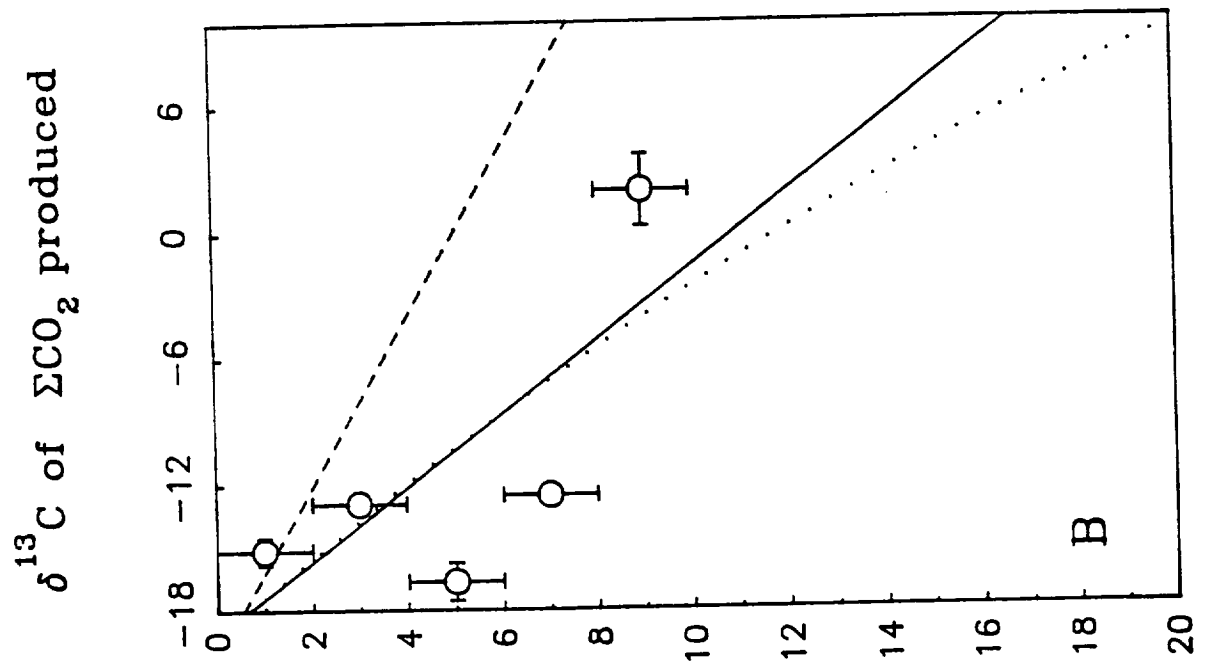


Fig. 3.3 The measured concentrations of ΣCO_2 and sulfate (symbols) and the model estimates determined using Eqn. 12 and the rate data shown in Fig. 3.2 (solid line) (A). The measured isotopic signature of the ΣCO_2 (symbols) and the modelled estimates determined using Eqn. 12 and the individual rates of $\Sigma^{12}\text{CO}_2$ and $\Sigma^{13}\text{CO}_2$ production (solid line) (B).

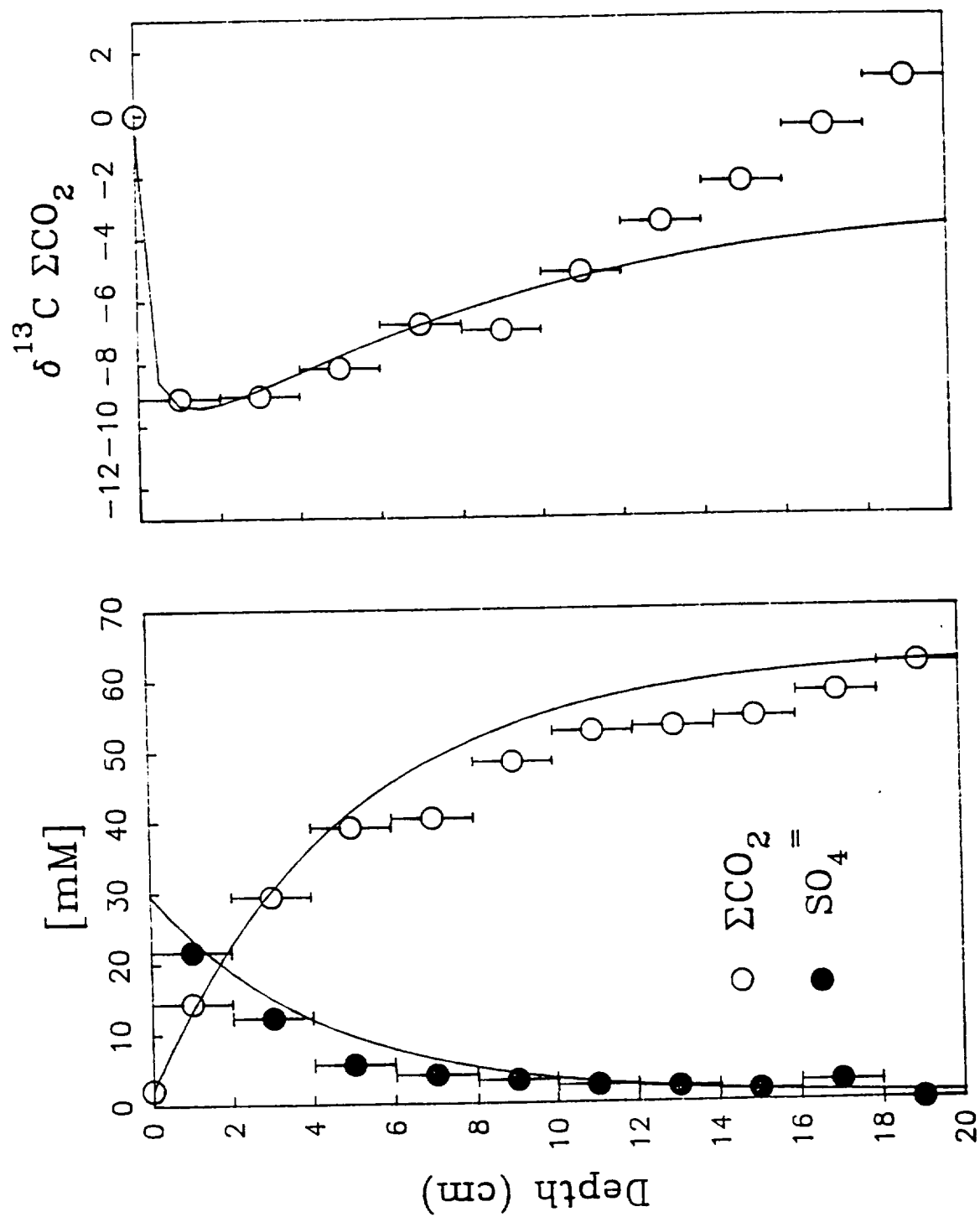


Fig. 3.4 The sulfate gradient versus the ΣCO_2 $\delta^{13}\text{C}$ gradient for the upper 3 cm of sediment from porewater profiles collected from 1986 to 1991 at Cape Lookout. The sulfate and ΣCO_2 $\delta^{13}\text{C}$ gradients were based on linear fits of concentration over the upper 3 cm (one cm intervals).

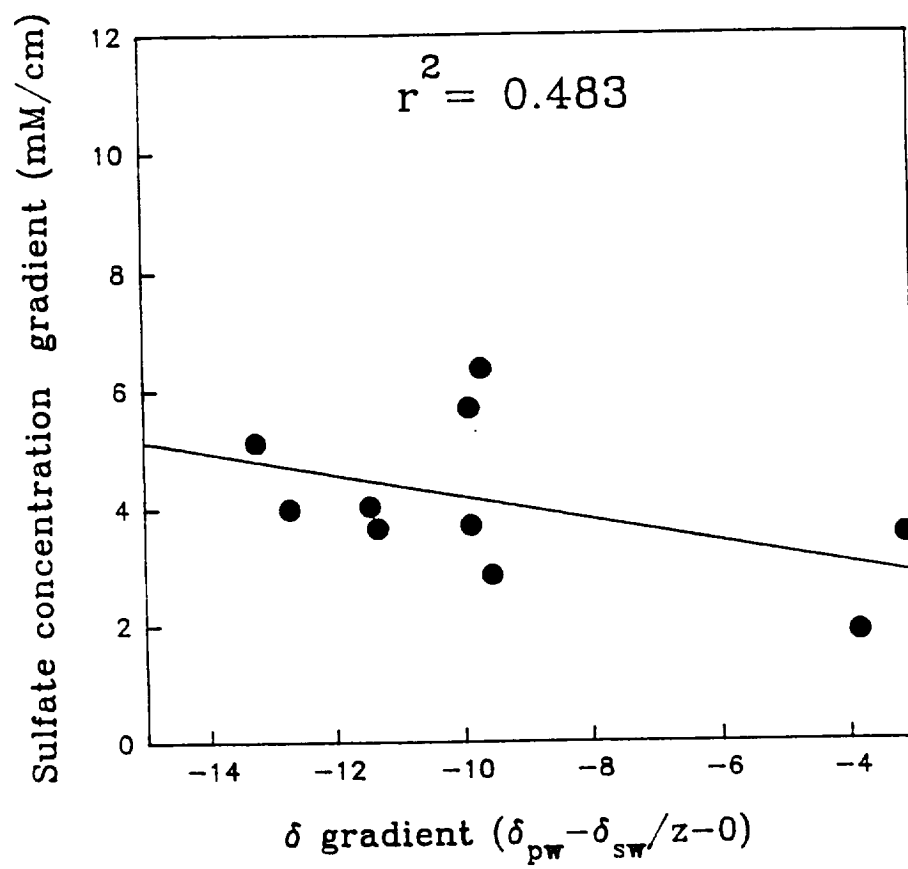


Fig. 3.5 **Porewater Calcium concentration versus time for the upper 10 cm from the incubation experiment.**

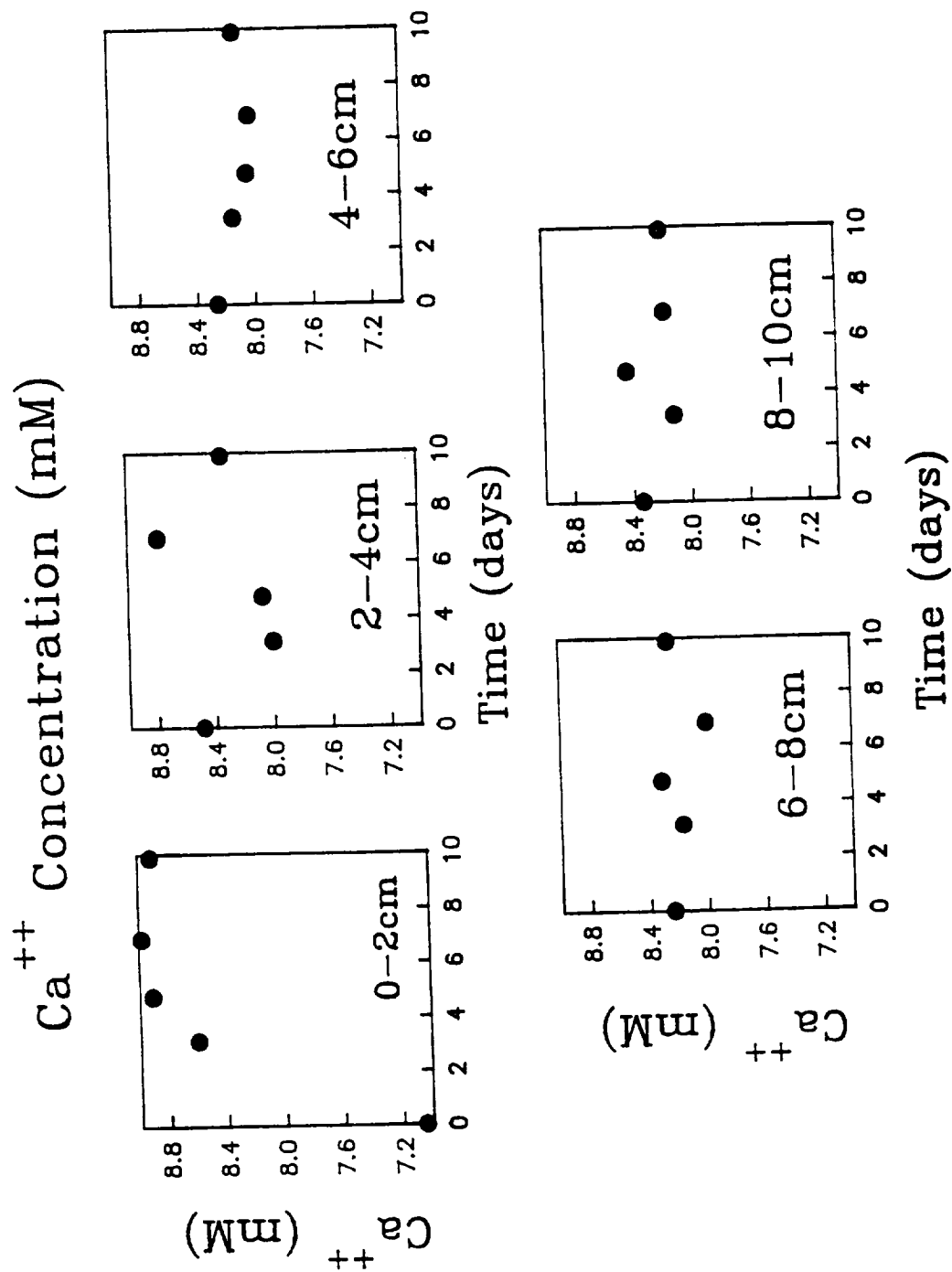


Fig. 3.6 **The relationship between the oxidation state of the organic carbon, the ratio of ΣCO_2 produced to sulfate reduced (τ) and the modelled isotopic signature of the methane produced.**

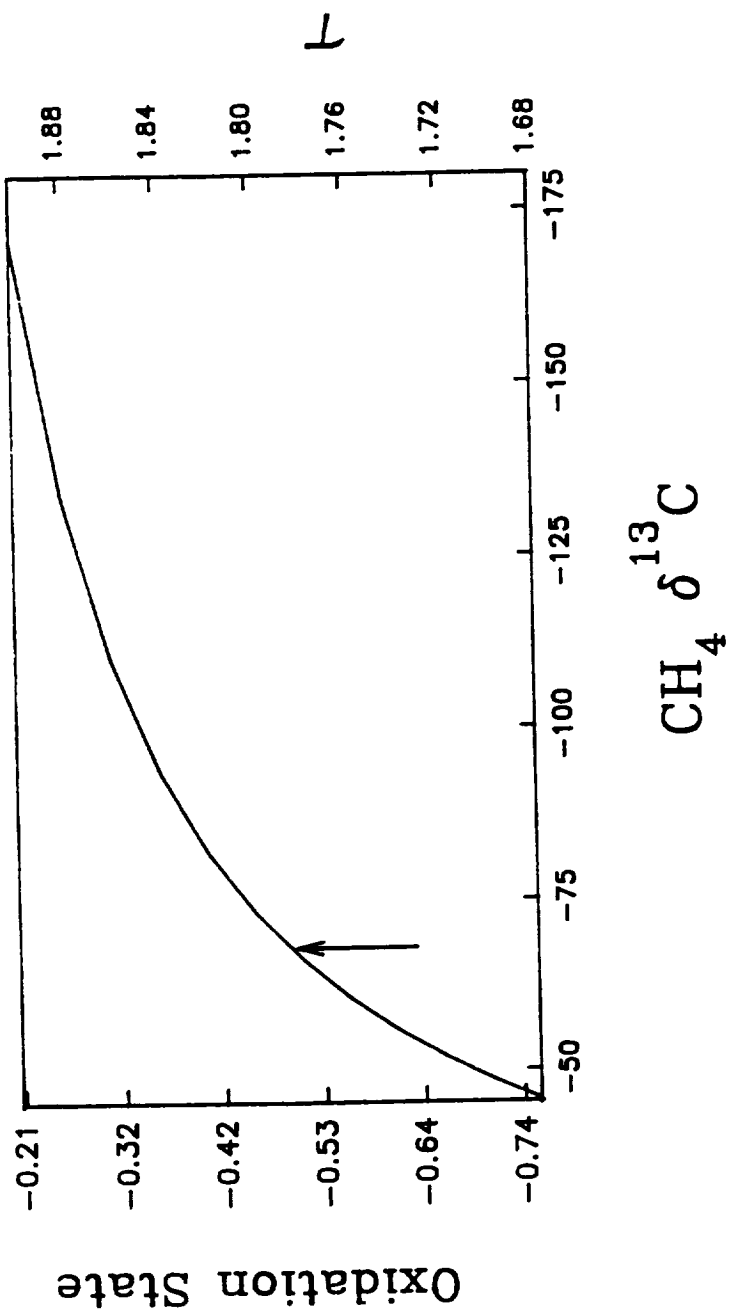


Fig. 3.7 The relationship of the relative rates of CO_2 and CH_4 production ($\tau-1$) and the apparent oxidation state (OS) of the fermented material. Data is from Tarvin and Buswell (1934). Curve is described by Eqn. 18.

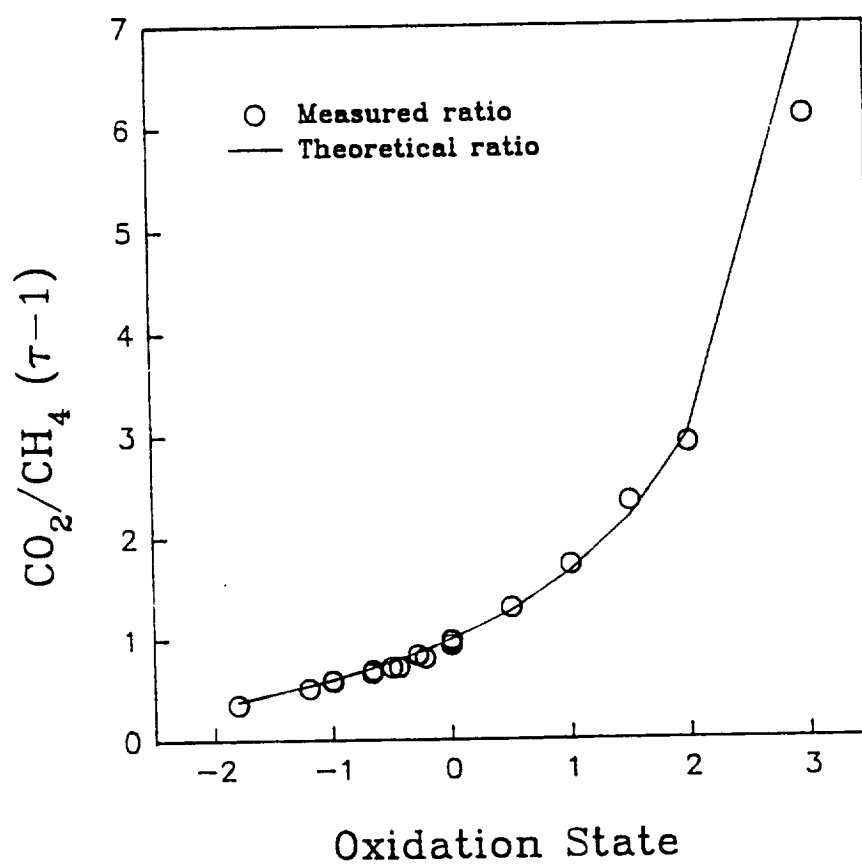


Table 3.1 Regression coefficients (r^2) for the $\text{SO}_4^{=}$, ΣCO_2 , and $\Sigma\text{CO}_2 \delta^{13}\text{C}$ incubation data

Depth	$\text{SO}_4^{=}$	ΣCO_2	$\Sigma\text{CO}_2 \delta^{13}\text{C}$
0-2 cm	0.92	0.99	0.99
2-4 cm	0.94	0.98	0.98
4-6 cm	0.75	0.96	0.96
6-8 cm	0.85	0.89	0.89
8-10 cm	0.56	0.84	0.84

Table 3.2 Curve fit parameters, estimated depth integrated rates (10 cm), and associated isotopic compositions from tube incubation experiment.

Process	R_0	a	*Depth Integrated Rate	$\delta^{13}\text{C}$
Total ΣCO_2 Produced	0.103	0.2037	0.439	-13.1
ΣCO_2 Produced from Sulfate Reduction	0.103	0.2341	0.397	-19.2
ΣCO_2 Produced from Methanogenesis	--	--	0.0420	+44.2
Methane Produced	--	--	0.0539	-65.9
Sulfate Reduction	0.058	0.2341	0.223	--

*Units of $\text{mmol}\cdot\text{cm}^{-2}\cdot\text{hr}^{-1}$

REFERENCES

- ALPERIN M.J. (1988) The carbon cycle in an anoxic marine sediment. Ph.D. Dissertation University of Alaska, Fairbanks.
- ALPERIN M.J., BLAIR N.E., ALBERT D.B., HOEHLER T.M. and MARTENS C.S. (1992) Factors that control the stable carbon isotopic composition of methane produced in an anoxic marine sediment. *Global Biogeochem. Cycles* 6, 271-291.
- BALABANE M., GALIMOV E., HERMANN M. and LETOLLE R. (1987) Hydrogen and carbon isotope fractionation during experimental production of bacterial methane. *Global Biogeochem. Cycles* 2, 279-288.
- BELYAEV S.S., WOLKIN R., KENEALY W.R., DENIRO M.J. EPSTEIN S. and ZEIKUS J.G. (1983) Methanogenic bacteria from the Bondyuzhskoe oil field: General characterization and analysis of stable-carbon isotopic fractionation. *Appl. Environ. Microbiol.* 45, 691-697.
- BERNER R.A. (1980) Early diagenesis. Princeton University Press.
- BLAIR N.E. and CARTER W.D. (1992) The carbon isotope biogeochemistry acetate from a methanogenic marine sediment. *Geochim. Cosmochim. Acta* 56, 1247-1258.
- BLAIR N.E., BOEHME S.E., and CARTER W.D. (1993) The carbon isotope biogeochemistry of methane production in anoxic sediments. In *The Biogeochemistry of Global Change: Radiative Trace Gases* (ed. R.S. Oremland) Chapman and Hall.
- BOEHME S.E. (1989) Seasonal variation in the production of ΣCO_2 in a methane-producing sediment. M.S. North Carolina State University, Raleigh.
- BOEHME S.E., BLAIR N.E., CHANTON J.P. and MARTENS C.S. (in revision) A carbon isotope mass balance for an anoxic marine sediment: Isotopic signatures of diagenesis. Submitted to *Geochim. Cosmochim. Acta*.
- BURDIGE D. and MARTENS C.S. (1988) Biogeochemical cycling in an organic-rich coastal marine basin: 10. The role of amino acids in sedimentary carbon and nitrogen cycling. *Geochim. Cosmochim. Acta* 52, 1571-1584.
- CANUEL E.A., MARTENS C.S. and BENNINGER L.K. (1990) Seasonal variations in ^7Be activity in the sediments of Cape Lookout Bight, North Carolina. *Geochim. Cosmochim. Acta* 54, 237-245.

- CHANTON J.P. (1985) Sulfur mass balance and isotopic fractionation in an anoxic marine sediment. Ph.D. Dissertation, University of North Carolina, Chapel Hill.
- CHANTON J.P., MARTENS C.S., and KIPPHUT G.W. (1983) Lead-210 sediment geochronology in an organic-rich coastal marine basin. *Geochim. Cosmochim. Acta* 49, 1791-1804.
- CHANTON J.P., MARTENS C.S. and GOLDBERGER M.B. (1987) Biogeochemical cycling in an organic-rich coastal marine basin. 7. Sulfur mass balance, oxygen uptake and sulfide retention. *Geochim. Cosmochim. Acta* 51, 1187-1199.
- CLAYPOOL G.E. and KAPLAN I.R. (1974) The origin and distribution of methane in marine sediments. In *Natural Gases in Marine Sediments* (ed. I.R. Kaplan) pp. 99-139. Plenum Press.
- CRAIG H. (1957) Isotopic standards for carbon and oxygen and correction factors for mass-spectrometric analysis of carbon dioxide. *Geochim. Cosmochim. Acta* 12, 133-149.
- CRILL P.M. and MARTENS C.S. (1983) Spatial and temporal fluctuations of methane production in anoxic, coastal marine sediments. *Limnol. Oceanogr.* 25, 564-571..
- CRILL P.M. and MARTENS C.S. (1986) Methane production from bicarbonate and acetate in an anoxic marine sediment. *Geochim. Cosmochim. Acta* 50, 2089-2097.
- DEINES P., LANGMUIR D., HARMON R.S. (1974) Stable carbon isotope ratios and the existence of a gas phase in the evolution of carbonate groundwaters. *Geochim. Cosmochim. Acta* 38, 1147-1164.
- FOREE E.G. and MCCARTY P.L. (1970) Anaerobic decomposition of algae. *Env. Sci. Technol.* 4, 842-849.
- FRIEDMAN I. and O'NEIL J.R. (1977) Compilation of stable isotope fractionation factors of geochemical interest. U.S. Geological Survey Professional Paper 440-KK.
- FRIEDMAN I. and MURATA K.J. (1979) Origin of dolomite in Miocene Monterey Shale and related formations in the Temblor Range, California. *Geochim. Cosmochim. Acta* 43, 1357-1365.

- FRY B. and SHERR E.B. (1984) $\delta^{13}\text{C}$ measurements as indicators of carbon flow in marine and freshwater ecosystems. *Contrib. in Mar. Sci.* 27, 13-47.
- FUCHS G., THAUER R. ZEIGLER H. and STICHLER W. (1979) Carbon isotope fractionation by *Methanobacterium thermoautotrophicum*. *Arch. Microbiol.* 120, 135-139.
- GAMES L.M., HAYES J.M. and GUNSALUS R.P. (1978) Methane-producing bacteria: natural fractionations of the stable carbon isotopes. *Geochim. Cosmochim. Acta* 42, 1295-1297.2
- GUJER W. and ZEHNDER J.B. (1983) Conversion processes in anaerobic digestion. *Water Sci. Technol.* 15, 127-167.
- HADDAD R.I. (1989) Sources and reactivity of organic matter accumulating in a rapidly depositing, coastal environment. Ph.D. Dissertation, University of North Carolina, Chapel Hill.
- HADDAD R.I. and MARTENS (1987) Biogeochemical cycling in an organic-rich coastal marine basin: 9. Sources and accumulation rates of vascular plant-derived organic material. *Geochim. Cosmochim. Acta* 51, 2991-3001.
- HAYES J.M. (1983) Practice and principles of isotope measurements in organic geochemistry. In: *Organic Geochemistry of Contemporaneous and Ancient Sediments* (ed. W.G. Meinschein) Society of Economic Paleontology and Mineralogy. pp 5-1 - 5-31.
- HERCZEG A.L. (1988) Early diagenesis of organic matter in lake sediments: A stable carbon isotope study of pore waters. *Chem. Geol.* 72, 199-209.
- KING G.M. (1984) Utilization of hydrogen, acetate, and "non-competitive" substrates by methanogenic bacteria in marine sediments. *Geomicrobiol. J.* 3, 275-306.
- KING G.M., KLUG M.J. and LOVLEY D.R. (1981) Metabolism of acetate, methanol, and methylated amines in intertidal sediments of Lowes Cove, Maine. *Appl. Environ. Microbiol.* 45, 1848-1853.
- KLUMP J.V. and MARTENS C.S. (1981) Biogeochemical cycling in an organic-rich coastal marine basin. 2. Nutrient sediment-water exchange processes. *Geochim. Cosmochim. Acta* 45, 101-121.
- KLUMP J.V. and MARTENS C.S. (1989) The seasonality of nutrient regeneration in an organic-rich coastal sediment: Kinetic modeling of changing pore-water nutrient and sulfate distributions. *Limnol. Oceanogr.* 34, 559-577.

- LAZERTE B.D. (1981) The relationship between total dissolved carbon dioxide and its stable carbon isotope ratio in aquatic sediments. *Geochim. Cosmochim. Acta* 45, 647-656.
- LI Y.H. and GREGORY S. (1974) Diffusion of ions in sea water and in deep-sea sediments. *Geochim. Cosmochim. Acta* 38, 703-714.
- MARTENS C.S. (1976) Control of methane sediment-water bubble transport by macroinfaunal irrigation in Cape Lookout Bight, North Carolina. *Science* 192, 998-1000.
- MARTENS C.S. and KLUMP J.V. (1984) Biogeochemical cycling in an organic-rich coastal marine basin. 4. An organic carbon budget for sediments dominated by sulfate reduction and methanogenesis. *Geochim. Cosmochim. Acta* 48, 1987-2004.
- MARTENS C.S., BLAIR N.E., GREEN C.D. and DESMARAIS D.J. (1986) Seasonal variations in the stable carbon isotopic signature of biogenic methane in a coastal sediment. *Science* 233, 1300-1303.
- MCARTHUR J.M. (1989) Carbon isotopes in pore water, calcite, and organic carbon from distal turbidites of the Madeira Abyssal Plain. *Geochim. Cosmochim. Acta* 53, 2997-3004.
- MCCORKLE D.C. and EMERSON S.R. (1988) The relationship between pore water carbon isotopic composition and bottom water oxygen concentration. *Geochim. Cosmochim. Acta* 52, 1169-1178.
- MCCORKLE D.C., EMERSON S.R. and QUAY P.D. (1985) Stable carbon isotopes in marine porewaters. *Earth Planet. Sci. Lett.* 74, 13-26.
- MCNICHOL A.P., DRUFFEL E.R.M. and LEE C. (1991) Carbon cycling in coastal sediments: 2. An investigation of the sources of ΣCO_2 to pore water using carbon isotopes. In *Organic Substances and Sediments in Water* (ed. R.A. Baker) Lewis Publishers, Chelsea, MI.
- NISSENBAUM A., BAEDECKER M.J. and KAPLAN I.R. (1972) Studies on dissolved organic matter from interstitial water of a reducing marine fjord. *Adv. in Org. Geochem.* (ed. Braunschweig) Pergamon Press, Oxford, 427-440.
- OREMLAND R.S., MARSH L.M. and POLCIN S. (1982) Methane production and simultaneous sulphate reduction in anoxic, salt marsh sediments. *Nature* 290, 143-145.

- OREMLAND R.S., MILLER L.G., COLBERTSON C.W., ROBINSON S.W., SMITH R.L., LOVLEY D., WHITICAR M.J., KING G.M., KIENE R.P., IVERSEN N. and SARGENT M. (1993) Aspects of the biogeochemistry of methane in Mono Lake and the Mono Basin of California. In *The Biogeochemistry of Global Change: Radiative Trace Gases* (ed. R.S. Oremland) Chapman and Hall.
- PRESLEY B.J. and KAPLAN I.R. (1968) Changes in dissolved sulfate, calcium and carbonate from interstitial water of near-shore sediments. *Geochim. Cosmochim. Acta* 32, 1037-1048.
- REEBURGH W.S. (1982) A major sink and flux control for methane in marine sediments: Anaerobic consumption. In: *The Dynamic Environment of the Ocean Floor*. (eds. Fanning K. and Manheim F.T.) Heath, Lexington Mass. pp 203-217.
- SCHAFF T., LEVIN L., BLAIR N., DEMASTER D.J., POPE R., and BOEHME S. (1992) Spatial heterogeneity of benthos on the Carolina continental slope: large (110 km)-scale variation. *Mar. Ecol. Prog. Ser.* 88, 143-160.
- STUMM W. and MORGAN J.J. (1981) *Aquatic Chemistry*. John Wiley and Sons, New York.
- TARVIN D. and BUSWELL A.M. (1934) The methane fermentation of organic acids and carbohydrates. *J. Amer. Chem. Soc.* 56, 1751-1755.
- ULLMAN W.J. and ALLER R.C. (1982) Diffusion coefficients in near-shore marine sediments. *Limnol. oceanogr.* 27, 552-556.
- WHELEN T., BERNARD B.B. and BROOKS J.M. (1976) Carbon isotope variations in total carbon dioxide and methane from interstitial waters of nearshore sediments. In *Stable Isotopes in the Earth Sciences* (N.Z. DSIR Bull.) 220, pp.39-47.
- WHITICAR M.J. and FABER E. (1986) Methane oxidation in sediment and water column environments--Isotope evidence. *Org. Geochem.* 10, 759-768.
- WHITICAR M.J., FABER E. and SCHOELL M. (1986) Biogenic methane formation in marine and freshwater environments: CO₂ reduction vs. acetate fermentation--Isotope evidence. *Geochim. Cosmochim. Acta* 50, 693-709.

Part III

The Carbon Isotope Biogeochemistry of Methane Production in
Anoxic Sediments 1. Field Observations

Neal E. Blair*, Susan E. Boehme and W. Dale Carter, Jr.¹

Department of Marine, Earth and Atmospheric Sciences,

North Carolina State University

Raleigh, NC 27695-8208

¹ Present address: Archer Daniels Midland Company

P.O. Box 10640

Southport, NC 28461

ABSTRACT

The natural abundance $^{13}\text{C}/^{12}\text{C}$ ratio of methane from anoxic marine and freshwater sediments in temperate climates varies seasonally. Carbon isotopic measurements of the methanogenic precursors, acetate and dissolved inorganic carbon, from the marine sediments of Cape Lookout Bight, North Carolina have been used to determine the sources of the seasonal variations at that site. Movement of the methanogenic zone over an isotopic gradient within the dissolved CO_2 pool appears to be the dominant control of the methane $^{13}\text{C}/^{12}\text{C}$ ratio from February to June. The onset of acetoclastic methane-production is a second important controlling process during mid-summer. An apparent temperature dependence on the fractionation factor for CO_2 -reduction may have a significant influence on the isotopic composition of methane throughout the year.

INTRODUCTION

Methane, like other carbon-containing materials, is comprised of approximately 99% ^{12}C and 1% ^{13}C (20). Small but distinct source-related variations in the $^{13}\text{C}/^{12}\text{C}$ ratio are well documented (52,59). It is important to understand the processes which control the isotopic composition of methane for a variety of reasons. The $^{13}\text{C}/^{12}\text{C}$ of biogenic methane may provide information concerning the methanogenic ecosystem and the relative rates of methane-producing pathways as a function of season (7,9,15,44) or environment (59). The increasing concentration of tropospheric methane and its potential impact on global temperature and the stratospheric mixing ratios of water vapor and chlorine radicals (8,16,25) require a better understanding of the sources and sinks of that gas. A carbon isotope budget of atmospheric methane which includes seasonal effects would be a powerful constraint on source estimates (44,55). An understanding of the controls of the isotopic composition of biogenic methane would also aid hydrocarbon exploration as approximately 20% of the world's natural gas resources are biogenic in origin (50).

Attempts to model the carbon isotopic composition of methane have been hampered by insufficient information concerning the rates of the methanogenic processes and the isotopic signatures of the methanogenic precursors. Early models used a Rayleigh distillation calculation to simulate the isotope effects associated with methane production in a marine sediment (17,46). These models had three

major assumptions: 1. Methane was produced only via CO_2 -reduction, 2. Net CO_2 consumption occurred in the methanogenic zone, and 3. The system was closed to material fluxes of CO_2 and CH_4 . No information was available concerning the importance of acetate dissimilation or other pathways. Ignoring the CO_2 -production which occurs during methanogenesis (57) led to a significant error in the models. Subsequent treatments, which involved freshwater systems, considered both CO_2 -reduction and acetate dissimilation pathways as well as net CO_2 -production in the methanogenic zone (28,36). It was assumed that the acetate was utilized only by methanogens in the methanogenic zone, a point which is contradicted by ^{14}C -tracer studies (12,37,60). The isotopic composition of sedimentary acetate was not measured in those studies.

This report reviews our attempts to model the carbon isotopic composition of biogenic methane (5; N.E. Blair and S.E. Boehme, submitted). The ultimate goal of this project is to determine the source of the seasonal variations observed in the $^{13}\text{C}/^{12}\text{C}$ ratio of methane from the organic-rich marine sediments of Cape Lookout Bight, North Carolina (44). In general, the $^{13}\text{C}/^{12}\text{C}$ ratio increased in the summer months when methane production rates were highest (Table 1). Similar seasonal variations have been observed in freshwater environments (15) and may be a common phenomenon. The general approach in this project has been to measure the natural abundance $^{13}\text{C}/^{12}\text{C}$ ratios of methanogenic precursors, CO_2 and acetate, and combine those values with estimates of the relative rates of CO_2 -reduction and acetate dissimilation, to simulate the

seasonal variations with an open system model. In doing so, hypotheses concerning the controls of the isotopic composition of methane are tested. In a second study reported in this volume, results from a laboratory microcosm experiment are used to test the model (1).

Field Site

Cape Lookout Bight, North Carolina, is a 1-2 km² coastal basin located 115 km SW of Cape Hatteras on the Outer Banks (Fig. 1;40,43). Fine-grained sediment, with an organic content up to 4% dry weight (41), accumulates at a rate of 8-12 cm/yr (11,13) at the sampling station, A-1. The organic matter appears to be derived from phytoplankton and seagrass debris (32).

The rapid flux of metabolizable organic matter to the seabed results in a high rate of organic carbon remineralization (41). Sulfate reduction, occurring in the upper 10 cm of sediment during summer months, and methanogenesis, which occurs in the underlying zone (21), are the dominant diagenetic processes at this site and respectively account for $68 \pm 20\%$ and $32 \pm 16\%$ of the organic carbon remineralization (41). Approximately 20-30% of the methane is produced via acetate dissimilation and the remainder of the gas is formed primarily by CO₂-reduction (22).

METHODS

All $^{13}\text{C}/^{12}\text{C}$ ratios (R) are reported in the $\delta^{13}\text{C}$ notation which is defined (20) as:

$$\delta^{13}\text{C} = [(R_{\text{sample}} - R_{\text{PDB}})/R_{\text{PDB}}] \times 10^3 .$$

R_{PDB} is the carbon isotopic ratio of the international standard, Peedee Belemnite, and has the accepted value of 0.0112372 (33). The preparation of samples for isotopic analysis is discussed below in the appropriate sections.

Diver-collected cores were obtained at A-1 with 9.5 cm diameter lucite tubes. Pore water samples for sulfate and ΣCO_2 measurements were collected with a sediment press (49). Pore water samples for acetate $\delta^{13}\text{C}$ measurements were isolated with the press or by centrifugation. The porewater samples were frozen immediately after collection and stored at -86°C until analysis.

The acetate samples were treated as described previously (5,6,7). The acetate fraction was isolated by a series of cryogenic distillations coupled with a preparative liquid chromatography step. The acetate was converted to CO_2 for isotopic analysis with a gas chromatograph - combustion system (24,39).

The isotopic analysis of the acetate methyl group was accomplished by the pyrolysis of sodium acetate (6,45,47). A 200:1 mixture of NaOH and acetate (from the last distillation) was dried under N_2 at 135°C in a quartz tube (9 mm i.d. x 20 cm long). The tube was evacuated after drying and heated to 500°C . Methane, which

is derived from the methyl group, was quantitatively collected, measured and injected into the gas chromatograph-combustion system via a Toepler pump.

One to two milliliter subsamples of porewater were injected into evacuated 120 ml serum bottles (Wheaton) sealed with crimped 20 mm rubber stoppers (Alltech Assoc.) and frozen until analysis for ΣCO_2 concentrations and $\delta^{13}\text{C}$ values. Immediately prior to analysis, one ml of 1M phosphoric acid saturated with cupric sulfate was added to the thawed sample. The cupric sulfate was added to precipitate sulfide. The resulting CO_2 was removed from the bottle through a 23 gauge hypodermic needle connected to a vacuum line via a 1/4" Ultratorr union (Cajon). The CO_2 was purified cryogenically, quantitated with a manometer and sealed in a 6 mm o.d. pyrex tube for isotopic analysis. The analytical precision and accuracy of the ΣCO_2 extraction procedure were $\pm 4\%$ and $\pm 0.5\text{mM}$ respectively as determined by the measurement of CO_2 and bicarbonate standards (S.E. Boehme, M.S. thesis, North Carolina State University, Raleigh, 1989). The accuracy of the $\delta^{13}\text{C}$ measurements, as determined by the analysis of the NBS-20 carbonate standard (19), was ± 0.02 per mil.

The methane bubbles were collected from stirred sediment and stored in sealed bottles (44). The methane was converted to CO_2 at 780°C with CuO and purified cryogenically for isotopic analysis (24,39).

The $\delta^{13}\text{C}$ measurements of the CO_2 from the various preparations were analyzed on either a modified Nuclide 6-60 RMS (NASA-Ames

Research Center) or one of two Finnigan MAT 251 mass spectrometers (NCSU Stable Isotope Laboratory and the University of Georgia Center for Applied Isotope Studies). A cross-calibration of a CO₂ standard by the three facilities produced results consistent to within 0.25 per mil. Procedural blanks were collected and used to correct the results of all analyses.

Dissolved sulfate was measured on 5 mL of pore water by the gravimetric analysis of the precipitated barium salt (J.P. Chanton, Ph.D. thesis, Univ. North Carolina, Chapel Hill, 1985; 14). Sulfide was removed immediately after the recovery of the pore water sample by the addition of ZnCl₂ followed by the filtration of the zinc sulfide precipitate. The accuracy of this procedure is typically ± 0.5 mM.

RESULTS AND DISCUSSION

Ebullition is the primary mode of transport of methane from the sediments of Cape Lookout Bight, accounting for approximately 86% of the total flux of $7.4 \pm 2 \text{ mol-m}^{-2}\text{-yr}^{-1}$ (41,42, S.E. Boehme et al., in prep.). The rapid bubble transport from the methanogenic zone through the overlying sediments limits the exposure of the methane to oxidizing conditions which could alter its isotopic composition (2,18). Concordance between the $\delta^{13}\text{C}$ values of naturally- and diver-released bubbles and pore water methane supports that conclusion (44). Thus the $\delta^{13}\text{C}$ value of the methane is controlled primarily by its production.

In organic-rich marine sediments, methane is formed by CO_2 -reduction (17,22,46) and acetate dissimilation (22,35) with the latter process accounting for 20-50% of the total production. Accordingly, the isotopic composition of methane produced will be the result of a mass balance of material from those two sources. The isotopic composition of the methane from each pathway is dependent on the isotopic composition of the precursor, CO_2 or acetate, and the fractionation factor, α , (k_{12}/k_{13}) associated with each process.

Acetate Dissimilation

Acetoclastic methanogenesis is accomplished by the *Methanosarcina* and *Methanothrix* genera (58). Acetate is converted

to acetyl-CoA, after which the carbon-carbon bond of the acetyl moiety is cleaved (31,58). The methyl is reduced to methane and the carboxyl is oxidized to CO₂ (10,54,61). The fractionation factor associated with the formation of methane via acetate dissimilation by cultures of *Methanosarcina barkerii* is 1.02-1.03 (34; J.B. Risatti and J.M Hayes, Geol. Soc. Am. Abstr. Progr., 1983, 15:671).

The $\delta^{13}\text{C}$ value of the acetate methyl group and the in situ fractionation factor for acetate dissimilation in Cape Lookout Bight sediments have been determined via intramolecular carbon isotope measurements of acetate isolated from pore water samples (5,7). The $\delta^{13}\text{C}$ value of the total acetate molecule ranges from -17.6 per mil in non-methanogenic surficial sediments to -2.8 per mil in methane-producing sediments (Fig. 2; 5). Near the sediment surface, the similarity of the $\delta^{13}\text{C}$ value of the acetate to that of the average particulate organic carbon fraction (-19.1 ± 0.3 ; 5,7) indicates that little net fractionation occurs during acetate cycling in the sulfate-reducing zone. However, a large fractionation occurs in the methanogenic zone which leaves the acetate enriched in ^{13}C .

Isotopic analysis of the methyl group and a mass balance calculation of the $\delta^{13}\text{C}$ value of the carboxyl group indicates that the fractionation affects both carbon atoms of acetate (Fig. 2). The magnitude of the ^{13}C -enrichment correlates well with the parameter f , which is defined by the equation

$$f = r_{\text{CH}_4} / (r_{\text{CH}_4} + r_{\text{CO}_2}) \quad (1)$$

where r_{CH_4} and r_{CO_2} are the respective rates of the conversion of the acetate methyl group to CH_4 and CO_2 (5). The downcore profile of f (Fig. 2) was determined from the turnover rate of U- ^{14}C acetate in Cape Lookout sediments (22,51). On average, $38 \pm 11\%$ ($f = .38$) of the methyl group is reduced to methane in the uppermost sediments of the sulfate-depleted zone (10-20 cm) at this site.

The *in situ* fractionation factor for the dissociation of the methyl group from acetate (α_{diss}) was estimated with the equation

$$\alpha_{\text{diss}} = 1 + (\delta_{\text{obs}} - \delta_{\text{syn}}) / [f(\delta_{\text{syn}} + 10^3)] \quad (2)$$

where δ_{obs} is the average $\delta^{13}\text{C}$ value of the methyl group in the 10-20 cm interval (-11.2 ± 3.0) and δ_{syn} represents the $\delta^{13}\text{C}$ value of the newly synthesized acetate (5). The average $\delta^{13}\text{C}$ value of the methyl group in the 0-5 cm interval (-23.2 ± 2.2) was used as an estimate for δ_{syn} because, as noted earlier, the similarity of the isotopic composition of the total acetate from that interval with the particulate organic fraction suggests that little fractionation occurs during the synthesis or uptake in the surficial sediments. The assumption is made that the synthetic isotope effect is also small in the methanogenic zone. It is assumed that the fractionation factor for the conversion of acetate to CO_2 and other non-methane products is 1.000. Using $f = .38 \pm .11$, α_{diss} was calculated to be 1.032 ± 0.014 . The excellent agreement between our estimate of the *in situ* α_{diss} with the culture-derived values of 1.02-1.03 (34; J.B. Risatti and J.M. Hayes, Geol. Soc. Am. Abstr. Progr. 15:671)

indicates that our assumptions are reasonable to a first approximation.

Under steady state conditions (33), the $\delta^{13}\text{C}$ value of the methane produced from acetate is given by

$$\delta^{13}\text{C}(\text{CH}_4/\text{Acet}) = \delta_{\text{syn}} - (1-f)(\alpha_{\text{diss}}-1)10^3. \quad (3)$$

Using the same values and assumptions as above for the appropriate parameters, the $\delta^{13}\text{C}$ value of the methane is calculated to be -43 ± 10 per mil. A similar ^{13}C -enrichment relative to methane produced via CO_2 -reduction (see below) has been observed in the laboratory microcosm experiment (1).

Approximately, 20 and 26% of the methane is derived from acetate in the upper 30 cm of sediment at Cape Lookout in July and August, respectively, with the remainder formed via CO_2 -reduction (22). Direct measurements of the relative rates of the two methanogenic processes are not available for other months. The $\delta^{13}\text{C}$ value of the acetate methyl group in the 8-16 cm interval in June, 1984 was -26 per mil (7), which is a value more similar to that found in the sulfate reducing sediments than in the underlying methanogenic zone. That suggests that little of the acetate was dissimilated to CH_4 and CO_2 ($f=0$) at that time. On the other hand, one must consider the possibility that the June value is the combined result of a synthetic isotope effect, similar to that associated with acetogenesis (30,48), and a methanogenic isotope effect. For the purposes of the model, the simpler scenario is

assumed, i.e. the synthetic isotope effect remains small and unchanged throughout the summer and $f=0$ in June. Accordingly, when $f=0$, then the proportion of methane produced from acetate relative to total methane production (F) must be zero. There is no information concerning F for any other months. For the purposes of the model $F=0$ for all months except July and August, where it equals .20 and .26 respectively (Fig. 3b).

CO₂-Reduction

¹²CO₂ is selectively converted to CH₄, creating an isotopic gradient in the dissolved inorganic carbon (Σ CO₂) pool as buried sediment encounters and passes through the methanogenic zone (46, Fig. 4; Table 2). At Cape Lookout Bight, the methanogenic zone moves along the $\delta^{13}\text{C}$ gradient in response to the seasonal changes in the depth of sulfate penetration (Fig.4). In addition, the $\delta^{13}\text{C}$ profiles of Σ CO₂ respond to the seasonal changes in organic matter remineralization rates. Thus, the methanogens are exposed to different isotopic compositions of CO₂ throughout the year because of the two phenomena. The temporal CO₂ signal has been estimated by calculating the isotopic composition of CO₂ in equilibrium with HCO₃⁻ at the peak of the CO₂-reducing zone for each month that Σ CO₂ profiles were available (Blair and Boehme, submitted; S.E. Boehme, Ph.D. thesis, North Carolina State University, Raleigh, in prep.). The peak of the CO₂-reduction zone approximately coincides with the shallowmost depth where the sulfate concentration is less than

1.0±0.5 mM (21,22). The relative contributions of the CO₂, HCO₃⁻ and CO₃⁼ to the ΣCO₂ pool were estimated, assuming mutual chemical equilibrium (53), for the average pore water pH of 6.95 (J.P. Chanton, Ph.D. thesis, Univ. North Carolina, Chapel Hill; N.E. Blair, unpublished results). The isotopic composition of the CO₂ was estimated by solving the following equations simultaneously,

$$\delta^{13}\text{C}(\Sigma\text{CO}_2) = x\delta^{13}\text{C}(\text{CO}_2) + y\delta^{13}\text{C}(\text{HCO}_3^-) + z\delta^{13}\text{C}(\text{CO}_3^{=}) \quad (4)$$

$$\alpha(\text{HCO}_3^-/\text{CO}_2) = [10^3 + \delta^{13}\text{C}(\text{HCO}_3^-)] / [10^3 + \delta^{13}\text{C}(\text{CO}_2)] \quad (5)$$

$$\delta^{13}\text{C}(\text{HCO}_3^-) = \delta^{13}\text{C}(\text{CO}_3^{=}), \quad (6)$$

where x,y,z represent the fractions of each of the dissolved components. The δ¹³C values of the HCO₃⁻ and CO₃⁼ ions are assumed to be equivalent (equation 6) to simplify the calculations. Theoretical studies indicate that the HCO₃⁻ ion may be enriched in ¹³C by 1.4-1.7 per mil for the temperature range involved (23). For the given pH, the CO₃⁼ ion represents less than 1% of the ΣCO₂ pool, thus the small isotopic difference is considered insignificant. The equilibrium fractionation factor is given by

$$\ln\alpha(\text{HCO}_3^-/\text{CO}_2) = (9.552/T) - 0.0241 \quad (7)$$

where temperature (T) is in Kelvin (26). The resulting CO₂ δ¹³C values as a function of time are shown in Fig. 3c. The seasonal

isotopic variations are large and clearly must have a significant effect on the methane $\delta^{13}\text{C}$ values.

The fractionation factor for CO_2 -reduction ranges from 1.03 to 1.06 in cultures (3,4,27,29). The evidence for a temperature effect on the fractionation factor, while expected, is equivocal and may be dependent on culture conditions. We have attempted to estimate the *in situ* fractionation factor using data associated with the two temperature extremes at this site. At 7.8°C (Feb.), the $\delta^{13}\text{C}$ values of the CH_4 and CO_2 were -61.7 and -3.6, respectively. Using the equation

$$\alpha_{\text{CO}_2} = [\delta^{13}\text{C}(\text{CO}_2) + 10^3] / [\delta^{13}\text{C}(\text{CH}_4) + 10^3], \quad (8)$$

α_{CO_2} was calculated to be 1.062, during a period of time when it has been assumed that methane was produced predominantly via CO_2 -reduction. In August ($T=26.5^\circ\text{C}$), the $\delta^{13}\text{C}$ of the methane was -57.7. Given that 26% of the methane is derived from acetate dissimilation, and $\delta^{13}\text{C}(\text{CH}_4/\text{Acet}) = -43$, then the $\delta^{13}\text{C}$ value of the methane produced via CO_2 -reduction ($\delta^{13}\text{C}(\text{CH}_4/\text{CO}_2)$) should be approximately -62.1. Finally, with $\delta^{13}\text{C}(\text{CO}_2) = -9.8$, we estimate $\alpha_{\text{CO}_2} = 1.056$ at 26.5°C . Fitting the two estimates to an Arrhenius temperature dependence, one obtains

$$\ln \alpha_{\text{CO}_2} = (25.0/T) - 0.029 \quad (9)$$

where temperature is in Kelvin. The seasonal variation of α_{CO_2} is

shown in Figure 3d. The isotopic composition of the methane produced from the CO₂ for the other months was calculated using

$$\delta^{13}\text{C}(\text{CH}_4/\text{CO}_2) = [\delta^{13}\text{C}(\text{CO}_2) + 10^3]/\alpha - 10^3 \quad (10)$$

and is shown in Figure 5a.

$\delta^{13}\text{C}(\text{CH}_4)$

The isotopic composition of the methane produced at A-1 is described simply by the mass balance relationship,

$$\delta^{13}\text{C}(\text{CH}_4) = F\delta^{13}\text{C}(\text{CH}_4/\text{Acet}) + (1-F)\delta^{13}\text{C}(\text{CH}_4/\text{CO}_2). \quad (11)$$

The calculated monthly $\delta^{13}\text{C}$ values, using the parameters in Figures 3a-d, are in excellent agreement with measured values for the period February to September (Fig. 5b). The movement of the methanogenic zone over the ΣCO_2 $\delta^{13}\text{C}$ gradient and the temporal variation of α_{CO_2} are responsible for the gradual depletion of ^{13}C in the methane between February and June. The onset of acetate dissimilation in July-August coupled with the change in $\delta^{13}\text{C}$ value of the CO₂ within the methanogenic zone results in a dramatic enrichment of ^{13}C in those months. The trend is reversed when acetate dissimilation ceases in late August. The subsequent ^{13}C -

depletion in October and November is caused by changes in α_{CO_2} and the $\delta^{13}\text{C}$ value of the CO_2 . The relatively poor fit of the model to the observed values in October and November may be because the model estimates instantaneous $\delta^{13}\text{C}$ values and the measured values represent a pooled product. The largest deviation between modelled and observed values would be expected at this time when the reservoir of methane is large and bubbling rates are low.

Implications for Freshwater Sediments

Methane produced in freshwater environments is often enriched in ^{13}C relative to biogenic gas from marine sediments (59). It has been hypothesized that this is due to the relatively greater importance of acetate dissimilation as a methane-producing pathway in freshwater systems (59). ^{14}C -tracer studies indicate that 50-70% of methane production is via acetoclastic processes ($F=0.5-0.7$; 12,37,53,60). Our calculations indicate that the methane derived from the acetate methyl group is enriched in ^{13}C relative to that from CO_2 -reduction, thus apparently confirming the hypothesis. The ^{13}C -enrichment is a consequence of the smaller fractionation factor and large degree of conversion of the methyl group to methane ($f=0.4$, see equation 3). In freshwater sediments, where $f=0.7-0.9$ (12,37,53;60), the potential ^{13}C -enrichment could be greater if the synthetic pathways of acetate and the associated isotope effects

are comparable to those at Cape Lookout. Other investigators, using culture and modelling results, have proposed that acetate synthesis in freshwater sediments occurs by a very different process, i.e. acetogenic CO₂-reduction (30). Acetate produced in this manner would be significantly depleted in ¹³C because the acetogenic process exhibits a large ($\alpha \cong 1.06$) isotope effect (30,48). However, ¹⁴C-tracer studies indicate that <2% of the acetate in eutrophic lake sediments is produced by CO₂-reduction (38). The results from Part 2 (1) suggest that the ecological niche of the acetogenic bacteria may be an opportunistic one. Application of the approach summarized in this report to freshwater systems should resolve the issue. Such work is currently underway.

SUMMARY

The isotopic composition of methane varies seasonally at a variety of sites (15,44). In the organic-rich marine sediments of Cape Lookout Bight, North Carolina, the carbon isotopic variations appear to be the result of three factors. During the period February-June, CO_2 -reduction is the dominant methanogenic pathway and the $\delta^{13}\text{C}$ variations are driven by the movement of the methanogenic zone along an isotopic gradient within the dissolved CO_2 pool. Changes in the relative rates of CO_2 -reduction and acetate dissimilation become the dominant factor from July to September. Throughout the whole time period, a temperature dependence on the fractionation factor for CO_2 -reduction may play a role controlling the methane $\delta^{13}\text{C}$ value.

The Cape Lookout model is the first to combine measured isotopic compositions of both methanogenic precursors, CO_2 and acetate, with measured rates of methanogenic processes. The agreement between model predictions and observed $\delta^{13}\text{C}$ values of methane verifies estimates of *in situ* fractionation factors associated with acetate cycling and methanogenesis. The model also indicates that methane produced by acetate dissimilation should be enriched in ^{13}C relative to that produced via CO_2 -reduction, thus verifying, in general terms, earlier hypotheses concerning the isotopic differences commonly observed between methane from freshwater and marine sediments (59).

ACKNOWLEDGEMENTS

We thank Chris Martens and his group for their invaluable assistance throughout this project. Jeff Chanton, Dan Albert, Bob Haddad and Carol Green provided critical field assistance. David Des Marais, Bill Showers and Randy Culp provided mass spectrometer time. We thank Marc Alperin for his helpful discussions and two anonymous colleagues for their critical reviews. Laboratory space and boating facilities were provided by the University of North Carolina Institute of Marine Sciences, Morehead City, NC. This research was supported by NASA grant NAGW-838 and PRF grant 17527-G2.

LITERATURE CITED

1. Alperin M.J., N.E. Blair, D.B. Albert and T.M. Hoehler. The carbon isotope biogeochemistry of methane production in anoxic sediments. 2. A laboratory experiment. This volume.
2. Alperin M.J., W.S. Reeburgh, and M.J. Whiticar. 1988. Carbon and hydrogen isotope fractionation resulting from anaerobic methane oxidation. *Global Biogeochem. Cycles* 2:279-288.
3. Balabane M., E. Galimov, M. Hermann, and R. Letolle. 1987. Hydrogen and carbon isotope fractionation during experimental production of bacterial methane. *Org. Geochem.* 11:115-119.
4. Belyaev S.S., R. Wolkin, W.R. Kenealy, M.J. DeNiro, S. Epstein, and J.G. Zeikus. 1983. Methanogenic bacteria from the Bondyuzhskoe Oil field: General characterization and analysis of stable-carbon isotopic fractionation. *Appl. Environ. Microbiol.* 45:691-697.
5. Blair N.E. and W.D. Carter, Jr. 1992. The carbon isotope biogeochemistry of acetate from a methanogenic marine sediment. *Geochim. Cosmochim. Acta* 56:1247-1258.
6. Blair N., A. Leu, E. Muñoz, J. Olsen, E. Kwong, and D.J. Des Marais. 1985. Carbon isotopic fractionation in heterotrophic microbial metabolism. *Appl. Environ. Microbiol.* 50:996-1001.
7. Blair N.E., C.S. Martens, and D.J. Des Marais. 1987. Natural abundances of carbon isotopes in acetate from a coastal maine sediment. *Science* 236:66-68.
8. Blake D.R. and F.S. Rowland. 1988. Continuing worldwide increase in tropospheric methane, 1978 to 1987. *Science* 239:1129-1131.
9. Burke R.A. Jr., C.S. Martens, and W.M. Sackett. 1988. Seasonal variations of D/H and $^{13}\text{C}/^{12}\text{C}$ ratios of microbial methane in surface sediments. *Nature* 332:829-831.
10. Buswell A.M. and F.W. Sollo, Jr. 1948. The mechanism of methane fermentation. *J. Am. Chem. Soc.* 70:1778-1780.
11. Canuel E.A., C.S. Martens and L.K. Benninger. 1990. Seasonal variations in ^7Be activity in the sediments of Cape Lookout Bight, North Carolina. *Geochim. Cosmochim. Acta* 54:237-245.
12. Cappenberg TH.E. and R.A. Prins. 1974. Interrelations between sulfate-reducing and methane-producing bacteria in bottom deposits of a fresh-water lake. III. Experiments with ^{14}C -labeled substrates. *Antonie van Leeuwenhoek* 40:457-469.

13. Chanton J.P., C.S. Martens and G.W. Kipphut. 1983. Lead-210 sediment geochronology in a changing coastal environment. *Geochim. Cosmochim. Acta* 47:1791-1804.
14. Chanton J.P., C.S. Martens, and M.B. Goldhaber. 1987. Biogeochemical cycling in an organic-rich coastal marine basin. 7. Sulfur mass balance, oxygen uptake and sulfide retention. *Geochim. Cosmochim. Acta* 51:1187-1199.
15. Chanton J.P. and C.S. Martens. 1988. Seasonal variations in ebullitive flux and carbon isotopic composition of methane in a tidal freshwater estuary. *Global Biogeochemical Cycles* 2:289-298.
16. Cicerone R.J. and R.S. Oremland. 1988. Biogeochemical Aspects of Atmospheric Methane. *Global Biogeochemical Cycles* 2:299-327.
17. Claypool G.E. and I.R. Kaplan. 1974. The origin and distribution of methane in marine sediments, p. 99-139. In I.R. Kaplan (ed.), *Natural Gases in Marine Sediments*-Plenum Press.
18. Coleman D.D., J.B. Risatti, and M. Schoell. 1981. Fractionation of carbon and hydrogen isotopes by methane-oxidizing bacteria. *Geochim. Cosmochim. Acta* 45:1033-1037.
19. Coplen T.B., C. Kendall and J. Hopple. 1983. Comparison of stable isotope reference samples. *Nature* 302:236-238.
20. Craig H. 1953. The geochemistry of the stable carbon isotopes. *Geochim. Cosmochim. Acta* 3:53-92.
21. Crill P.M. and C.S. Martens. 1983. Spatial and temporal fluctuations of methane production in anoxic, coastal marine sediments. *Limnol. Oceanogr.* 28:1117-1130.
22. Crill P.M. and C.S. Martens. 1986. Methane production from bicarbonate and acetate in an anoxic marine sediment. *Geochim. Cosmochim. Acta* 50:2089-2097.
23. Deines P., D. Langmuir and R.S. Harmon. 1974. Stable carbon isotope ratios and the existence of a gas phase in the evolution of carbonate ground waters. *Geochim. Cosmochim. Acta* 38:1147-1164.
24. Des Marais D.J. 1978. Variable-temperature cryogenic trap for the separation of gas mixtures. *Anal. Chem.* 50:1405-1406.
25. Dickinson R.E. and R.J. Cicerone. 1986. Future global warming from atmospheric trace gases. *Nature* 319:109-115.
26. Friedman I. and J.R. O'Neil. 1977. Compilation of stable isotope fractionation factors of geochemical interest. U.S. Geological Survey Professional Paper 440-KK.

27. Fuchs G., R. Thauer, H. Zeigler, and W. Stichler. 1979. Carbon isotope fractionation by *Methanobacterium thermoautotrophicum*. Arch. Microbiol. 120:135-139.
28. Games L.M. and J.M. Hayes. 1976. On the mechanisms of CO₂ and CH₄ production in natural anaerobic environments, p 51-73. In J.O. Nriagu (ed.), Proc. 2nd Int. Sym. on Environ. Biogeochem.- Michigan State Press.
29. Games L.M., J.M. Hayes, and R.P. Gunsalus. 1978. Methane-producing bacteria: natural fractionations of the stable carbon isotopes. Geochim. Cosmochim. Acta 42:1295-1297.
30. Gelwicks J.T., J.B. Risatti and J.M. Hayes. 1989. Carbon isotope effects associated with autotrophic acetogenesis. Org. Geochem. 14:441-446.
31. Grahame D.A. and T.C. Stadtman. 1987. In vitro methane and methyl coenzyme M formation from acetate: evidence that acetyl-CoA is the required intermediate activated form of acetate. Biochem. Biophys. Res. Commun. 147:254-258.
32. Haddad R.I. and C.S. Martens. 1987. Biogeochemical cycling in an organic-rich coastal marine basin: 9. Sources and accumulation rates of vascular plant-derived organic material. Geochim. Cosmochim. Acta 51:2991-3001.
33. Hayes J.M. 1983. Practice and principles of isotopic measurements in organic geochemistry, p 5-1 - 5-31. In W.G. Meinschein (ed.) Organic Geochemistry of Contemporaneous and Ancient Sediments - Soc. Econ. Paleontol. and Mineralog.
34. Krzycki J.A., W.R. Kenealy, M.J. DeNiro, and J.G. Zeikus. 1987. Stable carbon isotope fractionation by *Methanosarcina barkeri* during methanogenesis from acetate, methanol, or carbon dioxide-hydrogen. Appl. Environ. Microbiol. 53:2597-2599.
35. Kuivila K.M., J.W. Murray, and A.H. Devol. 1990. Methane production in the sulfate-depleted sediments of two marine basins. Geochim. Cosmochim. Acta 54:403-411.
36. LaZerte B.D. 1981. The relationship between total dissolved carbon dioxide and its stable carbon isotope ratio in aquatic sediments. Geochim. Cosmochim. Acta 45:647-656.
37. Lovley D.R. and M.J. Klug. 1982. Intermediary metabolism of organic matter in the sediments of a eutrophic lake. Appl. Environ. Microbiol. 43:552-560.

38. Lovley D.R. and M.J. Klug. 1983. Methanogenesis from methanol and methylamines and acetogenesis from hydrogen and carbon dioxide in the sediments of a eutrophic lake. *Appl. Environ. Microbiol.* 45:1310-1315.
39. Matthews D.E. and J.M. Hayes. 1978. Isotope ratio monitoring GC-MS. *Anal. Chem.* 50:1465-1473.
40. Martens C.S. and J.V. Klump. 1980. Biogeochemical cycling in an organic-rich coastal basin-I. Methane sediment-water exchange processes. *Geochim. Cosmochim. Acta* 44:471-490.
41. Martens C.S. and J.V. Klump. 1984. Biogeochemical cycling in an organic-rich coastal marine basin. 4. An organic carbon budget for sediments dominated by sulfate reduction and methanogenesis. *Geochim. Cosmochim. Acta* 48:1987-2004.
42. Martens C.S. and J.P. Chanton. 1989. Radon as a tracer of biogenic gas equilibration and transport from methane-saturated sediments. *J. Geophys. Res.* D3 94:3451-3459.
43. Martens C.S., G.W. Kipphut and J.V. Klump. 1980. Sediment-water chemical exchange in the coastal zone traced by in situ radon-222 flux measurements. *Science* 208:285-288.
44. Martens C.S., N.E. Blair, C.D. Green, and D.J. Des Marais. 1986. Seasonal Variations in the Stable Carbon Isotopic Signature of Biogenic Methane in a Coastal Sediment. *Science* 233:1300-1303.
45. Meinschein W.G., G.G.L. Rinaldi, J.M. Hayes, and D.A. Schoeller. 1974. Intramolecular isotopic order in biologically produced acetic acid. *Biomed. Mass Spectrom.* 1:172-174.
46. Nissenbaum A., B.J. Presley, and I.R. Kaplan. 1968. Early diagenesis in a reducing fjord, Saanich Inlet, British Columbia-I. Chemical and isotopic changes in major components of interstitial water. *Geochim. Cosmochim. Acta* 36:1007-1027.
47. Oakwood T.S. and M.R. Miller. 1950. The decarboxylation of simple fatty acids. *J. Am. Chem. Soc.* 72:1849.
48. Preuß A., R. Schauder, G. Fuchs, and W. Stichler. 1989. Carbon isotope fractionation by autotrophic bacteria with three different CO₂ fixation pathways. *Z. Naturforsch.* 44c:397-402.
49. Reeburgh W.S. 1967. An improved interstitial water sampler. *Limnol. Oceanogr.* 12:163-165.
50. Rice D.D. and G.E. Claypool. 1981. Generation, accumulation and resource potential of biogenic gas. *Bull. AAPG* 65:5-25.

51. Sansone F.J. and C.S. Martens. 1982. Volatile fatty acid cycling in organic-rich marine sediments. *Geochim. Cosmochim. Acta* 46:1575-1589.
52. Schoell M. 1980. The hydrogen and carbon isotopic composition of methane from natural gases of various origins. *Geochim. Cosmochim. Acta* 44:649-661.
53. Schutz H., W. Seiler and R. Conrad. 1989. Processes involved in formation and emission of methane in rice paddies. *Biogeochemistry* 7:33-53.
54. Stadtman T.C. and H.A. Barker. 1949. Studies on the methane fermentation. VII. Tracer experiments on the mechanism of methane formation. *J. Biochem.* 21:256-264.
55. Stevens C.M. and F.E. Rust. 1982. The carbon isotopic composition of atmospheric methane. *J. Geophys. Res.* 87:4879-4882.
56. Stumm W. and J.J. Morgan. 1981. *Aquatic Chemistry*. 2nd edition, p 173-177. John Wiley and Sons, New York.
57. Tarvin D. and A.M. Buswell. 1934. The methane fermentation of organic acids and carbohydrates. *J. Am. Chem. Soc.* 56:1751-1755.
58. Thauer R.K., D. Moller-Zinkhan, and A.M. Spormann. 1989. Biochemistry of acetate catabolism in anaerobic chemotrophic bacteria. *Annu. Rev. Microbiol.* 43:43-67.
59. Whiticar M.J., E. Faber, and M. Schoell. 1986. Biogenic methane formation in marine and freshwater environments: CO₂ reduction vs. acetate fermentation- Isotope evidence. *Geochim. Cosmochim. Acta* 50:693-709.
60. Winfrey M.R. and J.G. Zeikus. 1979. Anaerobic metabolism of intermediate methane precursors in Lake Mendota. *Appl. Environ. Microbiol.* 37:244-253.
61. Zeikus J.G. 1983. Metabolism of one-carbon compounds by chemotrophic anaerobes. *Adv. Microbiol. Physiol.* 24:215-299.

TABLE 1. Carbon isotopic compositions of methane bubbles from Cape Lookout Bight, North Carolina

Month	$\delta^{13}\text{C}$		
	1983 ¹	1984 ¹	1986 ²
February		-63.4	-60.0
April		-63.8	-61.7
May		-66.2	-60.8
June	-64.5	-64.1	
July	-62.2	-60.0	-58.5
August	-59.6	-57.6	-55.9
September	-60.3	-58.0	-58.0
October	-60.0		-58.3
November	-62.2		-59.4

¹ Data from (44).

² Data from S.E. Boehme, Ph.D. dissertation, North Carolina State University, Raleigh, in progress.

TABLE 2: Carbon isotopic composition ($\delta^{13}\text{C}$) of porewater ΣCO_2 from Cape Lookout Bight, North Carolina.

Depth (cm)	2/20/86		7/1/86	
	core 1	core 2	core 1	core 2
bottom water	0.7			
0-1	-2.6		-10.4	-9.4
1-2	-1.0	0.4	-11.6	-10.3
2-3	-1.0	1.2	-12.0	-11.2
3-4		-1.0	-11.8	-9.5
4-5	-1.9		-11.5	-9.6
5-6	-2.7		-11.1	
6-7	-2.2	-2.9		
7-8		-3.5	-9.7	-9.2
8-9		-3.2		
9-10	-1.6	-2.4	-7.5	-7.2
10-12				
11-12	0.0			
12-14		-2.2		
16-18		-0.5	-1.9	
20-22		1.4		
24-25	4.6			
24-26			3.8	2.8
28-30		5.1		
29-31	6.6			
32-34		6.7		7.0
35-36	8.1			
36-38		8.0		
37-39	7.8			

FIGURE CAPTIONS

Figure 1: Cape Lookout Bight, North Carolina. The sampling station is designated A-1.

Figure 2: The $\delta^{13}\text{C}$ values of acetate and its methyl group as a function of depth. The $\delta^{13}\text{C}$ values are averages of results from 8/86 and 7/87 (5). The fraction of the methyl group which is converted to methane (f) as a function of depth (22,51).

Figure 3: Model parameters as a function of time.

3a: Average monthly temperature at Cape Lookout (40,41,44 this study).

3b: The fraction of methane derived from the dissimilation of acetate (F).

3c: The $\delta^{13}\text{C}$ value of dissolved CO_2 in the methanogenic zone.

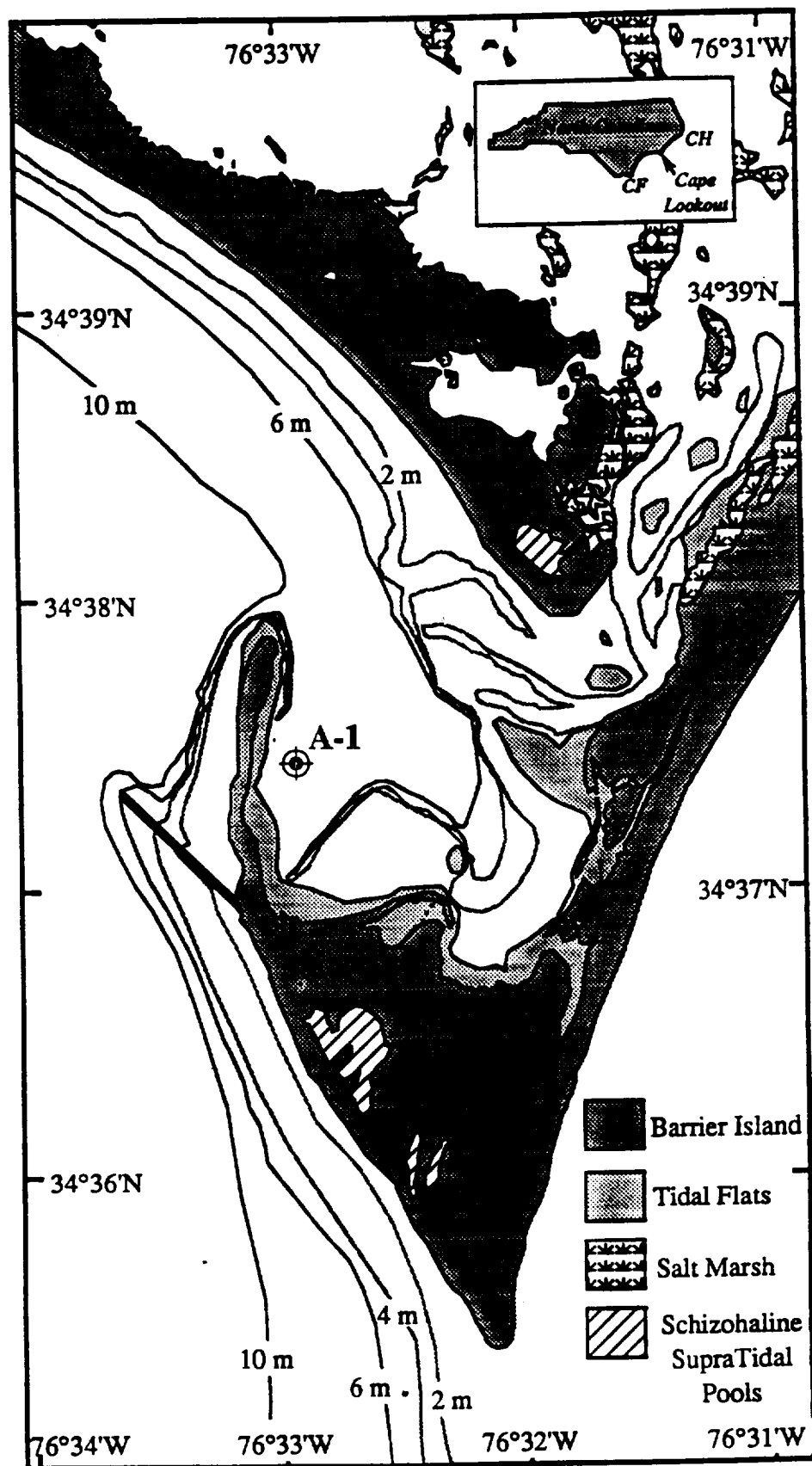
3d: The fractionation factor (α) for CO_2 -reduction.

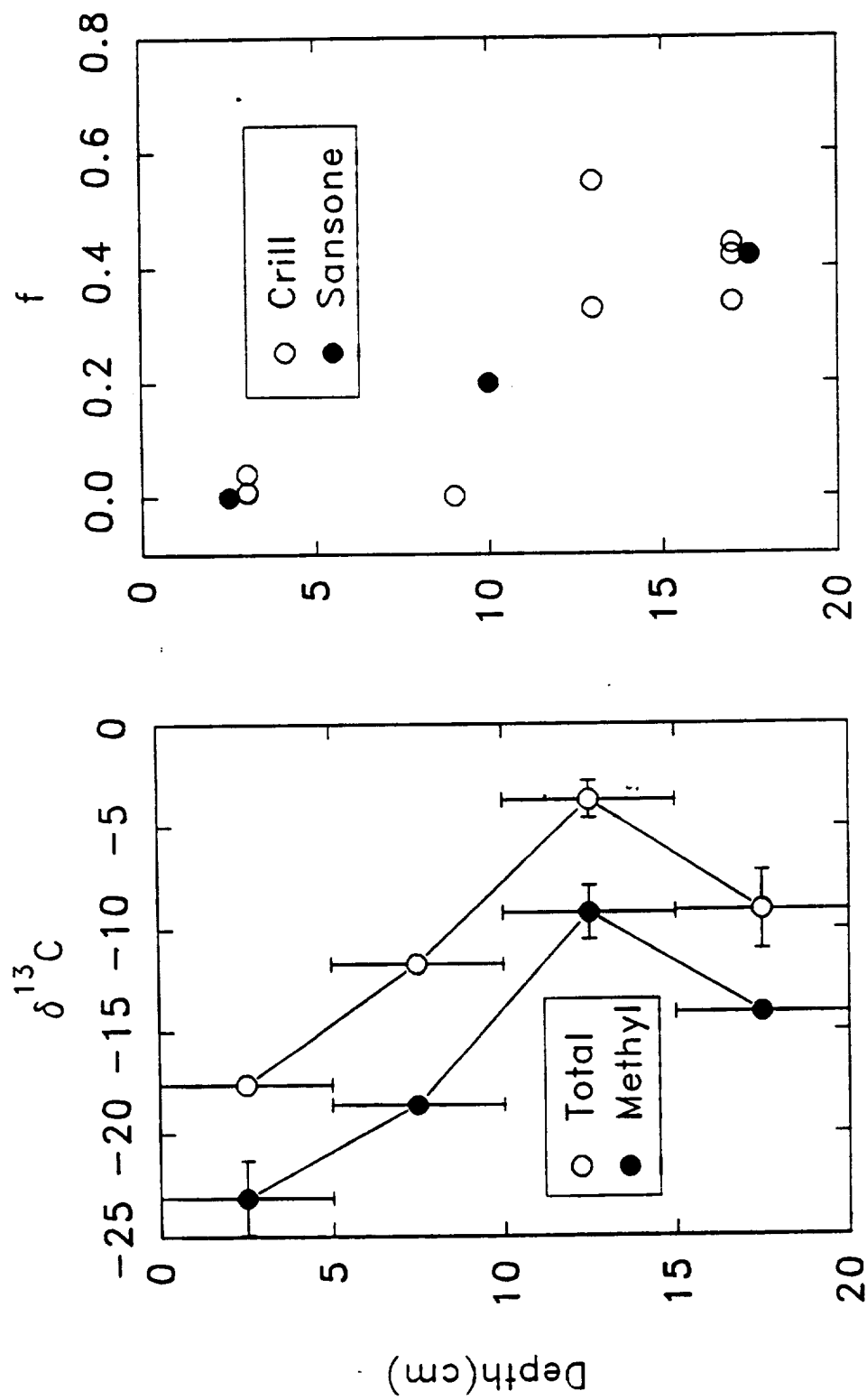
Figure 4: The $\delta^{13}\text{C}$ values of ΣCO_2 as a function of depth within the sediment from Cape Lookout. Profiles from February and July, 1986 are shown. The dotted horizontal lines represent the depths at which dissolved sulfate concentrations are equal to or less than 1.0 ± 0.5 mM in February and July.

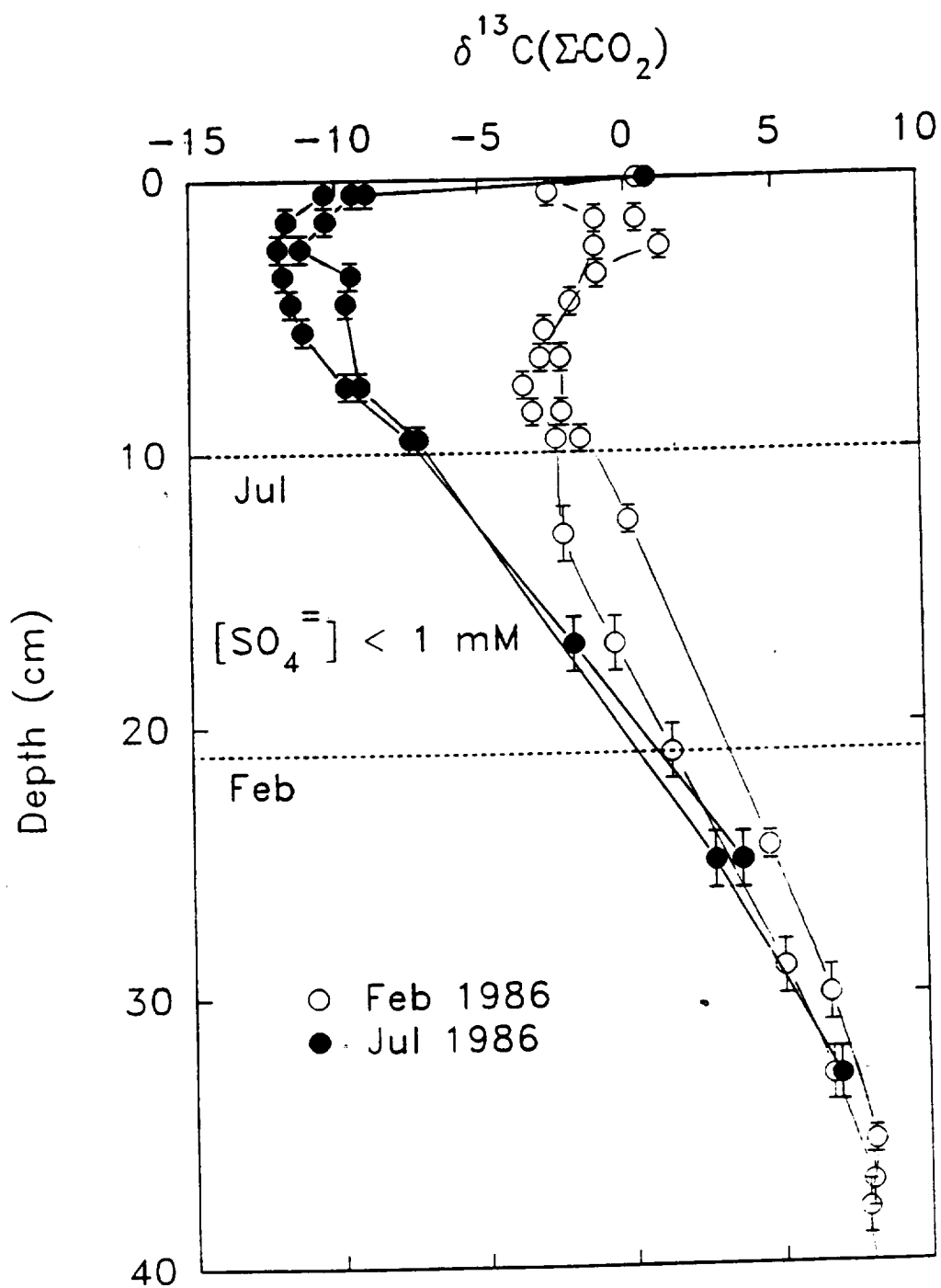
Figure 5: The measured and calculated $\delta^{13}\text{C}$ values of methane from Cape Lookout.

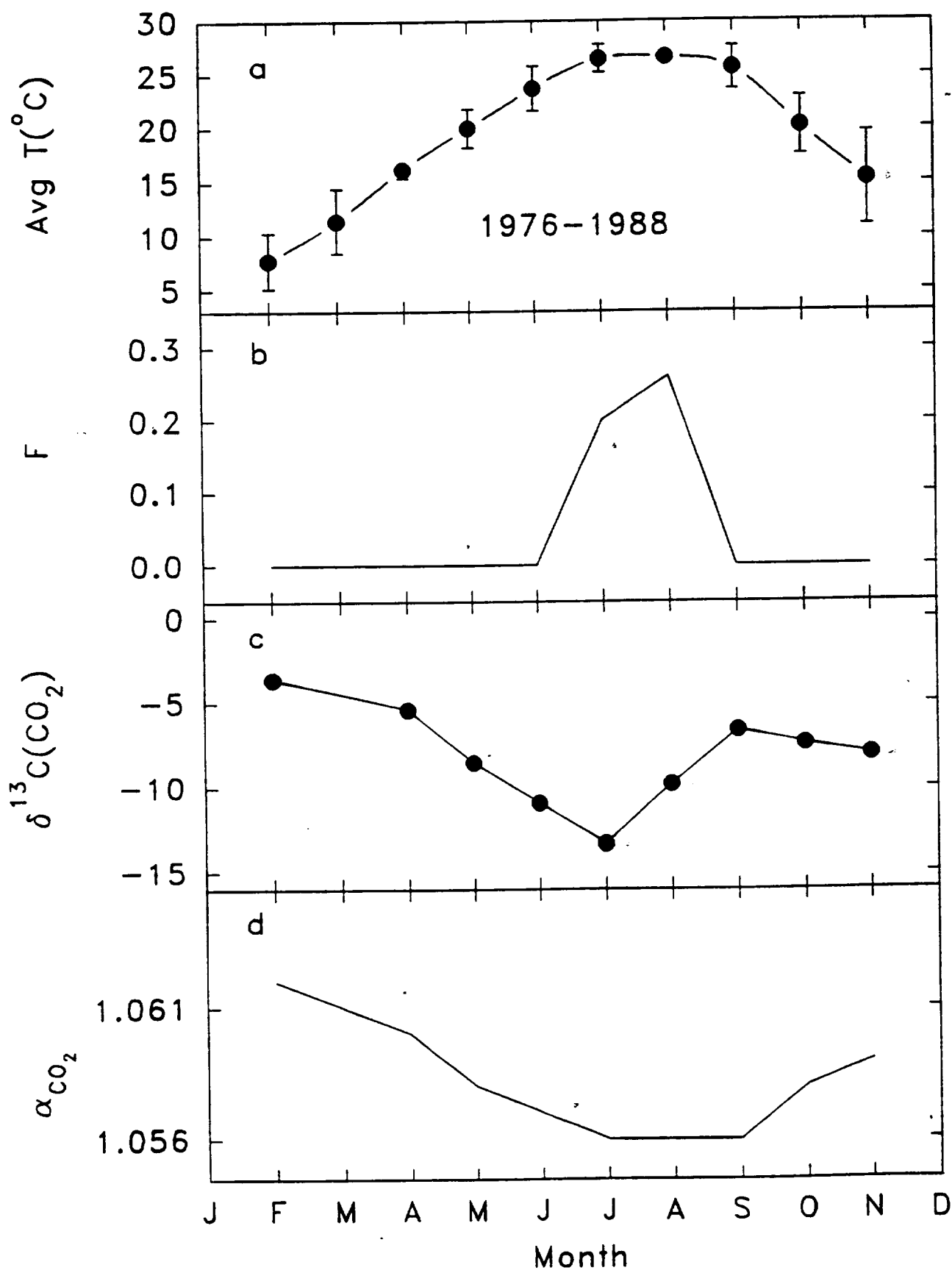
5a: Calculated $\delta^{13}\text{C}$ values of methane produced from CO_2 -reduction.

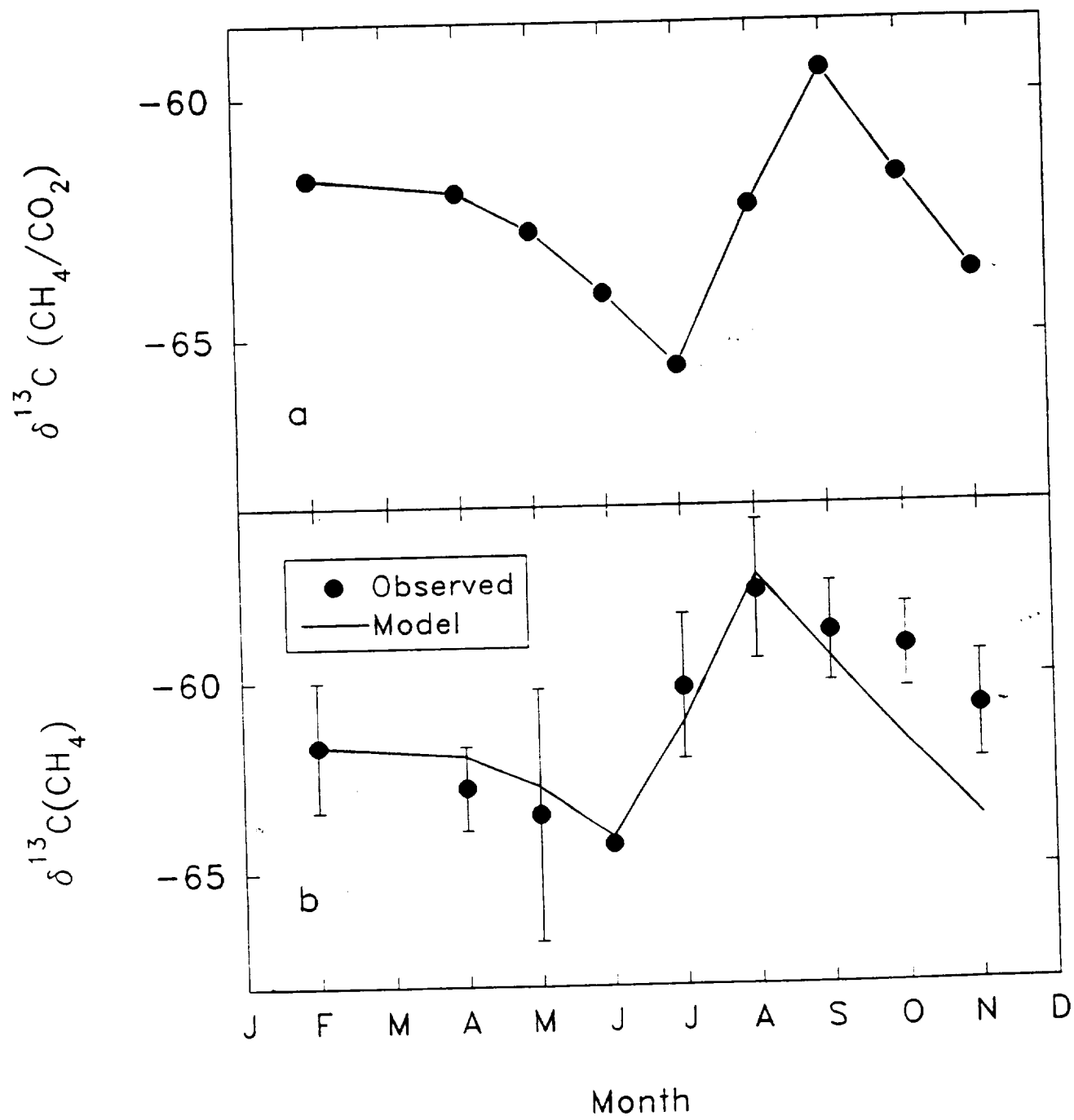
5b: The monthly average measured $\delta^{13}\text{C}$ values of methane bubbles for the period 1983-1984 and 1986 (●). The calculated $\delta^{13}\text{C}$ values using the model described in the text (—).











Reprinted from
GEOCHIMICA ET COSMOCHIMICA ACTA
Vol. 56, No. 3, March 1992

The carbon isotope biogeochemistry of acetate from a methanogenic marine sediment

N. E. BLAIR and W. D. CARTER JR.

Department of Marine, Earth, and Atmospheric Sciences, North Carolina State University, Raleigh, NC 27695-8208, USA

PERGAMON PRESS

New York / Oxford / Toronto / Paris / Frankfurt / Sydney

BLUE

The carbon isotope biogeochemistry of acetate from a methanogenic marine sediment

N. E. BLAIR and W. D. CARTER JR.*

Department of Marine, Earth, and Atmospheric Sciences, North Carolina State University, Raleigh, NC 27695-8208, USA

(Received May 14, 1991; accepted in revised form December 16, 1991)

Abstract—The $\delta^{13}\text{C}$ value of porewater acetate isolated from the anoxic sediments of Cape Lookout Bight, North Carolina, ranged from -17.6‰ in the sulfate reduction zone to -2.8‰ in the underlying methanogenic zone. The large ^{13}C -enrichment in the sulfate-depleted sediments appears to be associated with the dissimilation of acetate to CH_4 and CO_2 . Fractionation factors for that process were estimated to be 1.032 ± 0.014 and 1.036 ± 0.019 for the methyl and carboxyl groups. A subsurface maximum in $\delta^{13}\text{C}$ of the total acetate molecule, as well as the methyl and carboxyl carbons at 10–15 cm depth within the sediment column indicates that changes in the relative rates of acetate cycling pathways occur in the methanogenic zone. The methyl group of the acetate was depleted in ^{13}C by 7–14‰ relative to the carboxyl moiety. The intramolecular heterogeneity may be the result of both synthetic and catabolic isotope effects.

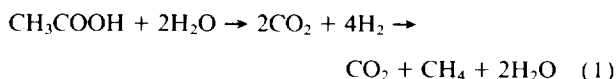
INTRODUCTION

ACETATE IS A KEY INTERMEDIATE in the early diagenesis of organic matter. Acetate can be produced by anaerobic bacteria via the degradation of a wide variety of organic compounds, including amino acids (BARKER, 1981; STAMS and HANSEN, 1984), carbohydrates (WINTER and WOLFE, 1980; BHARATI et al., 1980; LAUBE and MARTIN, 1981; LJUNGDAHL and WOOD, 1982; JONES et al., 1984; and many others), and organic acids and alcohols (BRYANT et al., 1977; MCINERNEY et al., 1979; MCINERNEY and BRYANT, 1981; KOCH et al., 1983; EICHLER and SCHINK, 1984; STIEB and SCHINK, 1985, 1986; KREMER et al., 1988). Bacteria capable of producing acetate via CO_2 -reduction with H_2 have also been identified (BRAUN et al., 1979, 1981; LEIGH et al., 1981; LJUNGDAHL and WOOD, 1982). The dominant microbial populations responsible for acetate synthesis and the relative importance of the different synthetic pathways in marine sediments are poorly understood.

Acetate is rapidly consumed in sediments by microorganisms linked with terminal oxidative processes such as sulfate reduction and methanogenesis. Sulfate-reducing bacteria appear to be responsible for the oxidation of >95% of the acetate in organic-rich marine sediments (WINFREY and WARD, 1983; SHAW et al., 1984). In sulfate-depleted marine and freshwater sediments, acetate is disproportionated to CH_4 and CO_2 (WARFORD et al., 1979; WINFREY and ZEIKUS, 1979a; SANSONE and MARTENS, 1981, 1982; LOVLEY and KLUG, 1982; CRILL and MARTENS, 1986; SCHUTZ et al., 1989; KUIVILA et al., 1990). Approximately 25–50% of the methane production in organic-rich marine sediments and as much as 60–70% in freshwater sediments results from the dissimilation of acetate (CAPPENBERG and PRINS, 1974; WINFREY and ZEIKUS, 1979a; LOVLEY and KLUG, 1982; CRILL and MARTENS, 1986; KUIVILA et al., 1990). The dissimilation process occurs only in the sulfate-depleted portion of the sed-

iment column because of the competition for acetate between the methanogens and sulfate reducers (SCHONHEIT et al., 1982; LOVLEY and KLUG, 1983a).

In addition to the methanogenic archaeobacteria, other microorganisms may be involved in the catabolism of acetate in sulfate-depleted sediments. Van Niel proposed the methane-producing pathway:



as an alternative process to the direct dissimilation of acetate to methane and CO_2 (BARKER, 1936). An organism capable of the first step of the reaction, the production of CO_2 and H_2 from acetate, has been isolated from a methane-producing thermophilic digester (ZINDER and KOCH, 1984). The microorganism, nicknamed "Reversibacterium," exists in a syntrophic relationship with hydrogen-utilizing methanogens. ^{14}C -tracer studies have indicated that acetate oxidation to CO_2 is an important process in sulfate-depleted marine sediments (WARFORD et al., 1979; SANSONE and MARTENS, 1981, 1982; CRILL and MARTENS, 1986). It has been proposed that an interspecies H_2 -transfer consortium between a sulfate reducer and a methanogen may be responsible for pathway (1) in marine sediments (SANSONE and MARTENS, 1982). Alternatively, the acetate oxidation may be mediated by a sulfur-reducing bacterium (WARFORD et al., 1979; WINFREY and ZEIKUS, 1979b) similar to the freshwater *Desulfuromonas acetoxidans* (GEBHARDT et al., 1985).

Isotope effects which might be associated with acetate cycling would have a significant, if not dominant, influence on the isotopic composition of the diagenetic products, ΣCO_2 and CH_4 (LAZERTE, 1981; WHITICAR et al., 1986). For instance, differences in the $\delta^{13}\text{C}$ and δD values of methane from marine and freshwater environments have been attributed to differences in the relative importance of the acetate dissimilation and CO_2 -reduction pathways (WHITICAR et al., 1986). Similarly, seasonal variations in the isotopic composition of methane from anoxic sediments have been hy-

* Present address: Archer Daniels Midland Co., PO Box 10640, Southport, NC 28461, USA.

pothesized to result from changes in acetate cycling processes (MARTENS et al., 1986; BURKE et al., 1988; CHANTON and MARTENS, 1988). Our ability to test those hypotheses, and more generally the development of quantitative models which describe the biogeochemical controls of the carbon isotopic compositions of ΣCO_2 and CH_4 , have been limited by the lack of information concerning the isotopic systematics of acetate turnover (GAMES and HAYES, 1976; LAZERTE, 1981).

In an attempt to address some of the issues in question concerning acetate cycling pathways and the associated isotopic fractionations, we have made $\delta^{13}\text{C}$ measurements of acetate and its methyl group isolated from the anoxic marine sediments of Cape Lookout Bight, North Carolina. Preliminary measurements suggested that large carbon isotope effects accompany the natural turnover of acetate (BLAIR et al., 1987). The measurements presented in this report provide new information concerning the relative rates and spatial distribution of acetate cycling processes, and the carbon isotope fractionation which occurs during the turnover of acetate.

FIELD SITE

Cape Lookout Bight, North Carolina, is a 1–2 km² coastal basin located 115 km SW of Cape Hatteras on the Outer Banks (MARTENS and KLUMP, 1980; MARTENS et al., 1980). Fine-grained sediment with an organic content up to 4% dry weight (MARTENS and KLUMP, 1984), accumulates at a rate of 8–12 cm/yr (CHANTON et al., 1983; CANUEL et al., 1990) at the sampling station, A-1. The organic matter appears to be derived from phytoplankton and seagrass debris (HADDAD and MARTENS, 1987).

The rapid flux of metabolizable organic matter to the seabed results in a high rate of organic carbon remineralization (MARTENS and KLUMP, 1984). Sulfate reduction, occurring in the upper 10 cm of sediment during summer months, and methanogenesis, which occurs in the underlying zone (CRILL and MARTENS, 1983), are the dominant diagenetic processes at this site and, respectively, account for $68 \pm 20\%$ and $32 \pm 16\%$ of the organic carbon remineralization (MARTENS and KLUMP, 1984). Acetate concentrations over 100 μM have been found in the summer months at the interface between the sulfate-reducing and methane-producing zones (SANSONE and MARTENS, 1982). Approximately 20–30% of the methane is produced via acetate dissimilation (CRILL and MARTENS, 1986).

METHODS

Diver-collected cores were obtained at A-1 with 9.5 cm diameter lucite tubes. Normally, the acetate cores were processed immediately after collection onboard ship. The porewater from cores collected on August 14, 1986, was isolated with a sediment press (REEBURGH, 1967). The porewater samples were frozen immediately after collection and stored at -86°C until analysis. One core from that date was transported to and processed at the Institute of Marine Sciences (Morehead City) in the same manner. Because of our concern for potential artifacts associated with the use of the sediment press and the possibility that the isotopic signature of the acetate may change rapidly after core recovery, samples collected on July 21, 1987, were treated in one of two methods. Each sampling interval was split with one portion immediately centrifuged at 8000 rpm for 10 min. The porewater sample (40 mL) was passed through a Whatman GFA filter, acidified with 5 mL of HPLC grade 85% H_3PO_4 (J. T. Baker)

and frozen in polypropylene bottles (Nalgene). The second portion of each sediment interval was rapidly mixed with 50 mL of a 1:1 methanol- H_2O mixture and frozen. The cores were sampled in less than 15 min. after retrieval. The methanol-porewater mixture was isolated later in the laboratory by centrifugation as described above.

The isotopic analysis of porewater acetate followed a modified procedure of BLAIR et al. (1985, 1987). The porewater sample was acidified to pH 1 with concentrated H_3PO_4 and distilled in vacuo cryogenically to produce a volatile acid fraction. The basified (pH > 11) distillate was dried in a Teflon[®] beaker under N_2 at 135°C . The dried salts were dissolved in 1.0 mL water and 0.9 mL concentrated H_3PO_4 . The resulting mixture was distilled in vacuo cryogenically. The distilling pot was maintained at 90 – 95°C . The resulting solids in the pot were redissolved with 1.0 mL of water and distilled as above. This procedure was repeated a third time with 2.0 mL of water. The volatile acids were concentrated approximately 25-fold with this method.

The volatile acids were separated on a 10 μm RP-8 Lichrosorb column (25 cm \times 4.6 mm i.d., Alltech Assoc.) and detected at 210 nm (Lambda-Max Model 481, Waters Chromatog. Div.). The mobile phase was 0.01 M H_2SO_4 maintained at 0.63 mL/min. The acetate was separated from the H_2SO_4 and concentrated by the following drying/distillation steps. The acetate fraction collected from the liquid chromatograph was brought to pH 11 with 20% NaOH and dried, as described above. The salts were dissolved in 50 μL water and 200 μL H_3PO_4 , and the resulting solution was distilled as above. The distillate was stored frozen until needed.

The isolated acetate was converted to CO_2 for isotopic analysis with a gas chromatograph-combustion system (MATTHEWS and HAYES, 1978; DES MARAIS, 1978). The Carlo Erba HRGC 5300 Mega series was outfitted with a packed column injector (150°C) and a Superox-FA wide bore capillary column (0.53 mm o.d., 30 m length, Alltech Assoc.). The helium flowrate was 3 mL/min and the temperature was programmed to hold at 80°C for 15 min. and ramped to 110°C at $10^\circ/\text{min}$. The sample was swept through the combustion furnace (2 mm i.d. quartz tube packed with 80–100 mesh CuO , 780 – 790°C) with a make-up gas (12 mL/min He). The resulting CO_2 was monitored with a thermal conductivity detector (Gow-Mac Model 40-400) and collected in a $\frac{1}{8}$ in. stainless steel multiple loop trap immersed in liquid nitrogen. The CO_2 was then purified cryogenically and stored in a 6 mm o.d. Pyrex breakseal until isotopic analysis. Acetate standards producing >0.3 $\mu\text{moles CO}_2$ per 10 μL injection were found to have $\delta^{13}\text{C}$ values within 0.4‰ of the accepted values, which were determined by either bomb combustion (BLAIR et al., 1985) or direct gas chromatograph (GC) combustion of large samples. This sample size would typically translate into an original porewater concentration of >30 μM . Smaller standards were depleted in ^{13}C by more than 0.5‰. Accordingly, all $\delta^{13}\text{C}$ analyses reported in this paper were from samples >0.3 $\mu\text{moles C/injection}$. The sensitivity of this procedure is comparable to that reported for an alternative method (GELWICKS and HAYES, 1990).

The isotopic analysis of the acetate methyl group was accomplished by the pyrolysis of sodium acetate (OAKWOOD and MILLER, 1950; MEINSCHEN et al., 1974; BLAIR et al., 1985). A 200:1 mixture of NaOH and acetate (from the last distillation) was dried under N_2 at 135°C in a quartz tube (9 mm i.d. \times 20 cm long). The tube was evacuated after drying and heated to 500°C . Methane, which is derived from the methyl group, was quantitatively collected, measured, and injected into the GC combustion system via Toepler pump. The purification of the methane was accomplished on a 2.5 m long \times 2 mm i.d. stainless steel column packed with 100–150 mesh Porasil B (Alltech Assoc.) at room temperature. The CO_2 resulting from the combustion of the methane was treated as above for isotopic analysis. As little as 1.6 μmoles of acetate could be analyzed with an accuracy and precision of 0.3‰.

Samples for the $\delta^{13}\text{C}$ measurements of the total organic carbon (TOC) fraction were prepared by one of two methods. Samples from 1983 were prepared by a bomb combustion method described previously (BLAIR et al., 1987). Samples from 1986–87 were treated with a modified procedure. Between 0.7 and 1.0 grams of wet sediment were slurried with 1N HCl until bubbling ceased, after which the sample was lyophilized. Approximately 20–30 mg of the homogenized sample were combusted in tin boats with a Carlo Erba 1500 CNS

analyzer (UNC-Chapel Hill, Marine Sciences). The resulting CO_2 was collected in a $\frac{1}{8}$ in. stainless steel multiple looped trap immersed in liquid nitrogen. The CO_2 was subsequently transferred cryogenically and sealed in a 6 mm o.d. Pyrex tube for later isotopic analysis. The $\delta^{13}\text{C}$ values of standards prepared by the CNS analyzer were within 0.3‰ of those prepared by the bomb combustion method referenced above.

Lipid fractions were prepared for isotopic analysis by sonicating 150 mg of freeze-dried sediment with 5 mL of 1:1 methanol-toluene (Burdick and Jackson) for 10 min. The mixture was vortexed for 2 min. The extract-sediment mixture was separated by centrifugation, and the sediment was reextracted as above. The extracts were combined, and the solvent was removed by rotary evaporation. The sample was saponified with a 1:1 aqueous 1 M KOH-methanol solution (J. T. Baker, Burdick and Jackson) at 77°C for 2 h. The KOH pellets had been pretreated by heating at 490°C for 25 min to remove organic contamination. The saponified lipid mixture was extracted three times with previously distilled petroleum ether (40–45°C) to produce the neutral lipid fraction. The KOH mixture was then acidified and reextracted with previously distilled CHCl_3 to produce the fatty acid fraction. The volumes of both fractions were reduced by rotary evaporation. The samples were transferred to Ag boats with CHCl_3 , and the solvent was removed in vacuo. The samples were converted to CO_2 for $\delta^{13}\text{C}$ analysis by bomb combustion (BLAIR et al., 1985).

The $\delta^{13}\text{C}$ measurements of the CO_2 from the various preparations were analyzed on either a modified Nuclide 6-60 RMS (NASA-Ames Research Center) or one of two Finnigan MAT 251 mass spectrometers (NCSU Stable Isotope Laboratory and the University of Georgia Center for Applied Isotope Studies). A cross-calibration of a CO_2 standard by the three facilities produced results consistent to within 0.25‰. Procedural blanks were collected and used to correct the results of all analyses.

Dissolved sulfate was measured on 5 mL of porewater by the gravimetric analysis of the precipitated barium salt (CHANTON, 1985; CHANTON et al., 1987). Sulfide was removed immediately after the recovery of the porewater sample by the addition of ZnCl_2 , followed by the filtration of the zinc sulfide precipitate. The accuracy of this procedure is typically ± 0.5 mM (CHANTON, 1985).

RESULTS

The $\delta^{13}\text{C}$ values of the TOC from Cape Lookout Bight averaged -19.08 ± 0.26 ‰ (Fig. 1), indicating that the organic matter is predominantly of marine origin (HAINES, 1976; GEARING et al., 1984; HADDAD and MARTENS, 1987). The fatty acid and neutral lipid fractions averaged $-22.1 \pm .5$ and $-22.9 \pm .3$ ‰, respectively (Fig. 1). Similar ^{13}C -depletions relative to the TOC have been observed in lipid fractions isolated from estuarine sediments (PARKER, 1964), the Eocene Messel shale (HAYES et al., 1987), and a wide variety of biological samples (ABELSON and HOERING, 1961; PARKER, 1964; DEGENS et al., 1968; DENIRO and EPSTEIN, 1977; MONSON and HAYES, 1982a,b). The nearly ubiquitous ^{13}C -depletion of lipids has been attributed to isotope effects associated with the biosynthesis and cycling of the lipid precursor, acetyl CoA (DENIRO and EPSTEIN, 1977; MONSON and HAYES, 1982a,b; BLAIR et al., 1985).

Porewater sulfate and acetate concentrations (Fig. 2) were similar to those observed previously at this site (SANSONE and MARTENS, 1982; CHANTON, 1985; CRILL and MARTENS, 1987). A subsurface maximum in acetate concentration frequently occurs between June and August at the same depth horizon where dissolved sulfate concentrations fall below 1 mM (SANSONE and MARTENS, 1982). The magnitude of the subsurface maximum was highly variable, similar to that seen in other studies at this site using different sediment processing and analytical methods (M. Alperin, per. comm.). The vari-

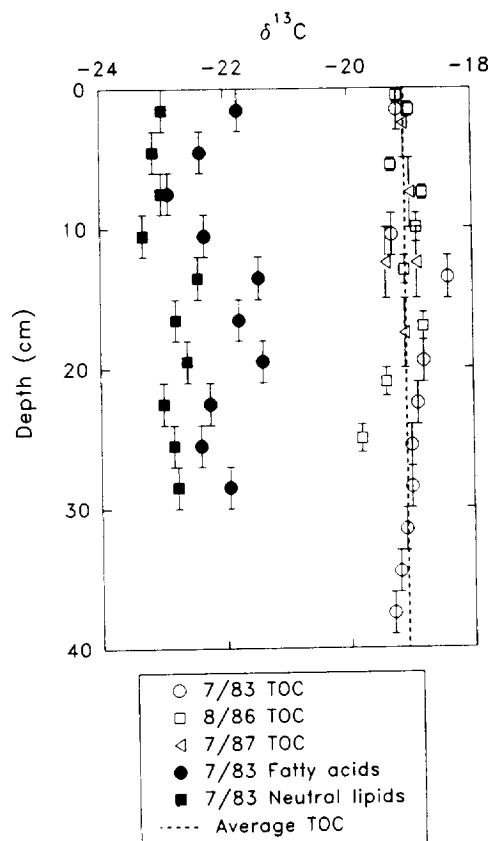


FIG. 1. $\delta^{13}\text{C}$ values of total organic carbon and lipid fractions. The TOC samples were collected on July 7, 1983 (○), August 14, 1986 (□), and July 21, 1987 (△). The fatty acid (●) and neutral lipid fractions (■) were from July 7, 1983. The TOC data is from Blair et al. (1987), Boehme et al. (unpubl. data), and this study.

ability between cores is thought to result from spatial heterogeneities in acetate cycling processes. No systematic differences were observed between splits of cores, which were processed by either the immediate centrifugation or methanol-poisoned/centrifugation treatments (Fig. 2C).

The $\delta^{13}\text{C}$ values of the porewater acetate exhibit excursions of nearly 15‰ with a pronounced subsurface maximum at the base of the sulfate reduction zone (Table 1; Fig. 3). The downcore variation is similar to that observed previously (BLAIR et al., 1987), but the absolute values are 5–10‰ heavier than the earlier data. The differences may represent true temporal variations as the 1983–84 data set was from June to early July. However, it should be noted that the core handling procedures were different in the two studies. In the original investigation, all cores were returned to the laboratory and refrigerated at 4°C until they could be processed (BLAIR et al., 1987). One core was treated similarly in this study. The results from that core (one total and two methyl $\delta^{13}\text{C}$ values) were approximately 1‰ lighter than those from a core processed immediately after collection onboard ship. Though the size of the data set prevents a rigorous statistical evaluation of the differences, it appears that the sample processing procedures were not responsible for the large differences between the two studies. Investigations are under way to resolve this issue.

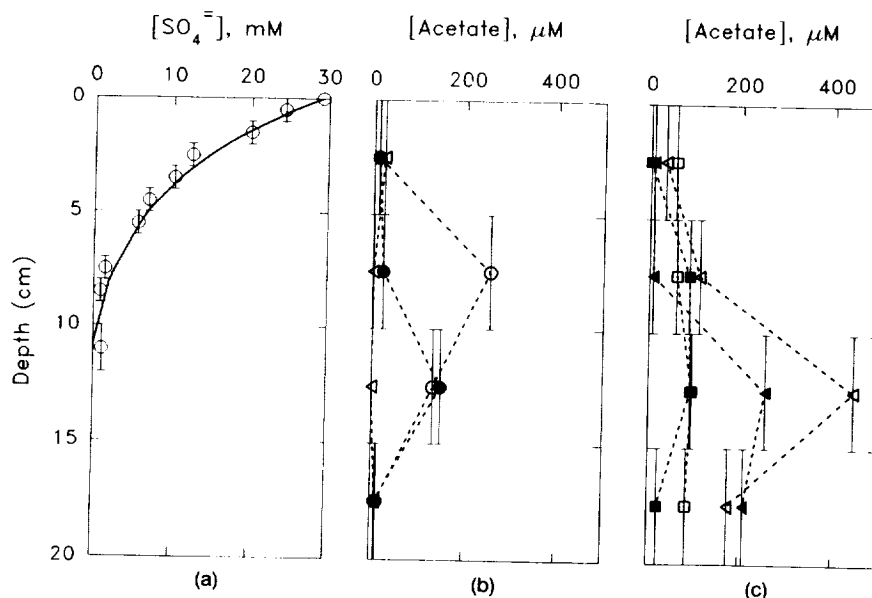


FIG. 2. Porewater sulfate and acetate concentration profiles. (a) Sulfate concentrations on August 14, 1986. (b) Acetate concentrations from triplicate cores collected on August 14, 1986. (c) Acetate concentrations from duplicate cores (triangles and squares) collected on July 21, 1987. Open and filled symbols represent methanol-killed and centrifuged-only samples, respectively (see Methods section for details).

The isotopic variability between cores from the same sampling date (0.2–2‰) was also of concern. No systematic differences were observed between the results of the different sampling procedures; thus, we conclude the noise is due to spatial heterogeneities on the meter scale within the seabed. Accordingly, the results from all treatments on a sampling date were averaged (Table 1; Fig. 3).

The $\delta^{13}C$ values of the acetate methyl group are 2–7‰ lighter than the total molecule (Table 1). The depth profile parallels that of the total acetate (Fig. 3). The $\delta^{13}C$ values of

the carboxyl group were determined by a mass balance calculation and are 5–14‰ enriched in ^{13}C relative to the methyl group.

DISCUSSION

In principle, the isotopic composition of sedimentary acetate should be controlled by the (1) isotopic composition of its precursors, (2) isotopic fractionations associated with its synthesis and consumption, and (3) relative rates of all

Table 1: $\delta^{13}C$ values of pore water acetate.

8/14/86			
Depth (cm)	CH ₃ COOH	CH ₃ -	-COOH ⁴
0-5	-17.6 ¹	-21.4(0.7) ²	-14.4 ¹
5-10	-11.4(1.0) ²	-18.6(0.4) ²	-4.2(2.4) ²
10-15	-4.6(0.2) ²	-10.5(0.4) ²	1.2(0.1) ²
15-20	-11.0(0.8) ²	-13.6(0.8) ²	-8.4(0.8) ²
7/21/87			
Depth (cm)	CH ₃ COOH	CH ₃ -	-COOH ⁴
0-5	-	-24.9(0.8) ²	-
5-10	-12.0 ¹	-18.5(0.2) ²	-5.3 ¹
10-15	-2.8(1.6) ³	-8.3(0.3) ²	4.4(1.2) ²
15-20	-7.2(2.1) ²	-14.4(0.5) ²	0.0(3.7) ²

¹ Single measurement (n=1)

² Difference between duplicate core $\delta^{13}C$ values and the mean.

³ Standard deviation (1 σ) for mean of triplicate core values.

⁴ Determined by mass balance calculation.

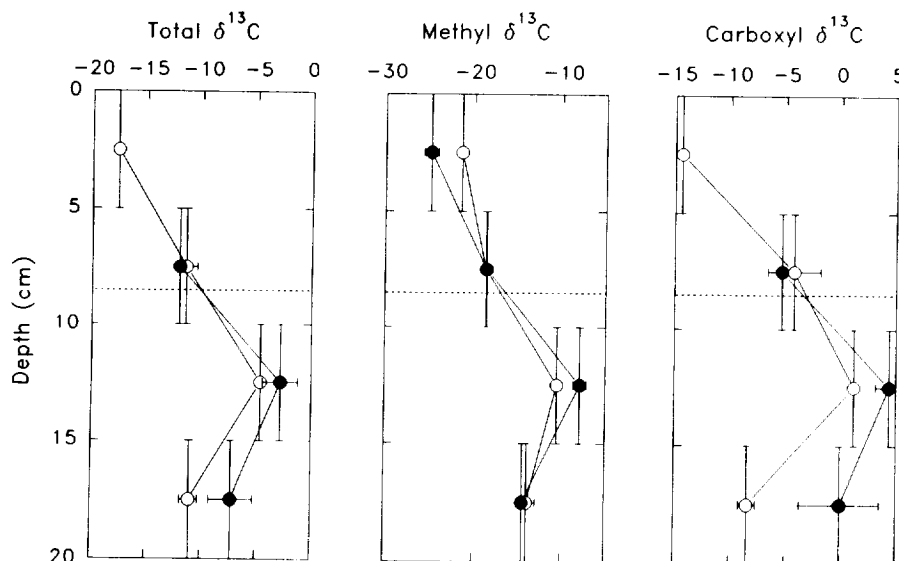


FIG. 3. $\delta^{13}\text{C}$ values of porewater acetate. The average $\delta^{13}\text{C}$ values of the total acetate, methyl, and carboxyl groups are from August 14, 1986 (○) and July 21, 1987 (●). The horizontal dashed line represents the <1 mM isopleth for dissolved sulfate.

processes which influence its pool size (BLAIR et al., 1985; BLAIR et al., 1987; GELWICKS et al., 1989). The downcore variations in the $\delta^{13}\text{C}$ value of acetate from Cape Lookout Bight indicate that changes in one or more of those factors occur as a function of depth within the sediment column. Each of those factors is discussed below.

Carbon Sources

The metabolizable organic carbon, which is the ultimate source of the acetate carbon, is estimated to have approximately the same average $\delta^{13}\text{C}$ value as the TOC fraction ($-19.08 \pm .26$) because the $\delta^{13}\text{C}$ value of the TOC remains unchanged as a function of depth (Fig. 1), even though 20–30% of the carbon is remineralized (MARTENS and KLUMP, 1984). The $\delta^{13}\text{C}$ value reflects a mixture of isotopically distinct sources. The sedimentary organic matter, and by inference, the metabolizable fraction, are derived from a variety of sources including phytoplanktic, microbial, and vascular plant remains (HADDAD and MARTENS, 1987; MARTENS et al., 1992). Visual inspection of cores and lignin analyses have indicated that *Halodule wrightii* and *Zostera marina*, the predominant seagrasses in the area (THAYER et al., 1978), and *Spartina alterniflora* are sources of the vascular plant matter (HADDAD and MARTENS, 1987). These plants typically have $\delta^{13}\text{C}$ values of -6 to -13‰ (THAYER et al., 1978; McMILLAN and SMITH, 1982; STEPHENSON et al., 1984; FRY and SHERR, 1984). This is in contrast to the $\delta^{13}\text{C}$ values of coastal plankton, which can range from -20 to -23‰ (HAINES, 1976; GEARING et al., 1984). The relative contributions of the vascular and nonvascular plant sources to the buried organic carbon pool have been estimated to be $17 \pm 23\%$ and $83 \pm 47\%$, respectively (HADDAD and MARTENS, 1987). The relative importance of those sources to the metabolizable fraction is unknown. While variations in the relative abundance of those sources within the sediment column

could influence the $\delta^{13}\text{C}$ depth profile of the acetate, no evidence for significant variations is apparent in either the TOC $\delta^{13}\text{C}$ (Fig. 1) or lignin profiles (HADDAD and MARTENS, 1987).

Isotopic heterogeneities which result from differences between compound classes also exist in the metabolizable fraction. Identified amino acid, carbohydrate, and lipid carbon represents $64 \pm 17\%$ of the metabolizable pool (BURDIGE and MARTENS, 1988, 1990; HADDAD, 1989; HADDAD and MARTENS, 1990; MARTENS et al., 1992). Lipid fractions are depleted in ^{13}C relative to the TOC fraction (Fig. 1). The $\delta^{13}\text{C}$ values of the amino acid and carbohydrate fractions are unknown. Large inter- and intramolecular carbon isotope heterogeneities exist in amino acids produced in a variety of algal and microbial cultures (ABELSON and HOERING, 1961; BLAIR et al., 1985; MACKO et al., 1987), and similar patterns may exist in sediments. The isotopic composition of carbohydrates from different sources is poorly characterized but the bulk carbohydrate pool is typically thought to be similar to that of the total biomass fraction of an organism (DEGENS et al., 1968; BLAIR et al., 1985). However, 3–4‰ differences have been observed between different carbohydrate fractions from marine plankton (DEGENS et al., 1968), and the leaves from the CAM-plant *Bryophyllum daigremontianum* (DELEENS and GARNIER-DARDART, 1977). The importance of the isotopic heterogeneity within the metabolizable carbon pool is dependent on the extent to which specific organic fractions bypass acetate as an intermediate during diagenesis.

Synthetic Isotope Effects

Little is known about the isotope effects associated with the anaerobic biosynthesis of acetate; however, any synthetic pathway could create a unique isotopic signature in the acetate that it produces. For example, the $\delta^{13}\text{C}$ values of the methyl and carboxyl groups of acetate produced aerobically from

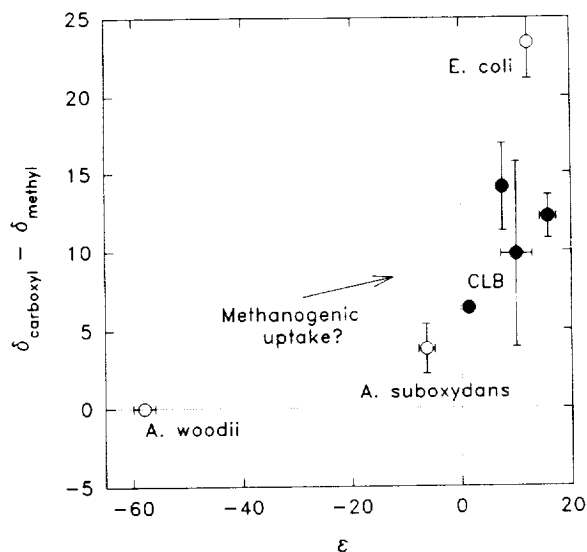
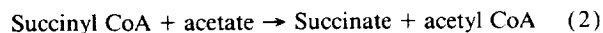


FIG. 4. Isotopic composition of acetate from various biological sources. The parameter, ϵ , is defined by the equation $\epsilon = [(R_{\text{acetate}}/R_{\text{substrate}}) - 1]10^3$, where R is the $^{13}\text{C}/^{12}\text{C}$ composition. The substrates for *A. woodii* (GELWICKS et al., 1989), *A. suboxydans* (RINALDI et al., 1974) and *E. coli* (BLAIR et al., 1985) were dissolved inorganic carbon, ethanol, and glucose, respectively. The substrate for the Cape Lookout sediments was assumed to have a $\delta^{13}\text{C}$ value of -19.1 .

glucose by *Escherichia coli* were approximately 0 and $+26\%$ relative to the glucose (BLAIR et al., 1985). The large enrichment of ^{13}C in the carboxyl group was proposed to result from the transformation of acetyl phosphate to acetyl-CoA. *Acetobacter suboxydans* expressed a smaller fractionation during the aerobic synthesis of acetate from ethanol where the methyl and carboxyl groups were -9 and 0% relative to the corresponding ethanol carbons (RINALDI et al., 1974). The CO_2 -reducing anaerobe, *Acetobacter woodii*, produced acetate which was isotopically homogeneous yet depleted in ^{13}C by as much as 57% relative to the total carbonate fraction (GELWICKS et al., 1989; PREUB et al., 1989). The isotope effect was believed to be associated with the enzyme carbon monoxide dehydrogenase (GELWICKS et al., 1989). The decarboxylation of lactate by the sulfate reducer, *Desulfovibrio desulfuricans*, produced CO_2 depleted in ^{13}C by 5 – 13% relative to the lactate carboxyl group (KAPLAN and RITTENBERG, 1964). The isotopic composition of the acetate which was produced was not measured; however, the carboxyl group of the acetate could be depleted in ^{13}C if the fractionation occurred during the actual decarboxylation step. A summary of the culture studies is shown in Fig. 4.

Catabolic Processes and Isotope Effects

The potential for isotope effects during the consumption of acetate is equally significant. Several biochemical strategies are used by sulfate- and sulfur-reducing bacteria to oxidize acetate to CO_2 (THAUER et al., 1989). *Desulfobacter postgatei* activates acetate to acetyl CoA via the reaction:



The acetyl CoA is subsequently oxidized to CO_2 via the citric acid cycle (BRANDIS-HEEP et al., 1983; GEBHARDT et al., 1983). *Desulfovibrio acetoxidans*, an anaerobe which grows on acetate and sulfur, utilizes similar pathways (GEBHARDT et al., 1985; THAUER et al., 1989). In contrast, *Desulfotomaculum acetoxidans* and *Desulfobacterium autotrophicum* activate acetate to acetyl CoA by the intermediate formation of acetyl phosphate. The acetyl CoA is oxidized to CO_2 via the carbon monoxide dehydrogenase pathway (SCHAUDER et al., 1986, 1989; SPORMANN and THAUER, 1988, 1989). To our knowledge, the carbon isotopic fractionation associated with the oxidation of acetate by either of those pathways has not been reported.

The methanogenic genera, *Methanosarcina* and *Methanotheroxirix*, are the only known microorganisms capable of dissimilating acetate to CH_4 and CO_2 (THAUER et al., 1989). In both genera, acetate is converted to acetyl CoA, after which the carbon-carbon bond of the acetyl unit is cleaved (GRAHAME and STADTMAN, 1987; THAUER et al., 1989). The methyl group is reduced to methane, and the carbonyl group is oxidized to CO_2 (BUSWELL and SOLLO, 1948; STADTMAN and BARKER, 1949; ZEIKUS, 1983). The fractionation factor (k^{12}/k^{13}) for methane formation from acetate by *Methanosarcina barkerii* is 1.02 – 1.03 (RISATTI and HAYES, 1983; KRZYCKI et al., 1987). The fractionation factors for acetate dissimilation by other species, including the marine methanogen, *Methanosarcina acetivorans* (SOWERS et al., 1984), have not been reported.

Relative Rates of Acetate Cycling Processes

The relative rates of the acetate cycling processes will have a major influence on the isotopic composition of that compound if any of the processes exhibit a significant isotope effect. The results of ^{14}C -tracer experiments can be used to estimate the relative rates of two processes, the oxidative and dissimilative pathways, by comparing the rates of conversion of the acetate methyl group to CO_2 or CH_4 . The fraction of the acetate methyl group, which is converted to methane (f), is defined by the equation:

$$f = r_{\text{CH}_4} / (r_{\text{CH}_4} + r_{\text{CO}_2}), \quad (3)$$

where r_{CH_4} and r_{CO_2} are the rates of the conversion of the acetate methyl group to CH_4 and CO_2 , respectively. By inference, f represents the fraction of acetate that is dissimilated directly by methanogens. If uniformly ^{14}C -labelled acetate is used to estimate turnover rate constants, f can be determined with the relationship:

$$f = 2k_{\text{CH}_4} / (k_{\text{CH}_4} + k_{\text{CO}_2}), \quad (4)$$

where k_{CH_4} and k_{CO_2} are the rate constants for CH_4 and CO_2 production from the total acetate molecule. It is assumed that the methane is derived solely from the methyl group. Similarly, the respiration index measurement (SANSONE and MARTENS, 1982) can be related to f by:

$$f = 2(1 - \text{RI}), \quad (5)$$

where the respiration index (RI) was determined with ^{14}C -labelled acetate and is defined as:

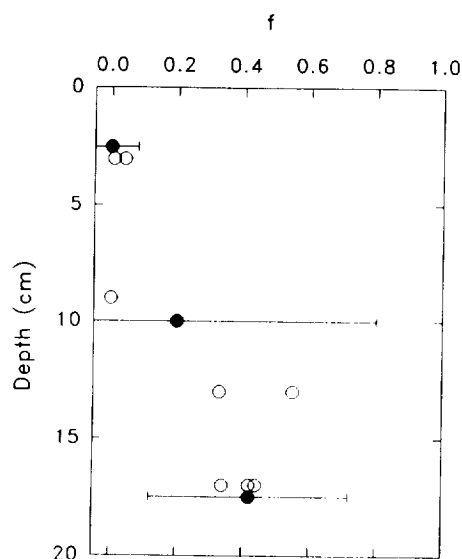


FIG. 5. The relative rate of acetate dissimilation as a function of depth. The parameter, f , was calculated using Eqns. (4) and (5) and ^{14}C -tracer data: ● (SANSONE and MARTENS, 1982); ○ (CRILL and MARTENS, 1986).

$$\text{RI} = \frac{^{14}\text{CO}_2 \text{ Production}}{(^{14}\text{CO}_2 \text{ Production} + ^{14}\text{CH}_4 \text{ Production})} \quad (6)$$

Data from SANSONE and MARTENS (1982) and CRILL and MARTENS (1986) were used to estimate f for Cape Lookout Bight (Fig. 5). The value of f increases from zero in the sulfate reduction zone to a maximum of 0.55 in the methanogenic zone. In comparison, 70–86% of acetate ($f = 0.70$ – 0.86) in freshwater sediments is dissimilated directly to CH_4 and CO_2 (CAPPENBERG and PRINS, 1974; WINFREY and ZEIKUS, 1979a; LOVLEY and KLUG, 1982). The fact that f is significantly less than 1.0 indicates that an oxidative process competes with the methanogenic dissimilation of acetate. The similarity in the downcore profiles of f and the acetate $\delta^{13}\text{C}$ values suggests that the relative rates of the oxidative and dissimilative processes may be important isotopic controls. This point will be tested with a model which is described in the next section.

The absolute rate constants for acetate turnover, which were reported in the two studies, differ by an order of magnitude or more (SANSONE and MARTENS, 1982; CRILL and MARTENS, 1986). This discrepancy has been attributed to a difference in the incubation times used in the tracer experiments (CRILL and MARTENS, 1986). The consistency of f calculated from the two data sets argues that the relative rates of the acetate cycling processes were insensitive to the differences in methodology.

An Isotopic Model for Porewater Acetate

A simple model is proposed to describe the isotopic composition of acetate in this system. The following equation can be used to describe the isotopic composition of the methyl group, δ_{me} :

$$\delta_{\text{me}} = (\delta_{\text{syn}} + 10^3)(\alpha_{\text{diss}}f + \alpha_{\text{ox}}[1 - f]) - 10^3, \quad (7)$$

where δ_{syn} is the isotopic composition of the biosynthesized methyl group before consumption, α_{diss} is the fractionation factor associated with the reduction of the methyl carbon to methane, and α_{ox} is the fractionation factor associated with the oxidation of the methyl group (BLAIR et al., 1985). Steady-state or near-steady-state conditions for the short time frame needed to turn over the acetate pool (15 min to one day, SANSONE and MARTENS, 1982; CRILL and MARTENS, 1986) and first-order kinetics for the uptake of acetate are assumed. The model is simplified by setting $\alpha_{\text{ox}} = 1.00$. This is a reasonable first approximation because the $\delta^{13}\text{C}$ value of the total acetate molecule in the 0–5 cm interval ($f = 0$) is within 1.5‰ of that estimated for the metabolizable organic carbon fraction. Accordingly, $\delta_{\text{syn}} = -23.2 \pm 2.2\text{‰}$, which is the average δ_{me} value for the 0–5 cm interval. Average values of f and δ_{me} for the 10–20 cm depth interval, 0.38 ± 0.11 and -11.2 ± 3.0 , respectively, were used with the following rearranged expression,

$$\alpha_{\text{diss}} = 1 + (\delta_{\text{me}} - \delta_{\text{syn}})/[f(\delta_{\text{syn}} + 10^3)], \quad (8)$$

to estimate α_{diss} . The resulting estimate for α_{diss} , 1.032 ± 0.014 , is in good agreement with that observed in acetoclastic cultures (RISATTI and HAYES, 1983; KRZYCKI et al., 1987). An analogous calculation can be done to determine the apparent fractionation factor on the carboxyl group associated with the uptake by methanogens. In that case, $\alpha_{\text{diss}}(\text{carboxyl})$ was found to be 1.036 ± 0.019 . The agreement between the estimate of α_{diss} from the model and the culture measurements suggests that the rate of the acetoclastic reaction relative to acetate oxidation and the isotopic fractionation associated with methanogenesis are the dominant controls of the downcore variations in δ_{me} . Source effects and the presence of other sinks of acetate, such as biologically unavailable dissolved and adsorbed pools (CHRISTENSEN and BLACKBURN, 1982; SHAW et al., 1984; PARKES et al., 1984; NOVELLI et al., 1988; GIBSON et al., 1989; MICHELSON et al., 1989), would appear to be limited to secondary roles as controlling factors of the isotopic composition of the methyl group.

The 4–6‰ ^{13}C -depletion of the acetate downcore within the 10–20 cm interval indicates that the methanogenic zone cannot be considered spatially homogeneous in terms of microbial processes and may be composed of smaller diagenetic horizons. There is insufficient information to resolve with confidence if the isotopic shift is due to a source or consumptive effect. However, the ^{14}C -tracer studies of CRILL and MARTENS (1986) suggest that the relative rates of acetate oxidation and dissimilation change within the methanogenic zone with the oxidative process becoming progressively more important below the depth of peak methane production. According to our model, such a trend would result in the observed isotopic change.

The isotope model can be used to estimate the $\delta^{13}\text{C}$ value of methane produced by acetate dissimilation. Assuming steady-state conditions (HAYES, 1983), the $\delta^{13}\text{C}$ of the methane is approximated by:

$$\delta(\text{CH}_4/\text{Acet}) = \delta_{\text{syn}} - (1 - f)(\alpha_{\text{diss}} - 1) \cdot 10^3. \quad (9)$$

Using the average value of f for the 10–20 cm methanogenic zone, $\delta(\text{CH}_4/\text{Acet})$ was calculated to be $-43 \pm 10\text{‰}$. Approximately 26% of the methane production at this site is provided by acetate; the remainder is generated principally by CO_2 -reduction (CRILL and MARTENS, 1986). A mass balance calculation using the average measured $\delta^{13}\text{C}$ value of $-59.5 \pm 2.0\text{‰}$ for methane produced in July and August at A-1 (MARTENS et al., 1986) indicates that the isotopic signature of the methane produced by CO_2 -reduction should be $-65 \pm 5\text{‰}$. This result appears to verify the hypothesis that the acetate-dissimilating pathway produces methane which is enriched in ^{13}C relative to that generated by CO_2 -reduction (WHITICAR et al., 1986). WHITICAR et al. (1986) hypothesized further that the isotopic differences observed between methane generated in freshwater and marine environments are the result of the distinctive isotopic signatures and the relative importance of the two pathways. Accordingly, freshwater environments, in which acetate dissimilation is the dominant pathway, typically produce methane which is relatively enriched in ^{13}C .

Similarly, the seasonal variations in methane $\delta^{13}\text{C}$ and δD values at Cape Lookout have been attributed, in part, to changes in the relative rates of the two methanogenic processes (MARTENS et al., 1986; BURKE et al., 1988). ^{14}C -tracer studies have suggested that the proportion of total methane production from acetate increased from 20% in mid-July 1983 to 29% in late August (CRILL and MARTENS, 1986). The statistical significance of the temporal trend cannot be evaluated; however, the apparent trend toward the greater importance of the acetate dissimilatory pathway in late summer should produce methane enriched in ^{13}C . The observed methane $\delta^{13}\text{C}$ values for mid-July and late August are -61.4 ± 1.1 and $-57.7 \pm .3\text{‰}$, respectively (MARTENS et al., 1986). This consistency between the model predictions and actual observations not only provides us with some measure of confidence in the general features of the model but also in the relative rates determined with the ^{14}C -tracer experiments. This is an important issue given the current controversial nature of acetate turnover rate measurements (CHRISTENSEN and BLACKBURN, 1982; SHAW et al., 1984; PARKES et al., 1984; NOVELLI et al., 1988; MICHELSON et al., 1989; GIBSON et al., 1989).

Speculations on Microbial Processes in Anoxic Sediments

The calculated $\delta^{13}\text{C}$ values of the carboxyl group exhibit a downcore trend nearly parallel to that of the methyl group (Fig. 3) suggesting that they are controlled, in part, by methanogenic activity. Two methanogenic-related processes may influence the carboxyl $\delta^{13}\text{C}$ value. The first involves the bond cleavage between the methyl and carbonyl groups of the acetyl intermediate in the acetoclastic reaction sequence. A normal kinetic isotope effect associated with that reaction would explain the methyl group $\delta^{13}\text{C}$ values as well. The fact that the isotopic fractionations associated with both the methyl and carboxyl groups are observed in the porewater pool of acetate implies that the steps leading to the isotopically discriminating reactions are reversible. Cell suspensions of *Methanosarcina*

barkeri catalyze rapid isotopic exchange between CO_2 and the carboxyl group of acetate (EIKMANN and THAUER, 1984). Similarly, cell extracts of the same methanogen promoted isotopic exchange between CO_2 and acetyl-CoA, thus providing direct evidence that the carbon-carbon bond cleavage of acetyl-CoA is reversible (FISCHER and THAUER, 1990).

The second process is the isotopic exchange between the carboxyl group and an external CO_2 pool, as demonstrated for *Methanosarcina barkeri*. Thus, the apparent fractionation factor determined for the carboxyl group may not be simply the result of a kinetic isotope effect as treated in our model. The importance of the exchange reaction as an isotopically controlling process will depend on the relative rates of the isotopic exchange and the overall dissimilative process. Other microorganisms, including *Desulfobacterium autotrophicum* (SCHAUDER et al., 1986), *Acetobacterium woodii* (WINTER and WOLFE, 1980), and the syntrophic acetate-oxidizer, "Reversibacterium," (ZINDER and KOCH, 1984) have exhibited similar isotopic exchange capabilities. Carbon monoxide dehydrogenase appears to be the enzyme responsible for the exchange reaction in all of those microorganisms (DIEKERT et al., 1985; THAUER et al., 1989). The extent to which isotopic exchange occurs between acetate and CO_2 in Cape Lookout or other organic-rich marine sediments is unknown but should clearly be investigated.

The similarity of the $\delta^{13}\text{C}$ value of the total acetate molecule in the upper 5 cm of sediment with that of the TOC fraction, along with the model results, suggests that the fractionation associated with the uptake by bacteria in the sulfate reduction zone is relatively small. This conclusion, which is admittedly based on a modest data base, merits discussion because of its implications. The intramolecular carbon isotopic difference (ca. 7‰) in the 0–5 cm interval indicates that large isotopic fractionations occur during the biosynthesis of acetate. For an isotope effect of that magnitude not to be reflected in the $\delta^{13}\text{C}$ value of the total molecule, a large portion of the metabolizable carbon must be shunted through acetate in the sulfate reduction zone. This would also explain why the isotopic heterogeneity within the metabolizable organic carbon fraction does not manifest itself more obviously. Qualitatively, the isotope data is consistent with previous estimates that 40–60% of the remineralized organic carbon is shunted through acetate in the sulfate reduction zone of coastal sediments (SORENSEN et al., 1981; WINFREY and WARD, 1983). A more quantitative estimate of the flow of carbon through acetate would require substantial information concerning the biosynthetic fractionations.

The similarity of the $\delta^{13}\text{C}$ value of the surficial acetate to that of the TOC fraction would appear to preclude the possibility that a significant portion of the acetate could be produced by acetogenic CO_2 -reduction because of the large isotope effect associated with that process (GELWICKS et al., 1989; PREUB et al., 1989). Instead, it is likely that the acetate is synthesized via the more direct fermentation of organic species. In contrast, isotope models have suggested that CO_2 -reduction is an important source of acetate in freshwater sediments (LAZERTE, 1981; GELWICKS et al., 1989). This con-

tradicts the results of other studies, which indicate that <2% of the acetate in eutrophic lake sediments was produced via CO₂-reduction (LOVLEY and KLUG, 1983b). The apparent contradiction clearly illustrates how little is known concerning acetate cycling and the associated isotope effects in different environments and points out the need for further studies.

SUMMARY AND CONCLUSIONS

The impressive intramolecular carbon isotopic heterogeneity and downcore $\delta^{13}\text{C}$ variations exhibited by the dissolved acetate at Cape Lookout Bight are compelling evidence for the presence of large isotope effects associated with some aspect of acetate cycling. The downcore $\delta^{13}\text{C}$ profiles are consistent with the hypothesis that both oxidative and dissimilative processes consume acetate in the methanogenic zone of the sediment (WARFORD et al., 1979; SANSONE and MARTENS, 1982). The dominant isotopic fractionation appears to be associated with the methanogenic dissimilation of acetate. A fractionation factor for the conversion of the methyl group of acetate to methane was estimated to be 1.032 ± 0.014 , which is in good agreement with that previously measured in culture (RISATTI and HAYES, 1983; KRZYCKI et al., 1987). The isotopic measurements of the acetate methyl group coupled with estimates of rates of acetate cycling have provided direct evidence in support of the hypothesis that methane produced by the dissimilation of acetate is enriched in ^{13}C relative to that produced by CO₂-reduction (WHITICAR et al., 1986).

The secondary controls of the isotopic composition of acetate are virtually unknown. Experiments employing chemical inhibitors for microbial processes, e.g., MoO₄²⁻ for sulfate reduction, and radiotracer rate determinations coupled with the natural abundance $^{13}\text{C}/^{12}\text{C}$ measurements will provide important information concerning both synthetic and catabolic isotope effects. Culture studies of acetate-producing and -consuming anaerobic microorganisms and their associated isotope effects are needed to establish the isotopic signatures of the different metabolic pathways. If the isotopic signature of the sedimentary acetate can be understood, it would be a sensitive indicator of in situ processes and their relative rates. The isotopic measurements should prove useful in monitoring temporal and spatial changes in the sedimentary microbial ecosystem and the related diagenetic processes. As an example in this study, the $\delta^{13}\text{C}$ measurements have indicated that the methanogenic zone should not be viewed as a homogeneous microbial ecosystem but instead appears to be stratified with respect to acetate cycling processes. The exact nature and cause of the stratification is unknown.

Isotopic measurements of diagenetic intermediates such as acetate provide information which is different from, but complementary to, that generated by other methods. In principle, by looking at the natural abundance isotopic composition of a compound from a sediment, we are viewing the result of in situ processes which have not been subjected to the same potential artifacts commonly associated with radiolabel and microbiological methods. Because of that characteristic, the isotopic measurements should serve as unique

constraints on models derived from the results of other methodologies.

Acknowledgments—We thank Chris Martens for his invaluable support throughout this project. Essential field assistance was provided by Jeff Chanton and Dan Albert. Bill Showers, David Des Marais, and Randy Culp provided the critical mass spectrometer analyses. We thank Emil Kwong and Susan Boehme for their assistance with the lipid and TOC $\delta^{13}\text{C}$ measurements, as well as Stan Mezynski for his glass blowing. Marc Alperin, Jeff Chanton, Cheryl Kelley, and Brian Popp provided helpful reviews of this manuscript. Laboratory space and boating facilities were provided by the University of North Carolina Institute of Marine Sciences, Morehead City, NC. This research was supported by NASA grant NAGW-838 and PRF grant 17527-G2.

Editorial handling: C. Lee

REFERENCES

- ABELSON P. H. and HOERING T. C. (1961) Carbon isotope fractionation in formation of amino acids by photosynthetic organisms. *Proc. Natl. Acad. Sci. USA* **47**, 623–632.
- BARKER H. A. (1936) On the biochemistry of the methane fermentation. *Arch. Microbiol.* **7**, 404–419.
- BARKER H. A. (1981) Amino acid degradation by anaerobic bacteria. *Ann. Rev. Biochem.* **50**, 23–40.
- BHARATI P. A. L., BAULAIGUE R., and MATHERON R. (1980) Breakdown of D-glucose by mixed cultures of *Escherichia coli*, *Desulfovibrio vulgaris*, and *Chromatium vinosum*. *Curr. Microbiol.* **4**, 371–376.
- BLAIR N., LEU A., MUNOZ E., OLSEN J., KWONG E., and DES MARAIS D. (1985) Carbon isotopic fractionation in heterotrophic microbial metabolism. *Appl. Environ. Microbiol.* **50**, 996–1001.
- BLAIR N. E., MARTENS C. S., and DES MARAIS D. J. (1987) Natural abundances of carbon isotopes in acetate from a coastal marine sediment. *Science* **236**, 66–68.
- BRANDIS-HEEP A., GEBHARDT N. A., THAUER R. K., WIDDEL F., and PFENNIG N. (1983) Anaerobic acetate oxidation to CO₂ by *Desulfohalobacter postgatei*. 1. Demonstration of all enzymes required for the operation of the citric acid cycle. *Arch. Microbiol.* **136**, 222–229.
- BRAUN M., SCHOBERTH S., and GOTTSCHALK G. (1979) Enumeration of bacteria forming acetate from H₂ and CO₂ in anaerobic habitats. *Arch. Microbiol.* **120**, 201–204.
- BRAUN M., MAYER F., and GOTTSCHALK G. (1981) *Clostridium acetium* (Wieringa), a microorganism producing acetic acid from molecular hydrogen and carbon dioxide. *Arch. Microbiol.* **128**, 288–291.
- BRYANT M. P., CAMPBELL L. L., REDDY C. A., and CRABILL M. R. (1977) Growth of *Desulfovibrio* in lactate or ethanol media low sulfate in association with H₂-utilizing methanogenic bacteria. *Appl. Environ. Microbiol.* **33**, 1162–1169.
- BURDIGE D. J. and MARTENS C. S. (1988) Biogeochemical cycling in an organic-rich coastal basin: 10. The role of amino acids in sedimentary carbon and nitrogen cycling. *Geochim. Cosmochim. Acta* **52**, 1571–1584.
- BURDIGE D. J. and MARTENS C. S. (1990) Biogeochemical cycling in an organic-rich coastal marine basin: 11. The sedimentary cycling of dissolved, free amino acids. *Geochim. Cosmochim. Acta* **54**, 3033–3052.
- BURKE R. A., MARTENS C. S., and SACKETT W. M. (1988) Seasonal variations of D/H and $^{13}\text{C}/^{12}\text{C}$ ratios of microbial methane in surface sediments. *Nature* **332**, 829–831.
- BUSWELL A. M., and SOLLO F. W., JR. (1948) The mechanism of methane fermentation. *J. Amer. Chem. Soc.* **70**, 1778–1780.
- CANUEL E. A., MARTENS C. S., and BENNINGER L. K. (1990) Seasonal variations in ^7Be activity in the sediments of Cape Lookout Bight, North Carolina. *Geochim. Cosmochim. Acta* **54**, 237–245.

- CAPPENBERG Th. E. and PRINS R. A. (1974) Interrelations between sulfate-reducing and methane-producing bacteria in bottom deposits of a fresh-water lake. III. Experiments with ^{14}C -labeled substrates. *Antonie van Leeuwenhoek* **40**, 457–469.
- CHANTON J. P. (1985) Sulfur mass balance and isotopic fractionation in an anoxic marine sediment. Ph.D. thesis, Univ. North Carolina at Chapel Hill.
- CHANTON J. P. and MARTENS C. S. (1988) Seasonal variations in ebullitive flux and carbon isotopic composition of methane in a tidal freshwater estuary. *Global Biogeochem. Cycles* **2**, 289–298.
- CHANTON J. P., MARTENS C. S., and KIPPUTH G. W. (1983) Lead-210 sediment geochronology in a changing coastal environment. *Geochim. Cosmochim. Acta* **47**, 1791–1804.
- CHANTON J. P., MARTENS C. S., and GOLDBERGER M. B. (1987) Biogeochemical cycling in an organic-rich coastal marine basin. 7. Sulfur mass balance, oxygen uptake and sulfide retention. *Geochim. Cosmochim. Acta* **51**, 1187–1199.
- CHRISTENSEN D. and BLACKBURN T. H. (1982) Turnover of ^{14}C -labelled acetate in marine sediments. *Mar. Biol.* **71**, 113–119.
- CRILL P. M. and MARTENS C. S. (1983) Spatial and temporal fluctuations of methane production in anoxic, coastal marine sediments. *Limnol. Oceanogr.* **28**, 1117–1130.
- CRILL P. M. and MARTENS C. S. (1986) Methane production from bicarbonate and acetate in an anoxic marine sediment. *Geochim. Cosmochim. Acta* **50**, 2089–2097.
- CRILL P. M. and MARTENS C. S. (1987) Biogeochemical cycling in an organic-rich coastal marine basin. 6. Temporal and spatial variations in sulfate reduction rates. *Geochim. Cosmochim. Acta* **51**, 1175–1186.
- DEGENS E. T., BEHRENDT M., GOTTHARDT B., and REPPMANN E. (1968) Metabolic fractionation of carbon isotopes in marine plankton-II. Data on samples collected off the coasts of Peru and Ecuador. *Deep-Sea Res.* **15**, 11–20.
- DELEENS E. and GARNIER-DARDART J. (1977) Carbon isotope composition of biochemical fractions isolated from leaves of *Bryophyllum daigremontianum* Berger, a plant with Crassulacean acid metabolism: Some physiological aspects related to CO_2 dark fixation. *Planta* **135**, 241–248.
- DENIRO M. J. and EPSTEIN S. (1977) Mechanism of carbon isotope fractionation associated with lipid synthesis. *Science* **197**, 261–263.
- DES MARAIS D. J. (1978) Variable-temperature cryogenic trap for the separation of gas mixtures. *Anal. Chem.* **50**, 1405–1406.
- DIEKERT G., FUCHS G., and THAUER R. K. (1985) Properties and function of carbon monoxide dehydrogenase from anaerobic bacteria. In *Microbial Gas Metabolism. Mechanistic, Metabolic and Biotechnological Aspects* (ed. R. K. POOLE and C. S. DOW) pp. 115–130. Academic Press.
- EICHLER B. and SCHINK B. (1984) Oxidation of primary aliphatic alcohols by *Acetobacterium carbinolicum* sp. nov., a homoacetogenic anaerobe. *Arch. Microbiol.* **140**, 147–152.
- EIKMANN B. and THAUER R. K. (1984) Catalysis of an isotopic exchange between CO_2 and the carboxyl group of acetate by *Methanosarcina barkeri* grown on acetate. *Arch. Microbiol.* **138**, 365–370.
- FISCHER R. and THAUER R. K. (1990) Methanogenesis from acetate in cell extracts of *Methanosarcina barkeri*: Isotope exchange between CO_2 and the carbonyl group of acetyl-CoA, and the role of H_2 . *Arch. Microbiol.* **153**, 156–162.
- FRY B. and SHERR E. B. (1984) $\delta^{13}\text{C}$ measurements as indicators of carbon flow in marine and freshwater ecosystems. *Contrib. Mar. Sci.* **27**, 13–47.
- GAMES L. M. and HAYES J. M. (1976) On the mechanisms of CO_2 and CH_4 production in natural anaerobic environments. In *Proc. 2nd Intl. Symp. Environ. Biogeochem.* (ed. NRIAGU J. O.) Ch. 5, pp. 51–73. Ann Arbor Mich. Science Press.
- GEARING J. N., GEARING P. J., RUDNICK D. T., REQUEJO A. G., and HUTCHINS M. J. (1984) Isotopic variability of organic carbon in a phytoplankton-based, temperate estuary. *Geochim. Cosmochim. Acta* **48**, 1089–1098.
- GEBHARDT N. A., LINDER D., and THAUER R. K. (1983) Anaerobic acetate oxidation of CO_2 by *Desulfobacter postgatei*. 2. Evidence from ^{14}C -labelling studies for the operation of the citric acid cycle. *Arch. Microbiol.* **136**, 230–233.
- GEBHARDT N. A., THAUER R. K., LINDER D., KAULFERS P.-M., and PFENNIG N. (1985) Mechanism of acetate oxidation to CO_2 with elemental sulfur in *Desulfuromonas acetoxidans*. *Arch. Microbiol.* **141**, 392–398.
- GELWICKS J. T. and HAYES J. M. (1990) Carbon-isotopic analysis of dissolved acetate. *Anal. Chem.* **62**, 535–539.
- GELWICKS J. T., RISATTI J. B., and HAYES J. M. (1989) Carbon isotope effects associated with autotrophic acetogenesis. *Org. Geochem.* **14**, 441–446.
- GIBSON G. R., PARKES R. J., and HERBERT R. A. (1989) Biological availability and turnover rate of acetate in marine and estuarine sediments in relation to dissimilatory sulphate reduction. *FEMS Microb. Ecol.* **62**, 303–306.
- GRAHAME D. A. and STADTMAN T. C. (1987) *In vitro* methane and methyl coenzyme M formation from acetate: Evidence that acetyl-CoA is the required intermediate activated form of acetate. *Biochem. Biophys. Res. Comm.* **147**, 254–258.
- HADDAD R. I. (1989) Sources and reactivity of organic matter accumulating in a rapidly depositing, coastal marine sediment. Ph.D. thesis, Univ. North Carolina at Chapel Hill.
- HADDAD R. I. and MARTENS C. S. (1987) Biogeochemical cycling in an organic-rich coastal marine basin: 9. Sources and accumulation rates of vascular plant-derived organic material. *Geochim. Cosmochim. Acta* **51**, 2991–3001.
- HADDAD R. I. and MARTENS C. S. (1990) Tales from a recent mudhole: Sources of organic matter driving early diagenesis in Cape Lookout Bight, N.C. *Eos* **71**, 99.
- HAINES E. B. (1976) Stable carbon isotope ratios in the biota, soils, and tidal water of a Georgia Salt Marsh. *Estuarine Coastal Mar. Sci.* **4**, 609–616.
- HAYES J. M. (1983) Practice and principles of isotopic measurements in organic geochemistry. In *Organic Geochemistry of Contemporary and Ancient Sediments* (ed. W. G. MEINSCHEN) pp. 5–1–5–31. Soc. Economic Paleontol. and Mineralog.
- HAYES J. M., TAKIGIKU R., OCAMPO R., CALLOT H. J., and ALBRECHT P. (1987) Isotopic compositions and probable origins of organic molecules in the Eocene Messel shale. *Nature* **329**, 48–51.
- JONES W. J., GUYOT J., and WOLFE R. S. (1984) Methanogenesis from sucrose by defined immobilized consortia. *Appl. Environ. Microbiol.* **47**, 1–6.
- KAPLAN I. R. and RITTENBERG S. C. (1964) Carbon isotope fractionation during metabolism of lactate by *Desulfovibrio desulfuricans*. *J. Gen. Microbiol.* **34**, 213–217.
- KOCH M., DOLFING J., WUHRMANN K., and ZEHNDER A. J. B. (1983) Pathways of propionate degradation by enriched methanogenic cultures. *Appl. Environ. Microbiol.* **45**, 1411–1414.
- KREMER D. R., NIENHUIS-KUIPER H. E., and HANSEN T. A. (1988) Ethanol dissimilation in *Desulfovibrio*. *Arch. Microbiol.* **150**, 552–557.
- KRZYCKI J. A., KENEALY W. R., DENIRO M. J., and ZEIKUS J. G. (1987) Stable carbon isotope fractionation by *Methanosarcina barkeri* during methanogenesis from acetate, methanol, or carbon dioxide-hydrogen. *Appl. Environ. Microbiol.* **53**, 2597–2599.
- KUIVILA K. M., MURRAY J. W., and DEVOL A. H. (1990) Methane production in the sulfate-depleted sediments of two marine basins. *Geochim. Cosmochim. Acta* **54**, 403–411.
- LAUBE V. M. and MARTIN S. M. (1981) Conversion of cellulose to methane and carbon dioxide by triculture of *Acetivibrio cellulolyticus*, *Desulfovibrio* sp., and *Methanosarcina barkeri*. *Appl. Environ. Microbiol.* **42**, 413–420.
- LAZERTE B. D. (1981) The relationship between total dissolved carbon dioxide and its stable carbon isotope ratio in aquatic sediments. *Geochim. Cosmochim. Acta* **45**, 647–656.
- LEIGH J. A., MAYER F., and WOLFE R. S. (1981) *Acetogenium kivui*, a new thermophilic hydrogen-oxidizing, acetogenic bacterium. *Arch. Microbiol.* **129**, 275–280.
- LJUNGDAHL L. G. and WOOD H. G. (1982) Acetate biosynthesis.

- In *Vitamin B 12*, Vol. 2 (ed. D. DOLPHIN), pp. 165–202. Wiley and Sons.
- LOVLEY D. R. and KLUG M. J. (1982) Intermediary metabolism of organic matter in the sediments of a eutrophic lake. *Appl. Environ. Microbiol.* **43**, 552–560.
- LOVLEY D. R. and KLUG M. J. (1983a) Sulfate reducers can out-compete methanogens at freshwater sulfate concentrations. *Appl. Environ. Microbiol.* **45**, 187–192.
- LOVLEY D. R. and KLUG M. J. (1983b) Methanogenesis from methanol and methylamines and acetogenesis from hydrogen and carbon dioxide in the sediments of a eutrophic lake. *Appl. Environ. Microbiol.* **45**, 1310–1315.
- MACKO S. A., FOGEL M. L., HARE P. E., and HOERING T. C. (1987) Isotopic fractionation of nitrogen and carbon in the synthesis of amino acids by microorganisms. *Chem. Geol.* **65**, 79–92.
- MARTENS C. S. and KLUMP J. V. (1980) Biogeochemical cycling in an organic-rich coastal basin—I. Methane sediment-water exchange processes. *Geochim. Cosmochim. Acta* **44**, 471–490.
- MARTENS C. S. and KLUMP J. V. (1984) Biogeochemical cycling in an organic-rich coastal marine basin. 4. An organic carbon budget for sediments dominated by sulfate reduction and methanogenesis. *Geochim. Cosmochim. Acta* **48**, 1987–2004.
- MARTENS C. S., KIPPURTH G. W., and KLUMP J. V. (1980) Sediment-water chemical exchange in the coastal zone traced by in situ radon-222 flux measurements. *Science* **208**, 285–288.
- MARTENS C. S., BLAIR N. E., GREEN C. D., and DES MARAIS D. J. (1986) Seasonal variations in the stable carbon isotopic signature of biogenic methane in a coastal sediment. *Science* **233**, 1300–1303.
- MARTENS C. S., HADDAD R. I., and CHANTON J. P. (1992) Organic matter accumulation, remineralization and burial in an anoxic coastal sediment. In *Organic Matter: Productivity, Accumulation, and Preservation in Recent and Ancient Sediments* (ed. J. K. WHELAN and J. W. FARRINGTON). Columbia Univ. Press (in press).
- MATTHEWS D. E. and HAYES J. M. (1978) Isotope ratio monitoring GC-MS. *Anal. Chem.* **50**, 1465–1473.
- MCINERNEY M. J. and BRYANT M. P. (1981) Anaerobic degradation of lactate by syntrophic associations of *Methanosarcina barkerii* and *Desulfovibrio* species and the effect of H₂ on acetate degradation. *Appl. Environ. Microbiol.* **41**, 346–354.
- MCINERNEY M. J., BRYANT M. P., and PFENNIG N. (1979) Anaerobic bacterium that degrades fatty acids in syntrophic association with methanogens. *Arch. Microbiol.* **122**, 129–135.
- MCMILLAN C. and SMITH B. N. (1982) Comparison of $\delta^{13}\text{C}$ values for seagrasses in experimental cultures and in natural habitats. *Aquat. Bot.* **14**, 381–387.
- MEINSCHEN W. G., RINALDI G. G. L., HAYES J. M., and SCHOELLER D. A. (1974) Intramolecular isotopic order in biologically produced acetic acid. *Biomed. Mass Spectr.* **1**, 172–174.
- MICHELSON A. R., JACOBSON M. E., SCRANTON M. I., and MACKIN J. E. (1989) Modeling the distribution of acetate in anoxic estuarine sediments. *Limnol. Oceanogr.* **34**, 747–757.
- MONSON K. D. and HAYES J. M. (1982a) Carbon isotopic fractionation in the biosynthesis of bacterial fatty acids. Ozonolysis of unsaturated fatty acids as a means of determining the intramolecular distribution of carbon isotopes. *Geochim. Cosmochim. Acta* **46**, 139–149.
- MONSON K. D. and HAYES J. M. (1982b) Biosynthetic control of the natural abundance of carbon 13 at specific positions within fatty acids in *Saccharomyces cerevisiae*. *J. Biol. Chem.* **257**, 5568–5575.
- NOVELLI P. C., MICHELSON A. R., SCRANTON M. I., BANTA G. T., HOBBS J. E., and HOWARTH R. W. (1988) Hydrogen and acetate cycling in two sulfate-reducing sediments: Buzzards Bay and Town Cove, Mass. *Geochim. Cosmochim. Acta* **52**, 2477–2486.
- OAKWOOD T. S. and MILLER M. R. (1950) The decarboxylation of simple fatty acids. *J. Amer. Chem. Soc.* **72**, 1849.
- PARKER P. L. (1964) The biogeochemistry of the stable isotopes of carbon in a marine bay. *Geochim. Cosmochim. Acta* **28**, 1155–1164.
- PARKES R. J., TAYLOR J., and JORCK-RAMBERG D. (1984) Demonstration, using *Desulfohalobacter* sp., of two pools of acetate with different biological availabilities in marine pore water. *Mar. Biol.* **83**, 271–276.
- PREUB A., SCHAUDER R., FUCHS G., and STICHLER W. (1989) Carbon isotope fractionation by autotrophic bacteria with three different CO₂ fixation pathways. *Z. Naturforsch.* **44c**, 397–402.
- REEBURGH W. S. (1967) An improved interstitial water sampler. *Limnol. Oceanogr.* **12**, 163–165.
- RINALDI G., MEINSCHEN W. G., and HAYES J. M. (1974) Carbon isotopic fractionations associated with acetic acid production by *Acetobacter suboxydans*. *Biomed. Mass Spectr.* **1**, 412–414.
- RISATTI J. B. and HAYES J. M. (1983) Biogenic acetate and the origin of sedimentary biogenic methane. *GSA Abstr. Prog.* **15**, 671.
- SANSONE F. J. and MARTENS C. S. (1981) Methane production from acetate and associated methane fluxes from anoxic coastal sediments. *Science* **211**, 707–709.
- SANSONE F. J. and MARTENS C. S. (1982) Volatile fatty acid cycling in organic-rich marine sediments. *Geochim. Cosmochim. Acta* **46**, 1575–1589.
- SCHAUDER R., EIKMANN B., THAUER R. K., WIDDEL F., and FUCHS G. (1986) Acetate oxidation to CO₂ in anaerobic bacteria via a novel pathway not involving reactions of the citric acid cycle. *Arch. Microbiol.* **145**, 162–172.
- SCHAUDER R., PREUSS A., JETTEN M., and FUCHS G. (1989) Oxidative and reductive acetyl CoA/carbon monoxide dehydrogenase pathway in *Desulfohalobacterium autotrophicum*. 2. Demonstration of the enzymes of the pathway and comparison of CO dehydrogenase. *Arch. Microbiol.* **151**, 84–89.
- SCHONHEIT P., KRISTJANSSON J. K., and THAUER R. K. (1982) Kinetic mechanism for the ability of sulfate reducers to out-compete methanogens for acetate. *Arch. Microbiol.* **132**, 285–288.
- SCHUTZ H., SEILER W., and CONRAD R. (1989) Processes involved in formation and emission of methane in rice paddies. *Biogeochem.* **7**, 33–53.
- SHAW D. G., ALPERIN M. J., REEBURGH W. S., and MCINTOSH D. J. (1984) Biogeochemistry of acetate in anoxic sediments of Skan Bay, Alaska. *Geochim. Cosmochim. Acta* **48**, 1819–1825.
- SORENSEN J., CHRISTENSEN D., and JORGENSEN B. B. (1981) Volatile fatty acids and hydrogen as substrates for sulfate-reducing bacteria in anaerobic marine sediment. *Appl. Environ. Microbiol.* **42**, 5–11.
- SOWERS K. R., NELSON M. J., and FERRY J. G. (1984) Growth of acetotrophic, methane-producing bacteria in a pH auxostat. *Curr. Microbiol.* **11**, 227–230.
- SPORMANN A. M. and THAUER R. K. (1988) Anaerobic acetate oxidation to CO₂ by *Desulfotomaculum acetoxidans*. Demonstration of enzymes required for the operation of an oxidative acetyl-CoA/carbon monoxide dehydrogenase pathway. *Arch. Microbiol.* **150**, 374–380.
- SPORMANN A. M. and THAUER R. K. (1989) Anaerobic acetate oxidation to CO₂ by *Desulfotomaculum acetoxidans*. Isotopic exchange between CO₂ and the carbonyl group of acetyl-CoA and topology of enzymes involved. *Arch. Microbiol.* **152**, 189–195.
- STADTMAN T. C. and BARKER H. A. (1949) Studies on the methane fermentation. VII. Tracer experiments on the mechanism of methane formation. *J. Biochem.* **21**, 256–264.
- STAMS A. J. M. and HANSEN T. A. (1984) Fermentation of glutamate and other compounds by *Acidaminobacter hydrogeniformans* gen. nov. sp. nov., an obligate anaerobe isolated from black mud. Studies with pure cultures and mixed cultures with sulfate-reducing and methanogenic bacteria. *Arch. Microbiol.* **137**, 329–337.
- STIEB M. and SCHINK B. (1985) Anaerobic oxidation of fatty acids by *Clostridium bryantii* sp. nov., a sporeforming, obligately syntrophic bacterium. *Arch. Microbiol.* **140**, 387–390.
- STIEB M. and SCHINK B. (1986) Anaerobic degradation of isovalerate by a defined methanogenic coculture. *Arch. Microbiol.* **144**, 291–295.
- STEPHENSON R. L., TAN F. C., and MANN K. H. (1984) Stable carbon isotope variability in marine macrophytes and its implications for food web studies. *Mar. Biol.* **81**, 223–230.
- THAUER R. K., MOLLER-ZINKHAN D., and SPORMANN A. M. (1989)

- Biochemistry of acetate catabolism in anaerobic chemotrophic bacteria. *Ann. Rev. Microbiol.* **43**, 43-67.
- THAYER G. W., PARKER P. L., LACROIX M. W., and FRY B. (1978) The stable carbon isotope ratio of some components of an eelgrass, *Zostera marina*, bed. *Oecologia (Berl.)* **35**, 1-12.
- WARFORD A. L., KOSIUR D. R., and DOOSE P. R. (1979) Methane production in Santa Barbara basin sediments. *Geomicrob. J.* **1**, 117-137.
- WHITICAR M. J., FABER E., and SCHOELL M. (1986) Biogenic methane formation in marine and freshwater environments: CO₂ reduction vs. acetate fermentation-Isotopic evidence. *Geochim. Cosmochim. Acta* **50**, 693-709.
- WINFREY M. R. and ZEIKUS J. G. (1979a) Anaerobic metabolism of immediate methane precursors in Lake Mendota. *Appl. Environ. Microbiol.* **37**, 244-253.
- WINFREY M. R. and ZEIKUS J. G. (1979b) Microbial methanogenesis and acetate metabolism in a meromictic lake. *Appl. Environ. Microbiol.* **37**, 213-221.
- WINFREY M. R. and WARD D. M. (1983) Substrates for sulfate reduction and methane production in intertidal sediments. *Appl. Environ. Microbiol.* **45**, 193-199.
- WINTER J. U. and WOLFE R. S. (1980) Methane formation from fructose by syntrophic associations of *Acetobacterium woodii* and different strains of methanogens. *Arch. Microbiol.* **124**, 73-79.
- ZEIKUS J. G. (1983) Metabolism of one-carbon compounds by chemotrophic anaerobes. *Adv. Microbiol. Physiol.* **24**, 215-299.
- ZINDER S. H. and KOCH M. (1984) Non-acetoclastic methanogenesis from acetate: Acetate oxidation by a thermophilic syntrophic co-culture. *Arch. Microbiol.* **138**, 263-272.

11

12

FACTORS THAT CONTROL THE STABLE
CARBON ISOTOPIC COMPOSITION OF
METHANE PRODUCED IN AN ANOXIC
MARINE SEDIMENT

M. J. Alperin

Curriculum in Marine Sciences, University of North
Carolina, Chapel Hill

N. E. Blair

Department of Marine, Earth, and Atmospheric
Sciences, North Carolina State University, Raleigh

D. B. Albert, T. M. Hoehler, and C. S. Martens

Curriculum in Marine Sciences, University of North
Carolina, Chapel Hill

Abstract. The carbon isotopic composition of methane produced in anoxic marine sediment is controlled by four factors: (1) the pathway of methane formation, (2) the isotopic composition of the methanogenic precursors, (3) the isotope fractionation factors for methane production, and (4) the isotope fractionation associated with methane oxidation. The importance of each factor was evaluated by monitoring stable carbon isotope ratios in methane produced by a sediment microcosm. Methane did not accumulate during the initial 42-day period when sediment contained sulfate, indicating little methane production from "noncompetitive" substrates. Following sulfate depletion, methane accumulation proceeded in three distinct phases. First, CO₂ reduction was the dominant methanogenic pathway and the isotopic composition of the methane produced ranged from -80 to -94 ‰. The acetate concentration increased during this phase, suggesting that acetoclastic methanogenic bacteria were unable to keep pace with acetate production. Second, acetate fermentation became the dominant methanogenic pathway as bacteria responded to elevated acetate concentrations. The methane produced during this phase was progressively enriched in ¹³C, reaching a

maximum $\delta^{13}\text{C}$ value of -42 ‰. Third, the acetate pool experienced a precipitous decline from >5 mM to <20 μM and methane production was again dominated by CO₂ reduction. The $\delta^{13}\text{C}$ of methane produced during this final phase ranged from -46 to -58 ‰. Methane oxidation concurrent with methane production was detected throughout the period of methane accumulation, at rates equivalent to 1 to 8% of the gross methane production rate. Thus methane oxidation was too slow to have significantly modified the isotopic signature of methane. A comparison of microcosm and field data suggests that similar microbial interactions may control seasonal variability in the isotopic composition of methane emitted from undisturbed Cape Lookout Bight sediment.

INTRODUCTION

Recent estimates place the current global methane flux to the atmosphere at $543 \pm 95 \times 10^{12} \text{ g CH}_4 \text{ yr}^{-1}$ [Cicerone and Oremland, 1988]. A relatively high level of precision ($\pm 17\%$) is possible because the global methane flux is calculated from three well-characterized parameters: the size of the atmospheric methane reservoir, the rate of change in atmospheric methane concentration, and the average residence time for atmospheric methane. Accurate estimates of reservoir size and rate of change are provided by concentration time series data from permanent stations throughout the world [Blake and Rowland,

Copyright 1992
by the American Geophysical Union.

Paper number 92GB01650.
0886-6236/92/92GB-01651\$10.00

1988]. Likewise, the residence time for methane is tightly constrained by atmospheric models of the hydroxyl radical field (calibrated with methyl chloroform distributions) and laboratory measurements of the rate coefficient for the methane-hydroxyl reaction [Prinn et al., 1987; Vaghjiani and Ravishankara, 1991; Taylor et al., 1991; Fung et al., 1991].

The contribution of individual sources to the total methane flux is much more difficult to constrain. The vast number and widespread geographic distribution of significant methane sources means that detailed studies of emission rates are limited to a relatively small number of representative systems. The precision of source strength estimates based on direct flux measurements is limited by spatial and temporal variability and uncertainty in the areal distribution of ecosystem types. The uncertainty of the global methane flux calculated by summing individual source terms is about $\pm 50\%$ [Tyler, 1991].

Quantitative knowledge of individual source strengths is of critical importance because atmospheric methane concentrations have more than doubled during the past 300 years [Pearman, 1986]. Since methane is a radiatively active trace gas, an increase in the atmospheric methane reservoir could alter the Earth's energy budget and contribute to global-scale climate change [Cicerone and Oremland, 1988]. In addition, methane serves as a sink for the hydroxyl radical and therefore plays an important role in regulating the oxidizing power of the atmosphere [Cicerone and Oremland, 1988]. Accurate source strength estimates are necessary to understand the underlying causes of increasing atmospheric inventories and to evaluate the efficacy of different mitigation strategies.

The isotopic composition of carbon in the methane molecule serves as a natural tracer of source. Methane produced during biomass combustion is enriched in ^{13}C relative to that produced by methanogenic bacteria [Stevens and Engelkemeir, 1988]. Fossil methane (from natural gas pipelines, coal mining activities, clathrate decomposition, and peat remineralization) can be distinguished on the basis of its low ^{14}C content [Wahlen et al., 1989]. The isotopic composition of atmospheric methane can provide a global-scale estimate of the contribution of bacterial, biomass burning, and fossil sources to the global methane budget [Quay et al., 1991].

The accuracy of source strength estimates based on isotopic constraints is limited by variability in the

isotopic composition of methane produced by individual sources. For example, $\delta^{13}\text{C}$ values of methane emitted from a particular ecosystem (such as a temperate wetland, Arctic tundra, or rice paddy) can vary by as much as 20 to 30 ‰ [Quay et al., 1988; Tyler et al., 1988; Chanton and Martens, 1988]. The factors that contribute to this variability are not well understood.

One important factor in controlling the stable carbon isotopic composition of bacterial methane is the mechanism of methane formation. Acetate fermentation and CO_2 reduction are thought to be the dominant methane production pathways in nature [Oremland, 1988]. However, methanogenic bacteria are known to produce methane from alternative compounds such as formate, methanol, methylated amines, and methylated sulfur compounds [Oremland, 1988]. These compounds serve as important methane precursors in some environments [Strayer and Tiedje, 1978; Oremland et al., 1982; King et al., 1983; King, 1988], but their widespread significance remains a matter of debate.

The isotopic composition of methane produced by a particular pathway depends on the $\delta^{13}\text{C}$ of the methane precursor and the isotope fractionation associated with the production process (i.e., the kinetic isotope effect). Therefore variations in $\delta^{13}\text{C}\text{-CH}_4$ are controlled by the relative contribution of different methane production pathways, the isotopic composition of the methane precursors, and the kinetic isotope effect for each pathway. In addition, aerobic and anaerobic methane oxidation can alter the isotopic composition of the residual methane reservoir [King et al., 1989; Alperin et al., 1988].

Most field-based studies designed to characterize the isotopic composition of methane emitted from specific sources have not conducted the process-level research necessary to understand the factors that control $\delta^{13}\text{C}\text{-CH}_4$ variability. In this study, we monitored the $\delta^{13}\text{C}$ of methane produced by a laboratory microcosm containing anoxic marine sediment from Cape Lookout Bight, North Carolina. We concurrently measured methane production rates from CO_2 and acetate, methane oxidation rates, $\delta^{13}\text{C}\text{-}\Sigma\text{CO}_2$, and a suite of key indicators of microbial processes. We observed large variations over time in the $\delta^{13}\text{C}$ of methane produced by the microcosm. These variations can be attributed both to shifts in the relative importance of CO_2 reduction and acetate fermentation, as well as changes in the isotopic composition of the methane precursors. The variability in $\delta^{13}\text{C}$ -

CH₄ can be understood in terms of syntrophic and competitive interactions between the microorganisms involved in organic matter remineralization. A comparison of microcosm and field data suggests that similar microbial interactions may control seasonal variability in the isotopic composition of methane emitted from Cape Lookout Bight sediment.

METHODS

Study Site and Sediment Sampling

Sediment was collected from Cape Lookout Bight, a shallow (10 m) barrier island lagoon located 70 km southwest of Cape Hatteras, North Carolina. Organic carbon deposition at this site ($165 \pm 20 \text{ mol m}^{-2} \text{ yr}^{-1}$) is among the highest reported for a coastal marine environment [Martens et al., 1992]. Sediment oxygen penetration is restricted to several hundred microns despite an air-saturated water column mixed by strong tidal currents. Sediment metabolism is dominated by microbial sulfate reduction and methane production, with methanogenesis accounting for about 30% of the annual integrated organic matter remineralization [Martens and Klump, 1984]. Metabolic rates exhibit strong seasonality driven by annual temperature changes of $>20^\circ\text{C}$ [Klump and Martens, 1989]. Sulfate concentration profiles are modulated by seasonal variations in sulfate reduction rates; the vertical extent of the sulfate reduction zone oscillates from $>30 \text{ cm}$ in the winter to $<10 \text{ cm}$ in the summer [Crill and Martens, 1987]. Methane production rates are highest immediately below the sulfate reduction zone [Crill and Martens, 1986] and sediments are methane-saturated below this horizon. During the summer, methane bubbles form below 10 cm and low tide ebullition occurs in response to reduced hydrostatic pressure [Martens and Klump, 1980]. The $\delta^{13}\text{C}$ of methane contained in these bubbles exhibits seasonal variations of $\sim 10 \text{ ‰}$ [Martens et al., 1986; Burke et al., 1987]. Sediment accumulation rates at this site are approximately 10 cm yr^{-1} [Chanton et al., 1983; Canuel et al., 1990].

Sediment samples used in this study were collected in July 1990 when sulfate reduction and methane production rates were at their annual maximum. Cores were collected by SCUBA diver in 22 cm x 13 cm diameter Plexiglass tubes. The tubes were gently inserted into the sediment and capped on top and bottom before being carefully withdrawn.

The cores were kept in the dark at in situ temperature (26.5°C) during transport to the laboratory.

Incubation Vessel

A large capacity syringe (hereafter referred to as the "magnum syringe") capable of long-term headspace-free incubations was constructed for this study (Figure 1). The vessel was designed as a syringe to allow for intermittent sample withdrawal without introducing a headspace. The presence of a headspace would significantly alter concentrations of dissolved methane and ΣCO_2 .

The syringe barrel was fabricated from 4-inch (10.16 cm) ID Kimax Beaded Process Pipe with a 10-mm bore stopcock (Teflon plug) welded to one end. The piston was constructed of solid polyvinyl chloride (PVC) machined to provide a slide-fit within the syringe barrel. A thin Teflon plate was secured to the bottom of the piston to prevent contact between sediment and PVC. Attempts at making a direct O-ring seal between the piston and the barrel failed due to variability in the inner diameter of the glass

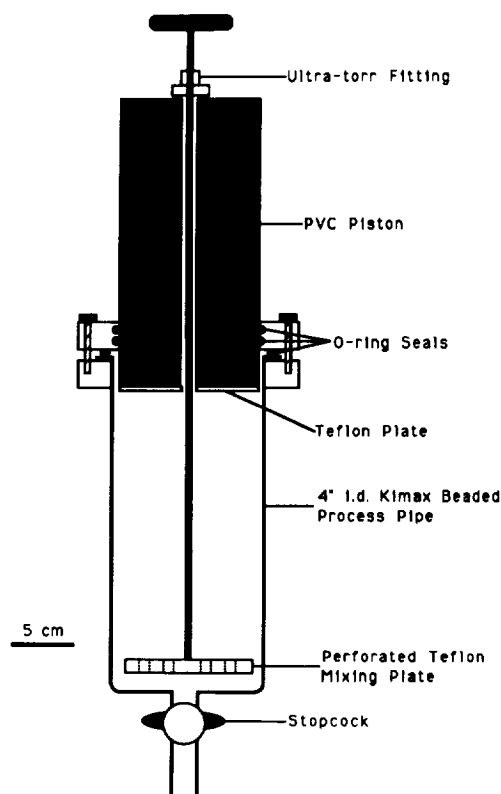


Fig. 1. Magnum syringe for incubating $\sim 2 \text{ L}$ sediment under headspace-free, anoxic conditions.

pipe. Therefore the piston was sealed to the barrel by means of a custom fabricated coupling that provided an O-ring seal to the barrel flange and a double O-ring seal around the piston. Sediment within the magnum syringe could be homogenized without air contact by churning with a perforated Teflon mixing plate connected to a Teflon rod that passed through a slightly oversized hole bored through the center of the piston. The mixing rod was sealed to the top of the piston with an Ultra-torr fitting (Cajon Vacuum Products) that provided a gas-tight seal while allowing for axial movement.

The magnum syringe was filled with sediment from the 0 to 3 cm depth interval. Six cores were pooled to give a total sediment volume of ~2 L. The piston was positioned in such a way as to exclude gas pockets and fastened in place by securing the coupling. The magnum syringe was sampled at weekly intervals by displacing 120 mL of sediment into two 60-mL catheter-tip plastic syringes that fit snugly in the arm of the stopcock. A large chain clamp immobilized the piston between sampling intervals. The sediment was homogenized prior to each sampling by churning sediment through the mixing plate. The magnum syringe was incubated in the dark at $22 \pm 1^\circ\text{C}$.

Concentration Measurements

Sulfate, acetate, and ΣCO_2 concentrations were determined on interstitial water extracted from whole sediment by centrifugation. Care was taken to prevent sediment and interstitial water from contacting air. Sediment was transferred to an argon-flushed 30-mL centrifuge tube and spun at 6000 G for 15 min. The centrifuge tube was filled to the top to minimize loss of gaseous CO_2 into the headspace volume. Following centrifugation, supernatant from just above the solid-liquid interface was pipetted using a long stainless steel needle fixed to a 5-mL glass syringe. The interstitial water was passed through a $0.45\text{-}\mu\text{m}$ syringe filter; the first milliliter of filtrate was discarded.

Sulfate concentrations were determined using a Dionex 2010i ion chromatograph. In order to minimize sulfide oxidation in the sample, 1.0-mL interstitial water was filtered directly into an argon-flushed vial containing 100- μL 10% (v/v) HCl and stripped of volatile sulfur compounds by bubbling with O_2 -free argon. The samples were diluted 1:10 with distilled water and passed thru an ONGUARD-Ag pretreatment cartridge (Dionex Corporation) to

remove chloride. The large quantity of chloride in interstitial water (~600 mM) interferes with low-level (<1 mM) sulfate determinations; after chloride removal the detection limit for sulfate was 5 μM .

Acetate concentrations were determined by HPLC using precolumn derivatization with 2-nitrophenylhydrazine [Albert et al., 1992]. The derivatives were prepared directly in the pore water and separated by a C8 reversed phase column with buffered, ion-pairing solvent. The detection limit for this method is 0.5 μM ; the precision is typically $\pm 5\%$.

Interstitial water for ΣCO_2 analysis was stored in 3.5-mL Pyrex screw-cap vials filled to just below the rim and capped with Teflon-faced silicone septa. Loss of CO_2 into the gas phase was prevented by displacing the headspace with a 4-mm Pyrex rod inserted through a hole in the septum. The ΣCO_2 concentrations were determined using the inorganic carbon channel of a Shimadzu TOC-5000 total carbon analyzer. Samples (25 μL) were injected directly into a gas stripping chamber containing 25% (v/v) H_3PO_4 . The CO_2 released upon acidification was quantified by a nondispersive infrared detector.

Whole sediment methane concentrations were measured by a headspace equilibration technique [Alperin and Reeburgh, 1985]. Whole sediment concentrations include methane dissolved in the pore water as well as methane bubbles trapped in the sediment. Sediment (2.5 mL) was transferred to a tared 30-mL serum vial containing 3-mL 0.1 N NaOH, sealed with a silicone stopper, and thoroughly vortex-mixed to disperse the sediment and equilibrate the gas and aqueous phase. An aliquot of the headspace was analyzed for methane by a Shimadzu Mini-2 gas chromatograph equipped with flame ionization detector. Standards were prepared by injecting pure methane into sealed 30-mL serum vials containing 3-mL 0.1 N NaOH and 2.5-mL distilled water. Samples and standards were kept at the same temperature and had equal volumes of aqueous phase and headspace, so corrections for the quantity of dissolved methane were not necessary. Whole sediment methane concentrations were converted to pore water units by dividing by sediment porosity.

Rate Measurements

Sulfate reduction [Albert et al., 1992], methane production from acetate [Crill and Martens, 1986],

methane production from CO_2 [Crill and Martens, 1986], and methane oxidation [Alperin and Reeburgh, 1985] rates were determined by previously described radiotracer techniques. Briefly, whole sediment was transferred to gas-tight 2.5-mL glass incubation syringes and injected with microliter quantities of radiotracer ($^{35}\text{SO}_4^{2-}$, $[\text{U-}^{14}\text{C}]\text{acetate}$, $[\text{U-}^{14}\text{C}]\text{-HCO}_3^-$, or $^{14}\text{CH}_4$). The samples were incubated at $22 \pm 1^\circ\text{C}$ for a time interval sufficient for 1 to 10% of the tracer pool to turnover. The incubation time was generally 24 hours, except samples injected with $[\text{U-}^{14}\text{C}]\text{acetate}$ which had incubation times ranging from 10 min to 27 hours. At two times (93 and 107 days), the samples amended with $[\text{U-}^{14}\text{C}]\text{acetate}$ were incubated sufficiently long that 40–60% of the tracer turned over. Methane production rates from acetate at these two times are considered to be underestimated.

Sediment samples assayed for sulfate reduction rate were "killed" by freezing the incubation syringes. For other rate measurements, the incubation was terminated by extruding the sediment into serum vials containing NaOH solution. The serum vials were quickly sealed with butyl-rubber or silicone stoppers and stored frozen and upside-down (to retard gas loss) until analysis. Collection and quantification of radioisotopes was according to published procedures (references given above). The rates were calculated from the following equation:

$$\text{Rate} = [\text{C}] \frac{a \alpha}{A t},$$

where $[\text{C}]$ is reactant concentration (i.e., sulfate, acetate, ΣCO_2 , or methane), a and A are activities of recovered product and added reactant, respectively, α is the fractionation factor for the tracer isotope (^{14}C or ^{35}S) relative to the dominant natural isotope (^{12}C or ^{32}S), and t is the incubation time. The isotope fractionation factor was taken to be 1.12 for methane production from CO_2 [Blair et al., 1992], 1.06 for methane production from acetate [Blair and Carter, 1992], 1.02 for methane oxidation [Alperin et al., 1988], and 1.045 for sulfate reduction [Jørgensen, 1978]. Note that isotope discrimination for ^{14}C is twice that for ^{13}C [Stern and Vogel, 1971].

Stable Isotope Measurements

The $\delta^{13}\text{C}$ - ΣCO_2 analyses were done on 1.0-mL aliquots of filtered interstitial water stored in 3-mL serum vials capped with silicone septa. Samples were acidified with 0.5-mL 1 M H_3PO_4 and stripped with helium into a gas purification line [Schaff et al.,

1992]. Air and CO_2 were separated by a GC column packed with porous silica beads (Unibeads 1S, Alltech Associates) and quantified by a thermal conductivity detector (Gow Mac Corporation). The CO_2 peak was collected in a cryogenic trap (-196°C) fashioned from six loops of 1/8 inch (0.318 cm) stainless steel tubing. The helium was pumped away, and the CO_2 was transferred to a Pyrex breakseal ampoule for introduction to the isotope ratio mass spectrometer.

For $\delta^{13}\text{C}$ - CH_4 analysis, 10-mL whole sediment was transferred to a 60-mL serum vial containing 5-mL 1N NaOH and sealed with a black butyl rubber stopper. The sample and base were thoroughly slurried and an aliquot of the headspace was transferred to a gas-tight syringe and injected into a combustion line. The sample was flushed with helium carrier gas through a cryogenic trap (-196°C) to remove CO_2 and H_2O and into a combustion tube packed with CuO at 780°C . The CO_2 and H_2O resulting from methane combustion were passed through a multiloop trap maintained at -120°C (to remove H_2O), and the CO_2 was collected in a breakseal ampoule.

Carbon isotopic analyses were performed with a Delta E ratio mass spectrometer (Finnigan-Mat) equipped with a modified low-volume inlet system [Hayes et al., 1977]. The precision of the $\delta^{13}\text{C}$ analysis was ± 0.1 ‰.

RESULTS

Changes in sulfate, methane, acetate, and ΣCO_2 concentrations during the 114-day incubation period are summarized in Figure 2. The sulfate concentration decreased from 18.6 mM at the outset to 0.19 mM at 42 days (Figure 2a). After 50 days, sulfate leveled off at 10 to 20 μM , comparable to the threshold concentration below which sulfate reduction stops for pure cultures of *Desulfobacter postgatei* [Ingvorsen et al., 1984].

The methane concentration remained relatively constant (~ 0.2 mM) until sulfate was depleted to < 0.2 mM (Figure 2a). Following sulfate depletion, the methane concentration increased, exceeding the saturation level (1.2 mM [Yamamoto et al., 1976]) after 70 days. Since the immobilized magnum syringe piston restricted headspace formation, subsequent methane production resulted in a pressure buildup. The coupling that sealed the piston to the barrel was not capable of containing positive pressures and methane was inadvertently lost. The

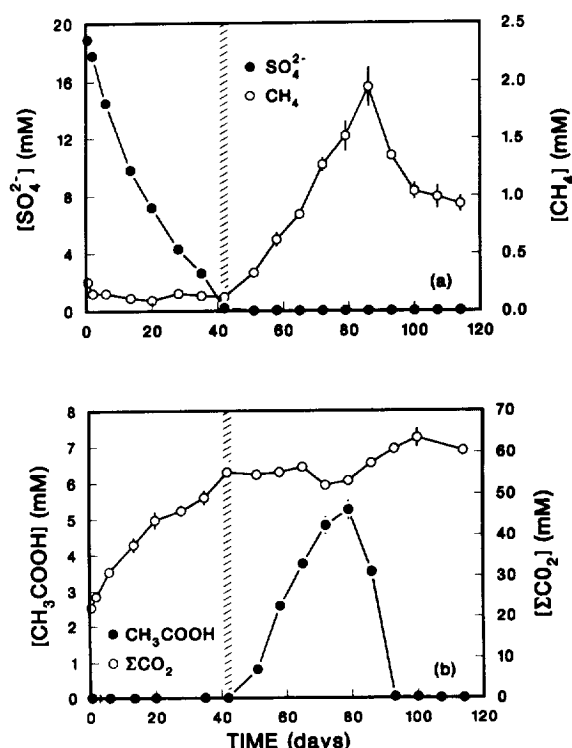


Fig. 2. Changes in pore water concentrations during the 114-day incubation period. (a) Sulfate and methane; (b) acetate and ΣCO_2 . With the exception of acetate, error bars represent the standard deviation of triplicate analyses. A standard deviation of $\pm 5\%$ is assumed for acetate concentrations. The absence of an error bar indicates that the standard deviation is smaller than the symbol. The hatched line denotes the time that pore water sulfate concentrations were depleted to <0.2 mM.

decrease in methane concentration after 85 days is due to gas loss from the magnum syringe rather than net methane consumption (see below).

The acetate concentration ranged from 1 to $9\text{ }\mu\text{M}$ during the initial 42-day period when sediment contained appreciable sulfate (Figure 2b). Acetate concentrations $<10\text{ }\mu\text{M}$ are typical for sulfate-containing marine sediment [Ingvorsen et al., 1984]. Following sulfate depletion, acetate began to accumulate in the sediment, reaching a peak concentration of 5.3 mM at ~ 80 days. The period of acetate accumulation was immediately followed by a period of dramatic depletion as concentrations fell to $5\text{ }\mu\text{M}$ in just 14 days.

The ΣCO_2 concentration increased rapidly during the period that sediment contained sulfate (Figure

2b). Sulfate and ΣCO_2 concentrations during the initial 42-day period are highly correlated ($r^2 = 0.99$), suggesting that sulfate served as the dominant terminal electron acceptor for organic matter remineralization. The slope of the ΣCO_2 versus sulfate plot ($\Delta[\Sigma\text{CO}_2]/\Delta[\text{SO}_4^{2-}]$) is -1.7 ± 0.1 , suggesting that sediment organic carbon remineralized in the magnum syringe experiment had an average oxidation state somewhat less than carbon in pure carbohydrate.

The rate of increase of ΣCO_2 tapered off following sulfate depletion. This is primarily due to a delay in ΣCO_2 production caused by pooling of carbon in the acetate reservoir. However, the gas loss that occurred when methane concentrations exceeded saturation may also have contributed to a reduced rate of dissolved ΣCO_2 accumulation. Gas equilibrated with sediment pore waters (pH 7) having a ΣCO_2 concentration of 50 mM will have a CO_2 partial pressure of 0.2 atm [Stumm and Morgan, 1981]. Therefore ΣCO_2 concentrations in samples collected after methane concentrations exceeded saturation should be regarded as lower limits.

Sulfate reduction, methane oxidation, and methane production rates are presented in Figure 3. Sulfate reduction rates measured by the ^{35}S tracer method are consistent with rates calculated from changes in sulfate concentration. Sulfate reduction rates fell off rapidly from the outset (Figure 3a), suggesting a rapid depletion of the most reactive fraction of the organic carbon pool [Westrich and Berner, 1984]. Since sulfate concentrations throughout most of the sulfate reduction period were well in excess of the half-saturation constant for sulfate reducing bacteria (0.2 mM [Ingvorsen et al., 1984]), it is unlikely that the initial decline in the sulfate reduction rate was due to sulfate limitation.

Methane oxidation rates remained near baseline level throughout the period that sediment contained sulfate (Figure 3a). Note that methane concentrations during the initial 42 days ($\sim 0.2\text{ mM}$, Figure 2a) were sufficient to support moderate rates of oxidation. Following sulfate depletion, methane oxidation rates began to increase, achieving maximum values between 80 and 100 days. The methane oxidation rate at all times represents a small fraction (1 to 8%) of the total methane production rate (see below). Methane oxidation rates integrated over the 114-day experiment account for only 2.4% of the integrated methane production. Net methane oxidation was not observed during this experiment.

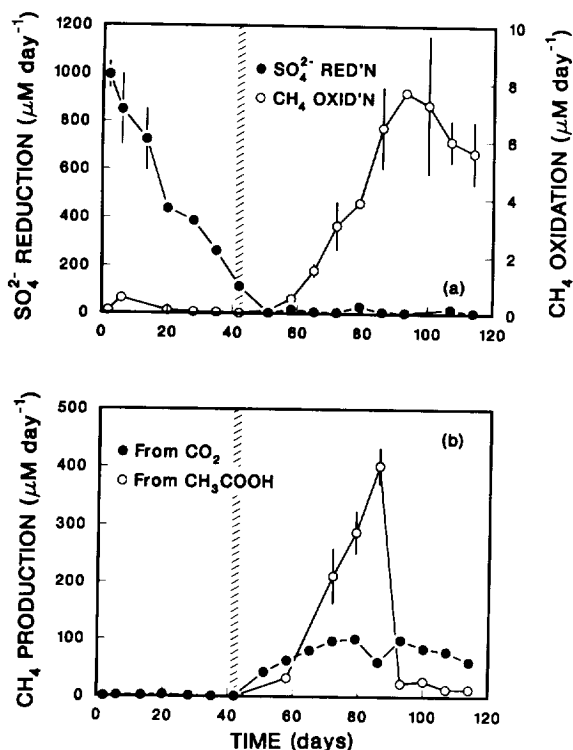


Fig. 3. Changes in rates of microbial processes during the 114-day incubation period. (a) Sulfate reduction and methane oxidation; (b) methane production from CO_2 and acetate. Rates of methane production from acetate at 93 and 107 days are considered to be underestimated because 40 to 60% of the tracer turned-over during the incubation period. The error bars represent the standard deviation of rates measured in two to four (generally 3) replicate samples. The absence of an error bar indicates that the standard deviation is smaller than the symbol. The hatched line denotes the time that pore water sulfate concentrations were depleted to <0.2 mM.

Methane production rates from CO_2 and acetate were negligible during the period that sediment contained sulfate (Figure 3b). The absence of CO_2 reduction and acetate fermentation in the presence of sulfate is consistent with the well-established principle that sulfate-reducing bacteria out-compete methanogens for H_2 and acetate [Kristjansson et al., 1982; Schonheit et al., 1982]. Following sulfate depletion, methane production rates from CO_2 and acetate began to increase, but the two methanogenic pathways followed very different patterns. Methane production from CO_2 increased steadily, reached a

maximum rate of $\sim 100 \mu\text{M d}^{-1}$, and gradually declined. In contrast, methane production from acetate began relatively slowly, increased sharply to $\sim 400 \mu\text{M d}^{-1}$, and then decreased dramatically to very low levels.

Relatively constant methane concentrations (Figure 2a) and very low rates of oxidation in sulfate-containing sediment (Figure 3a) suggest little methane production from "noncompetitive" substrates (i.e., compounds not metabolized by sulfate-reducing bacteria). Therefore acetate fermentation and CO_2 reduction are assumed to be the dominant pathways for methane production throughout the experiment. Total methane production rates (Figure 4a) are calculated as the sum of methane production from CO_2 and methane production from acetate.

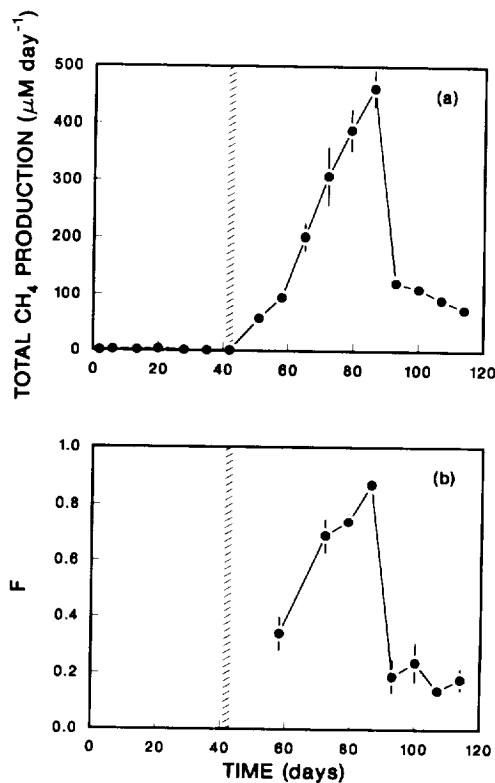


Fig. 4. Changes in total methane production rates and pathways during the 114-day incubation period. (a) Total methane production rates; (b) fraction of methane derived from acetate (F). The error bars were calculated by error propagation. The absence of an error bar indicates that the standard deviation is smaller than the symbol. The hatched line denotes the time that pore water sulfate concentrations were depleted to <0.2 mM.

The fraction of methane derived from acetate (F) varied considerably over the course of the experiment (Figure 4b). Following the sulfate-methane transition, CO₂ reduction accounted for the bulk of the methane production. As acetate accumulated in the pore waters (Figure 2b), the methanogenic pathway shifted and acetate became the major methane precursor. Acetate fermentation dominated methane production until the acetate reservoir was fully depleted. At this point, CO₂ reduction resumed its role as the dominant methanogenic pathway. Over the course of the experiment, acetate fermentation accounted for nearly 60% of the total methane production.

The ΣCO_2 and methane reservoir experienced large changes in isotopic composition over the course of the 114-day experiment (Figure 5). During the period that sediment contained sulfate, $\delta^{13}\text{C}-\Sigma\text{CO}_2$ values decreased only slightly (Figure 5a), despite a large increase in ΣCO_2 concentration (Figure 2b).

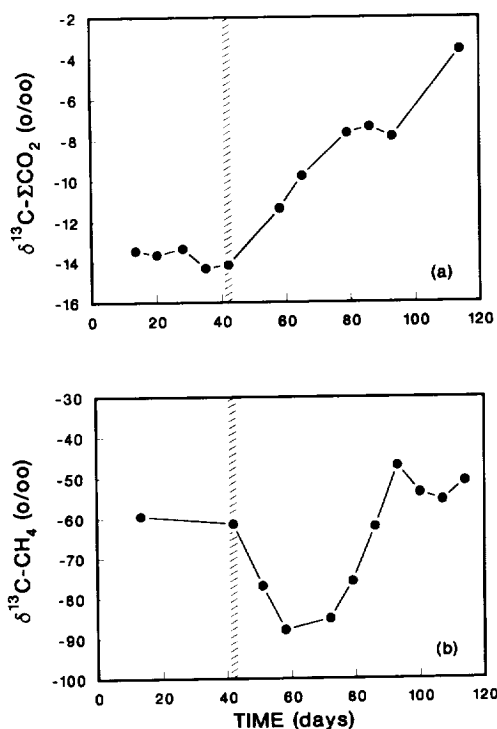


Fig. 5. Changes in $\delta^{13}\text{C}$ values during the 114-day incubation period. (a) $\delta^{13}\text{C}-\Sigma\text{CO}_2$; (b) $\delta^{13}\text{C}-\text{CH}_4$. Samples were not analyzed for $\delta^{13}\text{C}$ during the first 6 days of the experiment. The hatched line denotes the time that pore water sulfate concentrations were depleted to <0.2 mM.

This suggests that the CO₂ produced by organic matter remineralization had a $\delta^{13}\text{C}$ similar to the initial value of the ΣCO_2 pool. Following sulfate depletion, the ΣCO_2 reservoir became progressively enriched in ^{13}C .

The $\delta^{13}\text{C}-\text{CH}_4$ values remained nearly constant (-59 to -61 ‰) prior to the onset of methanogenesis (Figure 5b). The low methane concentrations during this initial period reflect methane that was present in the 0 to 3 cm interval at the time the sediment was collected. The initial $\delta^{13}\text{C}-\text{CH}_4$ values are similar to those for methane in gas bubbles collected from Cape Lookout Bight sediment in July (-59 to -62 ‰) [Martens et al., 1986; Burke et al., 1987]. Following sulfate depletion, the methane reservoir underwent substantial variations in $\delta^{13}\text{C}$. The $\delta^{13}\text{C}-\text{CH}_4$ initially dropped from -61 to -88 ‰, gradually increased to -47 ‰, and decreased slightly toward the end of the experiment.

DISCUSSION

The isotopic composition of methane in the magnum syringe varied by more than 40 ‰ over the course of the experiment (Figure 5b). In the following section, we evaluate the relative importance of changes in methanogenic pathway, precursor isotopic composition, and kinetic isotope effects in controlling the observed variations in $\delta^{13}\text{C}-\text{CH}_4$. Since integrated rates of methane production are ~ 40 times greater than methane oxidation, it is unlikely that methane oxidation played an important role in controlling the isotopic composition of methane.

The discussion is divided into four sections. The first section examines the relationship between $\delta^{13}\text{C}-\text{CH}_4$ and the methane production pathway. The second section provides constraints on variations in the isotopic composition of the major methane precursors (CO₂ and acetate). The third section describes the microbial interactions that may have played a role in regulating both methane production pathways and substrate isotopic composition. The final section compares the results of the microcosm experiment with in situ seasonal variations in isotopic composition of methane emitted from Cape Lookout Bight sediments.

$\delta^{13}\text{C}-\text{CH}_4$ Versus Methane Production Pathway

Measured $\delta^{13}\text{C}-\text{CH}_4$ values (Figure 5b) reflect the isotopic composition of methane accumulated in

the magnum syringe. Before we can examine the relationship between $\delta^{13}\text{C}\text{-CH}_4$ and methane production pathway, the $\delta^{13}\text{C}$ of the methane produced during a discrete time interval must be determined by an isotope mass balance calculation. Since the positive pressures that developed in the magnum syringe when methane concentrations exceeded saturation resulted in gas loss, methane concentrations must be corrected before mass balance constraints can be applied.

Methane concentrations corrected for gas loss.

Methane concentrations calculated by integrating production rate data are unaffected by gas loss from the magnum syringe and therefore reflect the total quantity of methane produced during the experimental period. The methane concentration at time t_2 is equal to the concentration at time t_1 plus the time integral of the total methane production rate (MPR) (Figure 4a):

$$[\text{CH}_4]_2 = [\text{CH}_4]_1 + \int_1^2 \text{MPR} \, dt \quad (1)$$

Calculated (equation (1)) and measured concentrations began to diverge as the methane concentration approached saturation (Figure 6). By the end of the experiment (114 days), the measured methane concentration represents less than 10% of the calculated value.

Isotopic composition of methane produced. The isotopic composition of methane produced in the magnum syringe ($\delta^{13}\text{C}\text{-MP}$) during any discrete time interval (e.g., t_1 to t_2) can be calculated by an isotope mass balance equation:

$$\delta^{13}\text{C}\text{-MP} = \frac{(\delta^{13}\text{C}\text{-CH}_4)_2 [\text{CH}_4]_2 - (\delta^{13}\text{C}\text{-CH}_4)_1 [\text{CH}_4]_1}{[\text{CH}_4]_{\text{PROD}}}, \quad (2)$$

where $[\text{CH}_4]_{\text{PROD}}$ is the concentration of methane produced during the time interval t_1 to t_2 .

Two factors must be considered before applying (2) to the magnum syringe experiment. First, the gas phase that appeared when methane concentrations exceeded saturation could lead to isotopic fractionation if there was an isotope effect associated with transfer of dissolved methane to the gas phase. Bernard et al. [1976] have shown that there is little isotopic fractionation between $\text{CH}_4(\text{aq})$ and $\text{CH}_4(\text{g})$

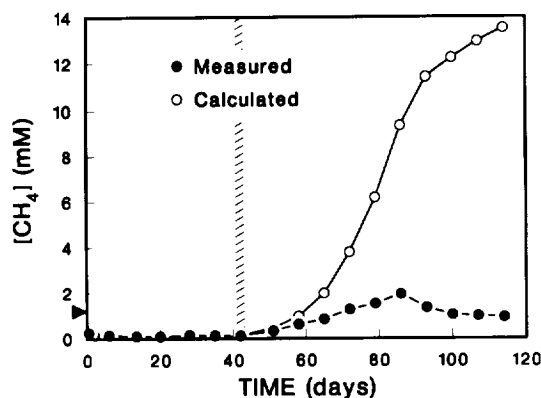


Fig. 6. Changes in measured and calculated methane concentrations during the 114-day incubation period. The method used to calculate methane concentrations is described in the text. The arrow on the concentration axis marks the dissolved methane concentration equivalent to a partial pressure of 1 atm. The hatched line denotes the time that pore water sulfate concentrations were depleted to <0.2 mM.

(0.3 ‰), so formation of a gas phase would not have an appreciable effect on the isotopic composition of the dissolved methane pool.

Application of (2) is further complicated by the large fraction of the methane production that was lost from the magnum syringe when positive pressures developed (Figure 6). Since effusive transport discriminates between ^{12}C - and ^{13}C -methane according to Graham's law [Mason and Kronstadt, 1967], gas loss via this mechanism would cause methane remaining in the magnum syringe to become enriched in ^{13}C . In order for effusive transport to occur, methane must pass through an orifice without colliding with other gas molecules. This requires that the diameter of the leak in the O-ring seal be less than the mean free path of the methane molecule (46 nm). The effusive flux through a hole this size can be calculated [Mason and Evans, 1969] by assuming the leak to have cylindrical geometry with length equal to the O-ring cross section (3 mm). The effusive flux ($\sim 10^{-8} \text{ mmol d}^{-1}$) is 7 orders-of-magnitude less than the actual leak rate (0.1 to 0.4 mmol d^{-1}) estimated from the difference between calculated and measured methane concentrations (Figure 6). This implies that pressure-driven gas transport from the magnum syringe must have occurred by other mechanisms. Since there is no mass discrimination during turbulent or viscous flow [Halsted and Nier, 1950], gas loss through faults in the O-ring coupling is unlikely to alter the $\delta^{13}\text{C}$ value of the methane.

Methane loss did reduce the size of the reservoir, however, so that the isotopic composition of any methane produced had a proportionately greater effect on the cumulative $\delta^{13}\text{C}$. The effect of gas loss on the isotopic composition of the methane reservoir was corrected in the following way. Cubic spline functions [Ahlberg et al., 1967] were fit to the measured and calculated methane concentration (Figure 6) and $\delta^{13}\text{C}$ - CH_4 data (Figure 5b) to allow interpolation at any t_1 and t_2 . Loss of methane from the magnum syringe was compensated by calculating the methane concentration at t_2 as

$$[\text{CH}_4]_2 = [\text{CH}_4]_1 + [\text{CH}_4]_{\text{PROD}}, \quad (3)$$

$$\text{where } [\text{CH}_4]_{\text{PROD}} = [\text{CH}_4]_2^* - [\text{CH}_4]_1^*. \quad (4)$$

The asterisks indicate calculated (as opposed to measured) methane concentrations. Thus $[\text{CH}_4]_2$ in (3) represents the methane concentration that would be present at t_2 if there was no gas loss during the time interval t_1 to t_2 . Any gas loss is treated as though it occurred during an infinitesimal time interval just after t_2 .

The $\delta^{13}\text{C}$ of methane produced during the time interval t_1 to t_2 was corrected for the effect of gas loss by combining (2), (3), and (4). The time step ($t_2 - t_1$) was made sufficiently small (0.1 day) that the calculated $\delta^{13}\text{C}$ -MP closely approximates the $\delta^{13}\text{C}$ of methane produced during any instant. The $\delta^{13}\text{C}$ value of methane produced during a finite time interval (e.g., between consecutive magnum syringe samples) was then calculated by integrating instantaneous $[\text{CH}_4]_{\text{PROD}}$ and $\delta^{13}\text{C}$ -MP values:

$$\delta^{13}\text{C-MP} = \frac{\int_A^B ([\text{CH}_4]_{\text{PROD}} \delta^{13}\text{C-MP}) dt}{\int_A^B [\text{CH}_4]_{\text{PROD}} dt}, \quad (5)$$

where A and B represent the beginning and end of the time interval of interest.

The $\delta^{13}\text{C}$ of methane produced by the sediment microcosm (calculated by equation (5)) varied between -94 and -42 ‰ (Figure 7). The range (52 ‰) is greater than that of the measured values because the cumulative reservoir represents an integrated isotopic composition. The isotopic composition of the cumulative reservoir tracks $\delta^{13}\text{C}$ -MP fairly closely (cf. Figures 5b and 7) because methane continuously escaped from the

magnum syringe once the methane concentration exceeded saturation.

There is no simple relationship between the $\delta^{13}\text{C}$ of the methane produced in the magnum syringe and the methane production pathway. For example, CO_2 reduction dominated methane production (accounting for ~70% of total production) both at the outset of the methanogenic period and toward the end of the experiment (Figure 4b). However, methane produced during the initial period (-80 to -94 ‰, Figure 7) was highly depleted in ^{13}C relative to the methane produced during the later period (-46 to -60 ‰). A simple relationship between $\delta^{13}\text{C}$ - CH_4 and methane production pathway is expected only if the methane produced by each mechanism has a distinct isotopic composition. The absence of such a relationship indicates variability in the $\delta^{13}\text{C}$ value of methane produced by a particular pathway. Such variability can be driven by changes in the isotopic composition of the methane precursors (CO_2 and acetate) and/or changes in the magnitude of the kinetic isotopic effect associated with each methane production mechanism.

Overall isotope mass balance. Conservation of mass requires that the end products of organic matter degradation (CO_2 and methane) have the same cumulative isotopic composition as the remineralized organic carbon. The isotopic composition of the

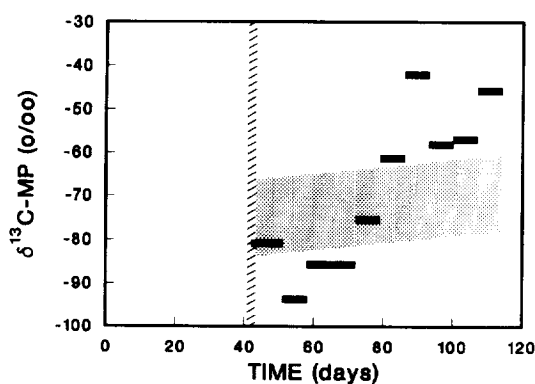


Fig. 7. Changes in isotopic composition of methane produced ($\delta^{13}\text{C}$ -MP) during the 114-day incubation period. The solid horizontal bars represent the $\delta^{13}\text{C}$ of methane produced between consecutive sampling intervals. The shaded region represents the $\delta^{13}\text{C}$ of methane produced by CO_2 reduction. Details of the calculations are given in the text. The hatched line denotes the time that pore water sulfate concentrations were depleted to <0.2 mM.

labile organic carbon should not be directly affected by the nature of the terminal electron acceptor. Therefore the $\delta^{13}\text{C}$ of organic carbon remineralized during the period of sulfate reduction ($\delta^{13}\text{C-C}_{\text{ORG}}[\text{SR}]$) should be similar to the $\delta^{13}\text{C}$ of organic carbon remineralized during the period of methane production ($\delta^{13}\text{C-C}_{\text{ORG}}[\text{MP}]$).

Since CO_2 is the sole end product of organic matter decomposition in sulfate-containing sediments (Figure 2), the $\delta^{13}\text{C}$ of organic carbon remineralized during the period of sulfate reduction is simply calculated as the $\delta^{13}\text{C}$ value of the ΣCO_2 produced:

$$\delta^{13}\text{C-C}_{\text{ORG}}[\text{SR}] = \frac{(\delta^{13}\text{C-}\Sigma\text{CO}_2)_{\text{FIN}} [\Sigma\text{CO}_2]_{\text{FIN}}}{[\Sigma\text{CO}_2]_{\text{FIN}} - [\Sigma\text{CO}_2]_{\text{INI}}} - \frac{(\delta^{13}\text{C-}\Sigma\text{CO}_2)_{\text{INI}} [\Sigma\text{CO}_2]_{\text{INI}}}{[\Sigma\text{CO}_2]_{\text{FIN}} - [\Sigma\text{CO}_2]_{\text{INI}}}, \quad (6)$$

where INI and FIN denote $[\Sigma\text{CO}_2]$ or $\delta^{13}\text{C-}\Sigma\text{CO}_2$ at the start of the experiment and at the time that sulfate became depleted (day 42), respectively. Between 14 and 42 days, the ΣCO_2 concentration increased from 37.6 to 55.2 mM (Figure 2b), while the $\delta^{13}\text{C-}\Sigma\text{CO}_2$ decreased from -13.4 to -14.1 ‰ (Figure 5a). The $\delta^{13}\text{C}$ value of organic carbon remineralized during the period of sulfate reduction ($\delta^{13}\text{C-C}_{\text{ORG}}[\text{SR}]$) is -15.6 ‰ (equation (6)). This value differs from the $\delta^{13}\text{C}$ of the bulk organic carbon in Cape Lookout Bight sediments (-18 to -20 ‰) [Blair et al., 1987; Martens et al., 1992; Blair and Carter, 1992], suggesting preferential remineralization of an organic matter component that is enriched in ^{13}C relative to the bulk phase. This result seems to contradict previous studies showing no downcore variations in $\delta^{13}\text{C}$ of particulate organic carbon in sediments from Cape Lookout Bight [Blair et al., 1987; Martens et al., 1992; Blair and Carter, 1992]. However, the quantity of organic carbon converted to CO_2 and methane during the 114-day experiment (40.4 mM) represents a small fraction (~2%) of the particulate organic carbon pool. Therefore it is not surprising that preferential remineralization of a ^{13}C -rich labile fraction is not detected in $\delta^{13}\text{C}$ profiles of total organic carbon.

Since CO_2 and methane are both end products of organic matter decomposition in sulfate-depleted sediments, the isotopic composition of organic carbon remineralized during the period of methane production is calculated as the weighted average $\delta^{13}\text{C}$ of the ΣCO_2 and methane produced:

$$\delta^{13}\text{C-C}_{\text{ORG}}[\text{MP}] = \frac{(\delta^{13}\text{C-}\Sigma\text{CO}_2)_{\text{FIN}} [\Sigma\text{CO}_2]_{\text{FIN}}}{[\Sigma\text{CO}_2]_{\text{FIN}} - [\Sigma\text{CO}_2]_{\text{INI}} + [\text{CH}_4]_{\text{FIN}} - [\text{CH}_4]_{\text{INI}}} - \frac{(\delta^{13}\text{C-}\Sigma\text{CO}_2)_{\text{INI}} [\Sigma\text{CO}_2]_{\text{INI}}}{[\Sigma\text{CO}_2]_{\text{FIN}} - [\Sigma\text{CO}_2]_{\text{INI}} + [\text{CH}_4]_{\text{FIN}} - [\text{CH}_4]_{\text{INI}}} + \frac{(\delta^{13}\text{C-CH}_4)_{\text{FIN}} [\text{CH}_4]_{\text{FIN}}}{[\Sigma\text{CO}_2]_{\text{FIN}} - [\Sigma\text{CO}_2]_{\text{INI}} + [\text{CH}_4]_{\text{FIN}} - [\text{CH}_4]_{\text{INI}}} - \frac{(\delta^{13}\text{C-CH}_4)_{\text{INI}} [\text{CH}_4]_{\text{INI}}}{[\Sigma\text{CO}_2]_{\text{FIN}} - [\Sigma\text{CO}_2]_{\text{INI}} + [\text{CH}_4]_{\text{FIN}} - [\text{CH}_4]_{\text{INI}}}, \quad (7)$$

where INI and FIN denote the concentration or $\delta^{13}\text{C}$ value at the start of the methane production period (day 42) and at the end of the experiment (day 114), respectively. The ΣCO_2 and methane concentrations at day 42 were 55.2 and 0.12 mM, respectively (Figure 2). The final methane concentration (13.5 mM, Figure 6) was calculated by correcting for gas loss using (1). The final ΣCO_2 concentration (64.6 mM) was also corrected for gas loss using an equation analogous to (1). The ΣCO_2 production rate was set equal to 0.7 times the total methane production rate (MPR). This stoichiometry is based on the oxidation state of labile organic carbon inferred from the $\Delta\Sigma\text{CO}_2/\Delta\text{SO}_4^{2-}$ ratio (-1.7). The $\delta^{13}\text{C-CH}_4$ and $\delta^{13}\text{C-}\Sigma\text{CO}_2$ values at day 42 were -61.4 ‰ and -14.1 ‰, respectively (Figure 5). The final $\delta^{13}\text{C-CH}_4$ value (-66.6 ‰) was corrected for gas loss by integrating $\delta^{13}\text{C-MP}$ (equation (5)) over the entire 114-day interval. Note that this value represents the cumulative $\delta^{13}\text{C-CH}_4$ and differs substantially from the measured value at day 114 (-50.8 ‰). The final $\delta^{13}\text{C-}\Sigma\text{CO}_2$ value (-3.9 ‰) was also corrected for gas loss using an equation analogous to (5). However, for the ΣCO_2 pool, isotopic fractionation between $\Sigma\text{CO}_2(\text{aq})$ and $\text{CO}_2(\text{g})$ [Deuser and Degens, 1967; Wendt, 1968] was taken into account. The $\delta^{13}\text{C}$ value of organic carbon remineralized during the period of methane production ($\delta^{13}\text{C-C}_{\text{ORG}}[\text{MP}]$) is -16.0 ‰ (equation (7)).

The isotope mass balance provides a check on the accuracy of the $\delta^{13}\text{C-MP}$ calculation. The $\delta^{13}\text{C}$ value of organic carbon remineralized during the period of sulfate reduction ($\delta^{13}\text{C-C}_{\text{ORG}}[\text{SR}]$) is based entirely on measured concentration and $\delta^{13}\text{C}$ values. In

contrast, the $\delta^{13}\text{C}$ value of organic carbon remineralized during the period of methane production ($\delta^{13}\text{C-C}_{\text{ORG}}[\text{MP}]$) is based on concentration and $\delta^{13}\text{C}$ values corrected for gas loss according to (2)-(5). Agreement between $\delta^{13}\text{C-C}_{\text{ORG}}[\text{SR}]$ (-15.6 ‰) and $\delta^{13}\text{C-C}_{\text{ORG}}[\text{MP}]$ (-16.0 ‰) indicates that calculated $\delta^{13}\text{C-MP}$ values are consistent with the constraint that the microcosm maintain an overall isotope mass balance.

$\delta^{13}\text{C-CH}_4$ From CO_2 and Acetate

The relationship between $\delta^{13}\text{C-CH}_4$ and the methanogenic pathway can be complicated by concurrent changes in the isotopic composition of the methanogenic substrates (CO_2 and acetate) and/or variability in the magnitude of the kinetic isotope effect for the methane production pathways (CO_2 reduction and acetate fermentation). In this section, we examine how these factors may have played a role in controlling the stable carbon isotopic composition of methane produced by the sediment microcosm.

Methane from CO_2 reduction. There is a large kinetic isotope effect associated with bacterial CO_2 reduction to methane. The magnitude of this effect is expressed as an isotope fractionation factor (α_{CR}), defined as the ratio of methane production rates from $^{12}\text{C-}$ and $^{13}\text{C-}\text{CO}_2$ normalized to the isotopic abundance in the reactant molecule [Rees, 1973]:

$$\alpha_{\text{CR}} = \frac{^{12}\text{C-MPC}/[^{12}\text{CO}_2]}{^{13}\text{C-MPC}/[^{13}\text{CO}_2]}, \quad (8)$$

where MPC denotes the rate of methane production via CO_2 reduction.

If we let $R_{\text{MPC}} = ^{13}\text{C-MPC}/^{12}\text{C-MPC}$ and $R_{[\text{CO}_2]} = [^{13}\text{CO}_2]/[^{12}\text{CO}_2]$, (8) can be written as

$$R_{\text{MPC}} = \frac{R_{[\text{CO}_2]}}{\alpha_{\text{CR}}}. \quad (9)$$

It follows from the definition of $\delta^{13}\text{C}$ [Craig, 1957] that

$$\delta^{13}\text{C-MPC} = \frac{\delta^{13}\text{C-CO}_2 + 10^3}{\alpha_{\text{CR}}} - 10^3, \quad (10)$$

where $\delta^{13}\text{C-MPC}$ represents the isotopic composition of methane produced from CO_2 reduction. This treatment assumes that CO_2 (as opposed to HCO_3^- or

CO_3^{2-}) is the form of inorganic carbon utilized by methanogenic bacteria [Fuchs et al., 1979].

The isotopic composition of methane produced from CO_2 at any time during the magnum syringe experiment can be determined from the $\delta^{13}\text{C}$ of the CO_2 pool and the isotope fraction factor (equation 10). While $\delta^{13}\text{C-CO}_2$ values are easily calculated from $\delta^{13}\text{C-}\Sigma\text{CO}_2$ data [Deuser and Degens, 1967], there is considerable uncertainty regarding the isotope fractionation factor for methane production from CO_2 . Laboratory cultures of methanogenic bacteria grown autotrophically on $\text{H}_2\text{-CO}_2$ yield fractionation factors that range from 1.025 to 1.061 (mean: 1.041, $n = 7$) [Oremland, 1988]. It is not clear whether this high degree of variability is due to differences in experimental conditions or differences between methanogenic species. For example, a single species (*Methanobacterium thermoautotrophicum*) grown in a sealed batch culture [Games and Hayes, 1976] and a flow-thru fermentation system [Fuchs et al., 1979] yielded isotope fractionation factors that differed by 10 ‰. Likewise, different species (*Methanobacterium barkeri* and *Methanosarcina bryantii*) grown under identical conditions had isotope fractionation factors that differed by 28 ‰ [Games and Hayes, 1976].

Aside from interspecies and intraspecies variability, there are reasons why in vitro fractionation factors may not apply to natural methanogen populations. First, the magnitude of the fractionation factor may be a function of the methane production rate. Laboratory cultures fed an 80/20 (v/v) mixture of $\text{H}_2\text{-CO}_2$ generally have higher production rates than methanogenic bacteria in natural ecosystems. Second, most laboratory measurements of isotope fractionation by methanogenic bacteria were conducted at elevated temperatures (37° to 65°C). Thermodynamics predicts that carbon isotope fractionation between CO_2 and methane decreases with increasing temperature [Bottinga, 1969], although it is not clear whether the kinetic isotope effect for bacterial methane production follows the same relationship. Third, the isotope fractionation factor may be species-specific and the bacteria used in the culture studies are unlikely to be representative of natural methanogen populations.

One approach to deriving fractionation factors applicable to methanogenic populations in aquatic sediments is based on in situ isotopic differences between methane and CO_2 . In sediment where CO_2 reduction is the exclusive methane source, the

isotope fractionation factor can be estimated from paired $\delta^{13}\text{C}$ - CO_2 and $\delta^{13}\text{C}$ - CH_4 data (equation (10)). Evidence based on the deuterium content of methane and its formation water suggests that CO_2 reduction is the dominant methanogenic pathway in many marine sediments [Whiticar et al., 1986]. An extensive compilation of paired $\delta^{13}\text{C}$ - CH_4 and $\delta^{13}\text{C}$ - CO_2 data from a wide variety of marine sediment environments predicts a fractionation factor for CO_2 reduction of 1.070 ± 0.020 [Whiticar et al., 1986].

A more rigorous approach to estimating fractionation factors for CO_2 reduction in aquatic sediments takes into account the contribution of different methane production pathways, the intramolecular isotopic composition of acetate, and the kinetic isotope effect for acetate fermentation. This approach was used to estimate fractionation factors for CO_2 reduction in Cape Lookout Bight sediments [Blair et al., 1992]. Isotope fractionation factors for summer (1.056 ± 0.004) and winter (1.062 ± 0.002) conditions fall within the range of values calculated from the paired $\delta^{13}\text{C}$ - CH_4 and $\delta^{13}\text{C}$ - CO_2 data.

The isotope fractionation factors for Cape Lookout Bight sediment [Blair et al., 1992] were used to calculate $\delta^{13}\text{C}$ -MPC values (equation (10)) for methane produced by the sediment microcosm. An average α_{CR} value (1.06) was used because seasonal variations are relatively small. A rather large range (± 0.01) was adopted to allow for uncertainty in the value of the isotope fractionation factor.

The stable carbon isotopic composition of methane derived from CO_2 is denoted by the stippled region in Figure 7; the upper and lower limits correspond to $\alpha_{\text{CR}} = 1.05$ and $\alpha_{\text{CR}} = 1.07$, respectively. The trend toward more positive $\delta^{13}\text{C}$ -MPC values with time is due to the shift in $\delta^{13}\text{C}$ - ΣCO_2 during the period of methane production (Figure 5a). The progressive enrichment of ^{13}C in the ΣCO_2 pool is due, at least in part, to the kinetic isotope effect associated with CO_2 reduction: $^{12}\text{CO}_2$ is converted to methane at a faster rate than $^{13}\text{CO}_2$, leaving the residual ΣCO_2 pool isotopically heavier.

The methane produced between 50 and 75 days is depleted in ^{13}C compared to the methane produced by CO_2 reduction. The methane produced after 85 days is enriched in ^{13}C relative to the methane derived from CO_2 . Although we cannot rule out the possibility that the isotope fractionation factor for CO_2 reduction varied over the course of the experiment, α_{CR} values substantially less than 1.05 or

greater than 1.07 are unlikely. Production of methane with $\delta^{13}\text{C}$ values well outside the range expected for CO_2 reduction are in all likelihood related to methane production from acetate.

Methane from acetate fermentation. The $\delta^{13}\text{C}$ of methane produced from acetate ($\delta^{13}\text{C}$ -MPA) cannot be calculated directly (using an equation analogous to equation (10)) because the $\delta^{13}\text{C}$ of acetate in the magnum syringe sediment is unknown. However, $\delta^{13}\text{C}$ -MPA can be estimated by an isotope mass balance calculation:

$$\delta^{13}\text{C-MPA} = \frac{(\delta^{13}\text{C-MP}) - (1-F) \delta^{13}\text{C-MPC}}{F}, \quad (11)$$

where F denotes the fraction of methane derived from acetate (Figure 4b). The large range in $\delta^{13}\text{C}$ -MPC values, due to uncertainty in the isotope fractionation factor for CO_2 reduction, limits the accuracy of the $\delta^{13}\text{C}$ -MPA calculation. It is possible, however, to place constraints on the isotopic composition of the methane produced by acetate fermentation. In the following section, we estimate $\delta^{13}\text{C}$ -MPA for two periods during the experiment: (1) the 51 to 58 day interval corresponding to minimum $\delta^{13}\text{C}$ -MP values and (2) the 86 to 93 day interval corresponding to maximum $\delta^{13}\text{C}$ -MP values.

During the 51 to 58 day interval, the methane produced by the sediment microcosm was depleted in ^{13}C ($\delta^{13}\text{C}$ -MP = -94‰) compared to the methane produced from CO_2 ($\delta^{13}\text{C}$ -MPC > -83‰) (Figure 7). This implies a source of ^{13}C -depleted methane derived from a pathway other than CO_2 reduction. Acetate fermentation is the most likely source of this methane; the lack of methane production in the presence of sulfate argues against significant methane production from noncompetitive substrates. Acetate fermentation accounted for 34% of the methane produced at 58 days (Figure 4b). Isotope mass balance (equation (11)) requires that the methane produced by acetate fermentation during the 51 to 58 day interval have a $\delta^{13}\text{C}$ value less than -115‰ . This extreme level of ^{13}C depletion is only possible if the methyl group of the acetate molecule is highly depleted.

Net acetate accumulation during the 51 to 58 day interval (Figure 2b) indicates that gross production exceeded consumption. Since acetoclastic methanogens were not substrate limited, isotopic fractionation of the acetate methyl carbon was not influenced by closed system effects. Under these conditions, the

carbon isotopic composition of the acetate methyl group ($\delta^{13}\text{C}-^*\text{CH}_3\text{COOH}$) can be calculated by rearranging an equation analogous to (10):

$$\delta^{13}\text{C}-^*\text{CH}_3\text{COOH} = \delta^{13}\text{C-MPA } \alpha_{\text{AF}} + (\alpha_{\text{AF}} - 1) 10^3, \quad (12)$$

where α_{AF} is the isotope fractionation factor for acetate dissimilation. Laboratory estimates of α_{AF} range from 1.02 to 1.03 for pure cultures of the acetate-utilizing methanogen *Methanosarcina barkeri* [Risatti and Hayes, 1983; Krzycki et al., 1987]. Comparable values (1.032 ± 0.014) were estimated for methanogenic sediments from Cape Lookout Bight [Blair and Carter, 1992]. The latter values, inferred from measured downcore shifts in the isotopic composition of the acetate methyl carbon, are adopted for the following calculations. Given a $\delta^{13}\text{C-MPA}$ of -115‰ for the 51 to 58 day interval (from equation (11)), we calculate a $\delta^{13}\text{C}$ of the acetate methyl carbon of -74 to -99‰ (equation (12)). The large range in the $\delta^{13}\text{C}-^*\text{CH}_3\text{COOH}$ values stems from uncertainty in α_{AF} .

Autotrophic acetogenic bacteria provide a mechanism for producing acetate with a methyl group that is highly depleted in ^{13}C . Gelwicks et al. [1989] have shown that pure cultures of *Acetobacterium woodii* grown autotrophically on CO_2 and H_2 produce isotopically homogeneous acetate that is depleted in ^{13}C by 59‰ relative to the ΣCO_2 pool. If the fractionation factor for *Acetobacterium woodii* in pure culture is applicable to microbial populations in the sediment microcosm, autotrophic acetogenesis during the 51 to 58 day interval would produce acetate with a methyl $\delta^{13}\text{C}$ value of -71‰ . Although this $\delta^{13}\text{C}-^*\text{CH}_3\text{COOH}$ value is slightly outside the range predicted above, it demonstrates the plausibility of extreme ^{13}C depletion in methane derived from autotrophically produced acetate.

At 86 days, acetate fermentation accounted for 87% of the methane produced by the sediment microcosm (Figure 4b). The methane produced during the 86 to 93 day interval was enriched in ^{13}C ($\delta^{13}\text{C-MP} = -42 \text{‰}$) compared to the methane derived from CO_2 reduction ($\delta^{13}\text{C-MPC} < -62 \text{‰}$) (Figure 7). Isotope mass balance constraints indicate that methane produced by acetate fermentation during this period had a $\delta^{13}\text{C}$ value of -37 to -39‰ (equation (11)).

The acetate pool was nearly quantitatively consumed during the 86 to 93 day interval (Figure 2a).

Assuming no isotopic fractionation during methyl group oxidation [Blair and Carter, 1992], the relationship between $\delta^{13}\text{C}-^*\text{CH}_3\text{COOH}$ and $\delta^{13}\text{C-MPA}$ is given by a closed-system Rayleigh equation [Hayes, 1983]:

$$\delta^{13}\text{C}-^*\text{CH}_3\text{COOH} = \delta^{13}\text{C-MPA} - \frac{(\alpha_{\text{AF}} - 1)(1-f)}{\alpha_{\text{AF}} f} [\ln(1-f)] 10^3, \quad (13)$$

where f is the fraction of the acetate methyl carbon pool converted to methane. The f value (0.80) was calculated from the rate of methane production from acetate at 86 days (Figure 3b) divided by the net acetate depletion rate during the 86 to 93 day interval (Figure 2b). From (13), we calculate $\delta^{13}\text{C}-^*\text{CH}_3\text{COOH}$ values ranging from -24 to -33‰ . Although the range of calculated values is large (reflecting uncertainty in α_{AF}), they overlap with values expected for acetate produced by fermentative processes (-21 to -25‰) [Blair and Carter, 1992].

The $\delta^{13}\text{C}$ of methane produced from acetate (calculated by isotope mass balance, equation (11)) varied from less than -115‰ (51 to 58 day interval) to greater than -39‰ (86 to 93 day interval). Such large variations cannot be accounted for by changes in the isotope fractionation factor for acetate dissimilation. Rather, the variations in $\delta^{13}\text{C-MPA}$ imply changes in the isotopic composition of the acetate methyl carbon.

Microbial Controls on $\delta^{13}\text{C-CH}_4$

We have shown that large variations in the $\delta^{13}\text{C}$ of methane produced by the sediment microcosm were driven by shifts in the relative rates of CO_2 reduction and acetate fermentation, as well as changes in the isotopic composition of the CO_2 pool and the acetate methyl carbon. In this section, we present a scenario describing the microbial processes that may have played a role in controlling the variations in isotopic composition of methane produced by the microcosm.

Organic matter degradation in the sediment microcosm can be divided into three distinct periods: (1) the sulfate reduction period, (2) the sulfate-methane transition period, and (3) the methane production period. During the sulfate reduction period (0 to 42 days), high sulfate reduction rates (Figure 3a) were supported by rapid degradation of relatively fresh organic matter. Sulfate concentrations (Figure 2a) throughout this period exceeded the level

at which sulfate-reducing bacteria become sulfate-limited (0.2 mM) [Ingvorsen et al., 1984]. In the presence of nonlimiting sulfate concentrations, sulfate-reducing bacteria maintain acetate and H_2 concentrations at a level too low to support growth of methanogenic bacteria [Lovley et al., 1982; Lovley and Klug, 1986]. The acetate and H_2 produced by organic matter degradation were essentially unavailable to methanogenic bacteria and total methane production rates were negligible (Figure 4a).

During the sulfate-methane transition period (42 to 60 days), sulfate concentrations dropped to threshold levels for uptake by sulfate-reducing bacteria (10 to 20 μM) [Ingvorsen et al., 1984]. Methane began to accumulate in the magnum syringe (Figure 2a), suggesting that methanogens had replaced sulfate reducers as the primary acetate and H_2 consumers. Methane production was initially dominated by CO_2 reduction (Figure 3b), possibly because methanogens growing on H_2 - CO_2 have faster doubling times than acetoclastic species [Vogels et al., 1988]. The first methane produced by the microcosm had a $\delta^{13}C$ of -80 ‰, within the range of values expected for methane produced from CO_2 (Figure 7).

The accumulation of acetate during the sulfate-methane transition period (Figure 2b) suggests that the existing population of acetate-utilizing methanogenic bacteria was unable to keep pace with acetate production. It is not known whether the H_2 reservoir experienced a similar accumulation, but relatively slow rates of CO_2 reduction during the sulfate-methane transition (Figure 3b) suggest that the population of methanogenic bacteria was not fully developed. These conditions would be favorable for H_2 -consuming acetogenic bacteria that normally cannot compete with sulfate-reducing or methanogenic bacteria [Lovley and Klug, 1983]. Most acetogenic bacteria capable of growing on H_2 - CO_2 are also able to grow by fermenting sugars to acetate [Dolfing, 1988]. Therefore acetogenic bacteria (unlike methanogens) can exist in a commensal relationship with sulfate-reducing bacteria, and would be well poised to take advantage of a temporary reduction in H_2 demand that might follow sulfate depletion. Acetate produced from H_2 - CO_2 by autotrophic acetogenic bacteria would be highly depleted in ^{13}C [Gelwicks et al., 1989]. Subsequent methane production from this acetate could account for the ^{13}C -depleted methane (-94 ‰) produced at the end of the transition period (Figure 7).

The methane production period (60 to 114 days) can be divided into two subperiods. During the first subperiod (60 to 90 days), methane production was dominated by acetate fermentation (Figure 3b). The high methane production rates were fueled by the large acetate pool that had begun accumulating during the sulfate-methane transition (Figure 2b). Methane production rates from CO_2 reached a plateau during this subperiod (Figure 3b), suggesting that H_2 -consuming methanogens were keeping pace with H_2 production. Since acetogens cannot successfully compete for H_2 with a well-developed methanogen population [Lovley and Klug, 1983], the acetate that accumulated throughout most of this subperiod was probably synthesized via the sugar fermentation pathway. The methyl carbon in acetate produced by sugar fermentation would be isotopically "heavy," and thus give rise to methane enriched in ^{13}C [Whiticar et al., 1986]. The ^{13}C -rich methane (-42 ‰) produced toward the end of the initial methane production subperiod (Figure 7) is consistent with the predominance of methane production from acetate synthesized by the fermentative pathway.

The second methane production subperiod (90 to 114 days) marks the return to a stable microcosm. Acetate concentrations were depleted to steady state levels (Figure 2b) and total methane production rates decreased gradually (Figure 4a) as the abundance of labile organic matter declined. Assuming that methanogens were the exclusive acetate and H_2 sinks during this period, the relative availability of acetate and H_2 must have been controlled by their respective production rates. Methane production was dominated by CO_2 reduction (Figure 3b), suggesting that H_2 was produced in stoichiometric excess of acetate.

The methane produced during the final subperiod was enriched in ^{13}C (-46 to -60 ‰) relative to the methane produced during the sulfate-methane transition (-80 to -94 ‰). Although CO_2 reduction accounted for ~70% of the methane produced during both these periods (Figure 4b), the methane precursors were enriched in ^{13}C during the latter period. The ΣCO_2 pool was progressively enriched in ^{13}C following sulfate depletion (Figure 5a), presumably due to preferential uptake of $^{12}CO_2$ by methanogenic and possibly autotrophic acetogenic bacteria. The ^{13}C enrichment in the acetate methyl group may be related to changes in the pathway of acetate synthesis (i.e., autotrophic acetogenesis during the sulfate-methane transition; sugar fermentation during the methane production period).

Comparison of Laboratory Microcosm and Natural Sediment

A laboratory microcosm is a highly artificial system. Removing sediment from its natural setting and placing it in a sealed container will inevitably lead to perturbations. The results of the microcosm experiment must be compared with in situ data to evaluate whether the processes that control isotopic variability in the sediment microcosm may also operate in undisturbed marine sediment.

The stable carbon isotopic composition of methane contained in gas bubbles emitted from Cape Lookout Bight sediments (Figure 8a) varies by ~ 10 ‰ over the course of a year [Martens et al., 1986; Burke et al., 1987]. Between February and May, $\delta^{13}\text{C-CH}_4$ values remain relatively constant at -63 to -65 ‰. For a short period at the end of May, $\delta^{13}\text{C-CH}_4$ values drop to -68.5 ‰. The transient decline is followed by a shift toward more positive $\delta^{13}\text{C}$ values that continues through the middle of August. Between August and November, $\delta^{13}\text{C-CH}_4$ values gradually decline from -57 to -62 ‰. Martens et al. [1986, p. 1300] hypothesize that the "observed seasonal isotopic variations are ... controlled by changes in pathways of methane production and cycling of acetate and molecular hydrogen within the sediments".

There is a dramatic increase in the acetate inventory in Cape Lookout Bight sediments between May and August (Figure 8b). The bulk of the summertime acetate inventory is contained in a narrow subsurface peak centered at 10 to 15 cm [Sansone and Martens, 1982]. The vertical extent of the sulfate reduction zone in Cape Lookout Bight decreases during the spring, as sulfate reduction rates increase in response to higher sediment temperatures [Crill and Martens, 1987]. The appearance of the subsurface acetate peak at the end of May corresponds to the sulfate-depletion depth crossing the 15 cm horizon [Sansone and Martens, 1982].

Sediment accumulation rates for Cape Lookout Bight (determined from ^7Be inventories) indicate that sediment residing at the 10 to 15 cm interval in May was deposited at the sediment surface during the late fall [Canuel et al., 1990]. As a result of relatively cool sediment temperatures, organic matter deposited in the fall is effectively preserved through the winter and spring, reaching the 10 to 15 cm horizon with a large fraction of its labile component intact. As sediments warm during the spring, this labile material is able to support high rates of acetate production.

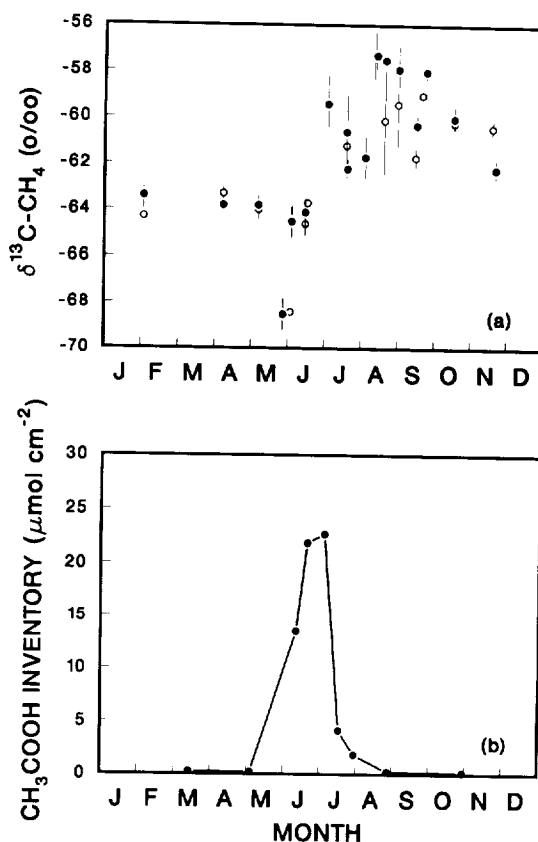


Fig. 8. Seasonal changes in Cape Lookout Bight sediment. (a) $\delta^{13}\text{C}$ of methane in gas bubbles collected during 1983 to 1984 (open circles denote data from Martens et al. [1986]; closed circles denote data from Burke et al. [1987]); (b) acetate inventory calculated by integrating acetate concentration-depth distributions (0 to 36 cm) determined on sediment cores collected in 1990. The error bars in Figure 8a denote the standard deviation based on two to four replicate samples.

The processes that lead to rapid acetate accumulation in the sediment column (Figure 8b) and the sediment microcosm (Figure 2b) are presumably similar: high rates of acetate production accompanied by a sudden reduction in the rate of acetate consumption. In the case of the sediment microcosm, the decline in acetate consumption appears to be caused by the cessation of sulfate reduction (due to sulfate-limitation) and a lag in acetate consumption by methanogenic bacteria (due the slow growth rate of acetoclastic methanogens).

There is a striking similarity in the relationship between $\delta^{13}\text{C-CH}_4$ and acetate concentration (or inventory) for both the microcosm and the undis-

turbed sediment (cf. Figures 2b, 7, and 8). For both systems, methane produced (or emitted) at the beginning of the acetate accumulation period is relatively depleted in ^{13}C . Likewise, methane produced (or emitted) during the period of rapid acetate depletion is relatively enriched in ^{13}C . Seasonal variations in $\delta^{13}\text{C}\text{-CH}_4$ ($\sim 10\text{‰}$) are much smaller than variations in the microcosm ($\sim 50\text{‰}$), presumably due to inertia imposed by the sediment column methane inventory.

The similarities between laboratory and field data suggest that similar processes control the isotopic composition of methane produced by the laboratory microcosm and natural sediment. The shoaling of the sulfate-depletion depth to the sediment horizon containing labile organic material may initiate a scenario similar to that described for the sediment microcosm. First, sulfate depletion may lead to a temporary reduction in competition for acetate and H_2 , resulting in acetate pooling and possibly, production of ^{13}C -depleted acetate by autotrophic acetogenic bacteria. The ^{13}C -depleted methane emitted at the end of May is consistent with a predominance of the CO_2 -reduction pathway (due to the slow growth rate of acetoclastic methanogens) and possibly, methane production from ^{13}C -depleted acetate. Second, acetate fermentation may become the dominant methane production pathway as the acetoclastic methanogens respond to the elevated acetate concentrations. Since acetogens cannot compete for H_2 with an active methanogen population, autotrophic acetogenesis is unlikely. The ^{13}C -rich methane emitted from June thru August is consistent with acetate dissimilation being the dominant methane production pathway. Third, the methane production pathway may shift in favor of CO_2 reduction after the acetate inventory is fully depleted. The shift toward ^{13}C -depleted methane from September thru November is consistent with increased importance of CO_2 reduction after depletion of the acetate reservoir.

CONCLUSIONS

The laboratory microcosm experiment demonstrates that a single sample of anoxic marine sediment incubated at constant temperature can produce methane with $\delta^{13}\text{C}$ values that vary from -94 to -42‰ . The variations in $\delta^{13}\text{C}\text{-CH}_4$ were caused by changes in the relative importance of acetate fermentation and CO_2 reduction, as well as changes in the isotopic composition of the methane precursors (acetate and CO_2). Concurrent methane oxidation and

production were observed, but oxidation was a small fraction (2.4%) of the gross production. It is unlikely that methane oxidation was an important factor in controlling the isotopic composition of methane.

Variations in the relative importance of CO_2 reduction and acetate fermentation can be understood in terms of changes in microbial processes that occurred as sediment bacteria responded to sulfate depletion. The initial predominance of the CO_2 reduction pathway is consistent with the relatively slow growth rate of acetate-utilizing methanogens. The subsequent shift in pathway to acetate fermentation appears to be a response to the elevated acetate concentrations that had accumulated following sulfate depletion. The return to CO_2 reduction as the dominant pathway toward the end of the microcosm experiment corresponds with the rapid and nearly quantitative depletion of the acetate pool.

The apparent changes in the isotopic composition of the acetate methyl carbon may be related to changes in the pathway of acetate synthesis, which in turn, were controlled by competition for H_2 . Changes in isotopic composition of the ΣCO_2 pool during the microcosm experiment are presumably due to isotopic fractionation associated with CO_2 reduction by methanogenic and possibly autotrophic acetogenic bacteria.

A comparison of microcosm and field data reveals a striking similarity in the relationship between $\delta^{13}\text{C}\text{-CH}_4$ and acetate concentration or inventory. This suggests that the processes that control in situ seasonal variations in the isotopic composition of methane emitted from Cape Lookout Bight sediments may be similar to those that controlled variations in the isotopic composition of methane produced by the sediment microcosm. This experiment demonstrates that laboratory-based process studies coupled with field measurements provide a powerful tool for interpreting and understanding stable isotope signatures in nature.

Acknowledgments. This work was supported by Technical Service contract OD4067NTEX from the Environmental Protection Agency (MJA) and grant OCE-9017979 from the National Science Foundation (CSM, DBA, MJA). Additional support was supplied by grant NAGW-838 from the National Aeronautics and Space Administration (NEB). We are grateful to David Meece for his thoughtful review of an earlier version of this paper. Some of the mathematical treatments presented in this paper benefited from discussions with Richard McCaffrey.

Stable carbon isotope analyses were done by Howard Mendlovitz, Julie Gunn, and Connie Crossley. The authors wish to thank Ken Sandbeck and Bill Reeburgh for supplying the $^{14}\text{CH}_4$. We also wish to thank two anonymous reviewers for their constructive comments.

REFERENCES

- Ahlberg, J., E. Nilson, and J. Walsh, *The Theory of Splines and Their Applications*, Academic, San Diego, Calif., 1967.
- Albert, D. B., C. Taylor, and C. S. Martens, Sulfate reduction rates and low molecular weight fatty acid concentrations in the water column and surficial sediments of the Black Sea, *Deep Sea Res.*, in press, 1992.
- Alperin, M. J., and W. S. Reeburgh, Inhibition experiments on anaerobic methane oxidation, *Appl. Environ. Microbiol.*, 50, 940-945, 1985.
- Alperin, M. J., W. S. Reeburgh, and M. J. Whiticar, Carbon and hydrogen isotope fractionation resulting from anaerobic methane oxidation, *Global Biogeochem. Cycles*, 2, 279-288, 1988.
- Bernard, B. B., J. M. Brooks, and W. M. Sackett, Natural gas seepage in the Gulf of Mexico, *Earth Planet. Sci. Lett.*, 31, 48-54, 1976.
- Blair, N. E., and W. D. Carter, The carbon isotope biogeochemistry of acetate from a methanogenic marine sediment, *Geochim. Cosmochim. Acta*, 56, 1247-1258, 1992.
- Blair, N. E., C. S. Martens, and D. J. Des Marais, Natural abundances of carbon isotopes in acetate from a coastal marine sediment, *Science*, 236, 66-68, 1987.
- Blair, N. E., S. E. Boehme, and W. D. Carter, The carbon isotope biogeochemistry of methane production in anoxic sediments. 1. A field study, in *The Biogeochemistry of Global Change: Radiative Trace Gases*, edited by R. S. Oremland, Chapman and Hall, London, in press, 1992.
- Blake, D. R., and F. S. Rowland, Continuing worldwide increase in tropospheric methane, 1978 to 1987, *Science*, 239, 1129-1131, 1988.
- Bottinga, Y., Calculated fractionation factors for carbon and hydrogen isotope exchange in the system calcite-carbon dioxide-graphite-methane-hydrogen-water vapor, *Geochim. Cosmochim. Acta*, 33, 49-64, 1969.
- Burke, R. A., Jr., C. S. Martens, and W. M. Sackett, Seasonal variations in the D/H and $^{13}\text{C}/^{12}\text{C}$ ratios of microbial methane in surface sediments, *Nature*, 332, 829-831, 1987.
- Canuel, E. A., C. S. Martens, and L. K. Benninger, Seasonal variations in ^7Be activity in the sediments of Cape Lookout Bight, North Carolina, *Geochim. Cosmochim. Acta*, 54, 237-245, 1990.
- Chanton, J. P., and C. S. Martens, Seasonal variations in ebullitive flux and carbon isotopic composition of methane in a tidal freshwater estuary, *Global Biogeochem. Cycles*, 2, 289-298, 1988.
- Chanton, J. P., C. S. Martens, and G. W. Kipphut, Lead-210 sediment geochronology in a changing coastal environment, *Geochim. Cosmochim. Acta*, 47, 1791-1804, 1983.
- Cicerone, R. J., and R. S. Oremland, Biogeochemical aspects of atmospheric chemistry, *Global Biogeochem. Cycles*, 2, 299-327, 1988.
- Craig, H., Isotopic standards for carbon and oxygen and correction factors for mass-spectrometric analysis of carbon dioxide, *Geochim. Cosmochim. Acta*, 12, 133-149, 1957.
- Crill, P. M., and C. S. Martens, Methane production from bicarbonate and acetate in anoxic marine sediment, *Geochim. Cosmochim. Acta*, 50, 2089-2097, 1986.
- Crill, P. M., and C. S. Martens, Biogeochemical cycling in an organic-rich coastal marine basin. 6. Temporal and spatial variations in sulfate reduction rates, *Geochim. Cosmochim. Acta*, 51, 1175-1186, 1987.
- Deuser, W. G., and E. T. Degens, Carbon isotope fractionation in the system $\text{CO}_2(\text{gas})$ - $\text{CO}_2(\text{aqueous})$ - $\text{HCO}_3^-(\text{aqueous})$, *Nature*, 215, 1033-1035, 1967.
- Dolfing, J., Acetogenesis, in *Biology of Anaerobic Microorganisms*, edited by A. J. B. Zehnder, pp. 417-468, John Wiley, New York, 1988.
- Fuchs, G., R. Thauer, H. Ziegler, and W. Stichler, Carbon isotope fractionation by *Methanobacterium thermoautotrophicum*, *Arch. Microbiol.*, 120, 135-139, 1979.
- Fung, I., J. John, J. Lerner, E. Matthews, M. Prather, L. P. Steele, and P. J. Steele, Three-dimensional model synthesis of the global methane cycle, *J. Geophys. Res.*, 96, 13,033-13,065, 1991.
- Games, L. M., and J. M. Hayes, On the mechanisms of CO_2 and CH_4 production in natural anaerobic environments, in *Environmental Biogeochemistry*, edited by J. O. Nriagu, pp. 51-73, Science, New York, 1976.

- Gelwicks, J. T., J. Bruno Risatti, and J. M. Hayes, Carbon isotope effects associated with autotrophic acetogenesis, *Org. Geochem.*, **14**, 441-446, 1989.
- Halsted, R. E., and A. O. Nier, Gas flow through the mass spectrometer viscous leak, *Rev. Sci. Instrum.*, **21**, 1019-1021, 1950.
- Hayes, J. M., Practice and principles of isotopic measurements in organic chemistry, in *Organic Geochemistry of Contemporaneous and Ancient Sediments*, edited by W. G. Meinschein, pp. 5-1 - 5-31, Society of Economic Paleontologists and Mineralogists, Tulsa, Okla., 1983.
- Hayes, J. M., D. J. Des Marais, D. W. Peterson, D. A. Schoeller, and S. P. Taylor, High precision stable isotope ratios from microgram samples, in *Advances in Mass Spectrometry*, vol. 7, edited by N. R. Daly, pp. 475-480, Heydon and Son, London, 1977.
- Ingvorsen, K., A. J. B. Zehnder, and B. B. Jørgensen, Kinetics of sulfate and acetate uptake by *Desulfovibrio postgatei*, *Appl. Environ. Microbiol.*, **47**, 403-408, 1984.
- Jørgensen, B. B., A comparison of the methods for the quantification of bacterial sulfate reduction in coastal marine sediments. I. Measurement with radiotracer techniques, *Geomicrobiol. J.*, **1**, 11-27, 1978.
- King, G. M., Methanogenesis from methylated amines in a hypersaline algal mat, *Appl. Environ. Microbiol.*, **54**, 130-136, 1988.
- King, G. M., M. J. Klug, and D. R. Lovley, Metabolism of acetate, methanol, and methylated amines in intertidal sediments of Lowes Cove, Maine, *Appl. Environ. Microbiol.*, **45**, 1845-1853, 1983.
- King, S. L., P. D. Quay, and J. M. Lansdown, The $^{13}\text{C}/^{12}\text{C}$ kinetic isotope effect for soil oxidation of methane at ambient atmospheric concentrations, *J. Geophys. Res.*, **94**, 18,273-18,277, 1989.
- Klump, J. V., and C. S. Martens, The seasonality of nutrient regeneration in an organic-rich coastal sediment: Kinetic modeling of changing pore-water nutrient and sulfate distributions, *Limnol. Oceanogr.*, **34**, 559-577, 1989.
- Kristjansson, J. K., P. Schönheit, and R. K. Thauer, Different K_s values for hydrogen of methanogenic bacteria and sulfate-reducing bacteria: An explanation for the apparent inhibition of methanogenesis by sulfate, *Arch. Microbiol.*, **131**, 278-282, 1982.
- Krzycki, D. R., W. R. Kenealy, M. J. DeNiro, and J. G. Zeikus, Stable carbon isotope fractionation by *Methanosarcina barkeri* during methanogenesis from acetate, methanol, or carbon dioxide-hydrogen, *Appl. Environ. Microbiol.*, **53**, 2597-2599, 1987.
- Lovley, D. R., and M. J. Klug, Methanogenesis from methanol and methylated amines and acetogenesis from hydrogen and carbon dioxide in the sediments of a eutrophic lake, *Appl. Environ. Microbiol.*, **45**, 1310-1315, 1983.
- Lovley, D. R., and M. J. Klug, Model for the distribution of sulfate reduction and methanogenesis in freshwater sediments, *Geochim. Cosmochim. Acta*, **50**, 11-18, 1986.
- Lovley, D. R., D. F. Dwyer, and M. J. Klug, Kinetic analysis of competition between sulfate reducers and methanogens for hydrogen in sediments, *Appl. Environ. Microbiol.*, **43**, 1373-1379, 1982.
- Martens, C. S., and J. V. Klump, Biogeochemical cycling in an organic-rich coastal marine basin. 1. Methane sediment-water exchange processes, *Geochim. Cosmochim. Acta*, **44**, 471-490, 1980.
- Martens, C. S., and J. V. Klump, Biogeochemical cycling in an organic-rich coastal marine basin. 4. An organic carbon budget for sediments dominated by sulfate reduction and methanogenesis, *Geochim. Cosmochim. Acta*, **48**, 1987-2004, 1984.
- Martens, C. S., N. E. Blair, C. D. Green, and D. J. Des Marais, Seasonal variations in the stable carbon isotopic signature of biogenic methane in a coastal sediment, *Science*, **233**, 1300-1303, 1986.
- Martens, C. S., R. I. Haddad, and J. P. Chanton, Organic matter accumulation, remineralization and burial in an anoxic coastal sediment, in *Productivity, Accumulation, and Preservation of Organic Matter: Recent and Ancient Sediments*, edited by J. K. Whelan and J. W. Farrington, pp. 82-98, Columbia University Press, New York, 1992.
- Mason, E. A., and R. B. Evans III, Graham's law: Simple demonstrations of gases in motion, Part 1, Theory, *J. Chem. Ed.*, **46**, 358-364, 1969.
- Mason, E. A., and B. Kronstadt, Graham's laws of diffusion and effusion, *J. Chem. Ed.*, **44**, 740-744, 1967.
- Oremland, R. S., The biogeochemistry of methanogenic bacteria, in *Biology of Anaerobic Microorganisms*, edited by A. J. B. Zehnder, pp. 641-705, John Wiley, New York, 1988.

- Oremland, R. S., L. M. Marsh, and S. Polcin, Methane production and simultaneous sulfate reduction in anoxic saltmarsh sediments, *Nature*, 296, 143-145, 1982.
- Pearman, G. I., D. Etheridge, F. de Silva, and P. J. Fraser, Evidence of changing concentrations of atmospheric CO₂, N₂O, and CH₄ from air bubbles in Antarctic ice, *Nature*, 320, 248-250, 1986.
- Prinn, R., D. Cunnold, R. Rasmussen, P. Simmonds, F. Alyea, A. Crawford, P. Fraser, and R. Rosen, Atmospheric trends in methylchloroform and the global average for the hydroxyl radical, *Science*, 238, 945-950, 1987.
- Quay, P. D., S. L. King, J. M. Lansdown, and D. O. Wilbur, Isotopic composition of methane released from wetlands: Implications for the increase in atmospheric methane, *Global Biogeochem. Cycles*, 2, 385-397, 1988.
- Quay, P. D., S. L. King, J. Stutsman, D. O. Wilbur, L. P. Steele, I. Fung, R. H. Gammon, T. A. Brown, G. W. Farwell, P. M. Grootes, and F. H. Schmidt, Carbon isotopic composition of atmospheric CH₄: Fossil and biomass burning source strengths, *Global Biogeochem. Cycles*, 5, 25-47, 1991.
- Rees, C. E., A steady-state model for sulphur isotope fractionation in bacterial reduction processes, *Geochim. Cosmochim. Acta*, 37, 1141-1162, 1973.
- Risatti, J. B., and J. M. Hayes, Biogenic acetate and the origin of sedimentary biogenic methane, *Geol. Soc. Am. Abstr. Prog.*, 15, 671, 1983.
- Sansone F. J., and C. S. Martens, Volatile fatty acid cycling in organic-rich marine sediments, *Geochim. Cosmochim. Acta*, 46, 1575-1589, 1982.
- Schaff, T., L. Levin, N. Blair, D. Demaster, R. Pope, and S. Boehme, Spatial heterogeneity of benthos on North Carolina continental slope; large (100 km) -scale variation, *Mar. Ecol. Prog. Ser.*, in press, 1992.
- Schonheit, P., J. K. Kristjansson, and R. K. Thauer, Kinetic mechanism for the ability of sulfate reducers to out-compete methanogens for acetate, *Arch. Microbiol.*, 132, 285-288, 1982.
- Stern, M. J., and P. C. Vogel, Relative ¹⁴C-¹³C kinetic isotope effects, *J. Chem. Phys.*, 55, 2007-2013, 1971.
- Stevens, C. M., and A. Engelkemeir, Stable carbon isotopic composition of methane from some natural and anthropogenic sources, *J. Geophys. Res.*, 93, 725-733, 1988.
- Strayer, R. F., and J. M. Tiedje, Kinetic parameters of the conversion of methane precursors to methane in hypereutrophic lake sediment, *Appl. Environ. Microbiol.*, 36, 330-340, 1978.
- Stumm, W., and J. J. Morgan, *Aquatic Chemistry*, 2nd ed., John Wiley, New York, 1981.
- Taylor, J. A., G. P. Brasseur, P. R. Zimmerman, and R. J. Cicerone, A study of the sources and sinks of methane and methyl chloroform using a global three-dimensional Lagrangian tropospheric tracer transport model, *J. Geophys. Res.*, 96, 3013-3044, 1991.
- Tyler, S. C., The global methane budget, in *Microbial Production and Consumption of Greenhouse Gases: Methane, Nitrogen Oxides, and Halomethanes*, edited by J. E. Rogers and W. B. Whitman, pp. 7-38, American Society for Microbiology, Washington, D. C., 1991.
- Tyler, S. C., P. R. Zimmerman, C. Cumberbatch, J. P. Greenberg, C. Westberg, and J. P. E. C. Darlington, Measurements and interpretation of $\delta^{13}\text{C}$ of methane from termites, rice paddies, and wetlands in Kenya, *Global Biogeochem. Cycles*, 2, 341-355, 1988.
- Vaghjiani, G. L., and A. R. Ravishankara, New measurement of the rate coefficient for the reaction of OH with methane, *Nature*, 350, 406-409, 1991.
- Vogels, G. D., K. T. Keltjens, and C. Van der Drift, Biochemistry of methane production, in *Biology of Anaerobic Microorganisms*, edited by A. J. B. Zehnder, pp. 707-770, John Wiley, New York, 1988.
- Wahlen, M., N. Tanaka, R. Henry, B. Deck, J. Zeglen, J. S. Vogel, J. Southon, A. Shemesh, R. Fairbanks, and W. Broecker, Carbon-14 in methane sources and in atmospheric methane: The contribution from fossil carbon, *Science*, 245, 286-290, 1989.
- Wendt, I., Fractionation of carbon isotopes and its temperature dependence in the system CO₂-gas-CO₂ in solution and HCO₃-CO₂ in solution, *Earth Planet. Sci. Lett.*, 4, 64-68, 1968.
- Westrich, J. T., and R. A. Berner, The role of sedimentary organic matter in bacterial sulfate reduction: The G model tested, *Limnol. Oceanogr.*, 29, 236-249, 1984.
- Whiticar, M. J., E. Faber, and M. Schoell, Biogenic methane formation in marine and freshwater environments: CO₂ reduction vs. acetate fermentation -- Isotope evidence, *Geochim. Cosmochim. Acta*, 50, 693-709, 1986.

Yamamoto, S., J. B. Alcauskas, and T. E. Crozier,
Solubility of methane in distilled water and
seawater, *J. Chem. Eng. Data*, 21, 78-80, 1976.

University of North Carolina, Chapel Hill, NC
27599-3300.

N. E. Blair, Department of Marine, Earth, and
Atmospheric Sciences, North Carolina State
University, Raleigh, NC 27695-8208.

D. B. Albert, M. J. Alperin, T. M. Hoehler, and
C. S. Martens, Curriculum in Marine Sciences,

(Received February 21, 1992;
revised June 24, 1992;
accepted July 9, 1992.)

